

Channel Change and Sediment Transport in the Puyallup River Watershed through 2022

Scott W. Anderson¹

¹U.S. Geological Survey, Washington Water Science Center, Tacoma, Washington, 98402, United States

*To whom correspondence should be addressed: swanderson@usgs.gov

This information product has been peer reviewed and approved for publication as a preprint by the U.S. Geological Survey.

Any use of trade, firm, or product names is for descriptive purposes only and does not imply endorsement by the U.S. Government.

Linear referencing

Locations along the Puyallup River are referenced here in terms of valley miles (VM) upstream from the East 11th St. bridge in Tacoma, Washington, the downstream-most span across the river. The bridge is located about 0.7 miles upstream of where the Puyallup River exits into Puget Sound at Commencement Bay. Distances were referenced to valley centerlines, as opposed to river centerlines, to provide a linear stationing system that was not tied to the wetted channel position at any one point in time. Centerlines were manually digitized based on visual inspection of bare-earth digital elevation models of the river valleys. Locations along the Carbon River are referenced in terms of valley miles upstream of the Puyallup River confluence. In the upper half of the watershed, and particularly in discussions of headwater sediment dynamics on the flanks of Mount Rainier, distances down-valley from 2022 glacier termini are used to provide a more intuitive and comparable measure of relative locations along a given river. Distances using this upstream-zero stationing system are noted as VM-DG, with DG indicating ‘downstream of 2022 glacier termini.’

For river stationing purposes, the South Puyallup River was treated as a continuation of the Puyallup River, with the North Puyallup River treated as a distinct tributary. Similarly, the South Mowich River was treated as a continuation of the Mowich River, with the North Mowich River treated as a distinct tributary. A crosswalk between the valley mile system used here and the river mile stationing used in Czuba and others (2010) in the lower half of the watersheds is provided below.

Czuba 2010 river			
River	mile	Valley mile	Feature
Puyallup River	0.00	-0.74	Mouth
	0.74	0.00	11th St. Bridge
	2.00	1.25	
	4.00	3.23	
	6.00	5.22	
	6.60	5.76	USGS 12101500
	8.00	7.19	
	10.00	8.83	
	10.34	9.09	White River confluence
	12.00	10.54	
	12.09	10.62	USGS 12096500
	14.00	11.96	
	16.00	13.57	
	17.63	15.15	Carbon River confluence
Carbon River	18.00	15.41	
	20.00	16.87	
	21.58	18.36	USGS 12093510
	22.00	18.77	
	24.00	20.71	
	25.67	22.18	USGS 12093500
	26.00	22.51	
	0.00	0.00	Confluence with Puyallup River
	2.00	2.00	
	4.00	3.83	
	5.87	5.48	USGS 12094300
	6.00	5.60	
	8.00	7.32	
	10.00	9.06	

Executive Summary

The Puyallup River drains a 990 square mile watershed in western Washington, with headwaters on the glacier-covered flanks of Mount Rainier. Major tributaries include the White, Carbon, and Mowich Rivers. In the levee-confined reaches of the lower watershed, loss of flood conveyance due to sand and gravel deposition has been a chronic issue. Over much of the 20th century, flood conveyance was maintained through sediment removal, but this practice ended in the late 1990s. Flood hazard management activities since the 1990s have primarily involved levee removal or setback projects. Assessments of 1984–2009 repeat cross sections suggested that sediment deposition rates were particularly high in reaches with recent levee setbacks. However, there have been no assessments of recent deposition rates since the 2009 surveys. There are also concerns that intensifying flood hydrology or increased sediment delivery from Mount Rainier may exacerbate deposition. However, assessment of those risks has been hindered by limited understanding of watershed-scale sediment delivery and routing, particularly for coarse sand and gravel.

The U.S. Geological Survey, in cooperation with Pierce County, initiated this study to improve understanding of sediment deposition in the lower Puyallup River watershed. This work is primarily based on differencing of multiple aerial lidar datasets collected during 2002–2022, supplemented by early 1990 photogrammetric elevation datasets, geomorphic assessments of streamgage data, historical topographic surveys from 1907, and previously collected sediment transport measurements. Analyses cover the Puyallup, Carbon, and Mowich Rivers, but do not include the White River.

During 2004–2020, repeat aerial lidar indicates that 1.3 ± 0.3 million yd^3 of sediment accumulated in the lower 20 valley miles (VMs) of the Puyallup River, averaging $80,000 \pm 20,000$ cubic yards per year (yd^3/yr). Deposition was observed during both 2004–11 and 2011–20 lidar differencing intervals. This continued a long-term depositional trend that extends back to at least 1977. From 2004 to 2011, deposition rates along the Soldiers Home levee setback reach, the only setback project downstream of VM 20 completed prior to 2011, were approximately four times higher than in adjacent unmodified reaches. From 2011 to 2020, two additional setback projects were completed; volumetric deposition rates over all three setback reaches were similar to adjacent unmodified reaches, suggesting elevated setback deposition in the 2004–11 interval may have been influenced by an extreme flood in November 2006. These levee setback projects increased the local cross-sectional area of the floodway, used as a rough proxy for relative flood conveyance, by 50 to 200 percent above 2004 conditions. If deposition continued at recent rates, cross-sectional area over the levee setback reaches would be reduced back to 2004 values by 2050–90.

Deposition also occurred over the lower six VMs of the Carbon River during 2004–20, though volumes (0.15 ± 0.09 million yd^3) were an order of magnitude lower than along the Puyallup River. Relatively lower deposition rates in the Carbon River are most likely the combined result of modestly lower incoming sediment loads, modestly steeper channel slope, and the additional sediment transport capacity provided by two large non-glacial tributaries that enter the Carbon River near VM 5.

Upstream of the depositional reaches described above, 2002–22 sediment storage trends along the Puyallup, Carbon, and Mowich Rivers were predominately negative (net erosion) up to the Mount Rainier National Park boundary. Net erosion was the result of bank and bluff erosion

exceeding deposition across wetted channel and bare gravel areas, as opposed to uniform vertical downcutting. Net erosion along these river valleys delivered 3.4 ± 0.6 million yd^3 to the river system, equivalent to $190,000 \pm 35,000 \text{ yd}^3/\text{yr}$. Most of that volume was supplied by erosion of relatively low (4–10 ft) surfaces along the Puyallup and Mowich Rivers and tall (300 ft) glacial bluffs along the lower Carbon River. Substantial aggradation from 1984 to 2009 reported by Czuba and others (2010) along reaches of the Puyallup River (VM 19–22) where levee confinement has recently been removed was most likely an artifact of methodologic bias.

The Puyallup, Mowich, and Carbon Rivers drain five distinct glaciated watersheds on the flanks of Mount Rainier, four of which were assessed in this study. All four watersheds were impacted by an extreme November 2006 rainstorm. Between 2002 and 2008, debris flows occurred in all four headwater areas, collectively eroding at least 2.1 million yd^3 of sediment. These debris flows formed distinct deposits one to two miles downstream of source areas, depositing 30-50 percent of the material eroded upstream. From 2008 to 2022, no headwater debris flows were observed and overall rates of geomorphic change in the headwaters were low. Rivers eroded into debris flow deposits emplaced over the 2002–08 interval, but re-deposited equivalent volumes of material within a half mile downstream.

Stage-discharge relations at five streamgages on upland rivers draining Mount Rainier show either net channel incision or dynamic variability with no long-term trend over the past 60–100 years. Observations of pervasive river valley erosion and stable or incising trends at long-term streamgages in the upper watershed do not support prior claims of widespread and accelerating aggradation of upland rivers draining Mount Rainier.

Erosion and deposition volumes estimated in this report were combined with sediment transport estimates from limited suspended sediment and bedload measurements, estimates of

sub-glacial erosion, and sediment delivery from non-glacial tributaries to construct watershed-scale sediment budgets for the Puyallup River watershed. During 2004–20, the estimated sediment load entering the depositional lowlands was well balanced by estimated inputs from, in order of relative magnitude, subglacial erosion (33–60 percent of total sediment load), erosion along the major river valleys (25–45 percent), erosion in recently deglaciated headwater areas (7–17 percent) and non-glacial tributaries (3–9 percent). These results are specific to the study period and represent total sediment loads, most of which is fine material carried in suspension. The relative sourcing of sand and gravel may be different than implied by this sediment budget.

Downstream of VM 12, comparison of 1907 and 2009 channel surveys show net lowering of the channel thalweg of 4–12 ft. A long-term gage near VM 22 shows lowering of 4–5 ft through the 1960s. Lowering at both locations was inferred to be a channel response to the substantial straightening, and so steepening, of the river during major phases of levee construction through the early and mid-20th century.

Application of a simple empirical bedload-discharge power-law relation to an ensemble of model-estimated daily mean discharge records in the lower Puyallup River between 1977 and 2100 projects that annual bedload transport capacity in the lower Puyallup River will increase by 20–60 percent by the middle of the 21st century. Actual changes in bedload transport and deposition rates will depend on concurrent changes in sediment supply and local hydraulics governing deposition.

This report presents several key conclusions. First, the persistence and spatial patterns of sand and gravel deposition along the lower Puyallup River support prior claims that deposition is fundamentally caused by decreases in channel slope moving downstream. Given this underlying cause and the abundance of sand and gravel available to be transported downstream, deposition

is likely to continue for the foreseeable future. Second, despite continued sediment deposition, recent levee setback projects in the lower Puyallup River will likely provide several decades of flood conveyance benefits relative to a no-action alternative. Third, while the rivers linking Mount Rainier to the Puget Sound lowlands have often been discussed as conduits that either pass or accumulate sediment from Mount Rainier, observations from 2002–22 show these river valleys acting as substantial sediment sources, delivering three times more sediment than recently deglaciated headwater areas on Mount Rainier. While the persistence and underlying cause of recent river valley erosion remain unknown, sediment storage dynamics along these river valleys are likely to be a major control on sand and gravel delivery to the lower watershed.

Introduction

The Puyallup River and its major tributaries are sediment-rich systems with headwaters on Mount Rainier, a glacier-covered stratovolcano of the Cascade Range in the State of Washington (Figure 1). Historically, the lower watershed contained dynamic river channels with braided or anastomosing planforms (Figure 2A). However, those channels were progressively straightened, narrowed, and leveed over the early and mid-20th century as the Puget Sound lowlands were developed (Figure 2B, C; Czuba and others, 2010; the Puget Sound lowlands are defined as areas previously covered by the Puget lobe of the Cordilleran ice sheet, shown on Figure 1).

Sediment deposition and associated losses in flood conveyance have been long-standing issues in these lower reaches of the mainstem rivers (Dunne, 1986; Prych, 1988; Sikonia, 1990; Czuba and others, 2010; Herrera Environmental Consultants, 2010; Anderson and Jaeger, 2021). In the mid-20th century, flood conveyance was maintained through manual removal of the accumulated sediment and vegetation clearing (Czuba and others, 2010). However, declines in funding and concerns about aquatic habitat impacts caused sediment removal to taper through the 1980s and ultimately stop in the late 1990s (Czuba and others, 2010). Since then, flood management activities have largely centered on the removal, abandonment, or setback of existing levees, particularly in the Puyallup River upstream of valley mile (VM) 15 (Table 1).

Czuba and others (2010) documented substantial aggradation along the Puyallup River between 1984 and 2009, a period encompassing the end of sediment removal and the start of major modifications to existing levee systems. Aggradation rates were highest in the reaches where levees had recently been removed or set back. Czuba and others (2010) attributed this to

the fact that levee setbacks or removals allowed high flows to spread and slow, reducing sediment transport capacity. Since that 2010 report, there have been multiple additional levee setback projects completed along the Puyallup River, and more are in various stages of planning (Katz and others, 2022). There have been no subsequent assessments of channel change since that 2010 report. However, detailed topographic data derived from aerial light detection and ranging (lidar) surveys have been collected over the lower Puyallup River watershed three times between 2004 and 2020, providing an opportunity to extend observations of deposition and erosion beyond 2009, and to do so with substantially increased spatial resolution (~3–6 ft) than prior cross-section surveys.

Sediment transport in the lower Puyallup River watershed is substantially influenced by Mount Rainier. That influence occurs both via contemporary processes, such as glacial erosion and mass wasting occurring on its flanks, and through the legacy of glacier and lahar deposits emplaced along the major river valleys downstream of Mount Rainier since the late Pleistocene (Crandell, 1963; Czuba and others, 2012a; Scott and Collins, 2021). Given the prominence of Mount Rainier in the watershed and the potential that changes in sediment delivery from Mount Rainier could have a substantial impact on deposition rates in the lower watershed, Czuba and others (2012a, b) conducted a wide range of analyses of sediment delivery and transport in upland watersheds draining Mount Rainier. Czuba and others (2012a) posited that variations in flood hydrology were likely to be the most direct control on sediment delivery rates to the Puget Sound lowlands, given high sediment availability throughout the watershed. However, Czuba and others (2012a) also presented a conceptual model of watershed sediment delivery in which contemporary rockfall, glacier erosion, and debris flows along the flanks of Mount Rainier supplied most of the coarse material in transport in the lower watershed, emphasizing a close

connection between upland sediment delivery rates and sediment transport in the lower watershed over decadal timescales.

Table 1. Summary of major levee modifications in the Puyallup and Carbon Rivers; U/S – upstream; D/S – downstream; VM - valley mile. Based on information from Todd Essman, Pierce County, written communication, May 1, 2023.

River	Levee name	Year of modification	U/S VM	D/S VM	Note
Puyallup River	Various	1996-2009	25.3	22.0	Near-continuous system of straight, narrow levees on both banks that sustained substantial damage in 1996 flood, not repaired
	County	1996-2009	21.9	20.6	Left bank; damaged in floods starting 1996, not repaired
	Ford	1998	21.8	20.1	Right-bank; damaged in 1996, setback alignment built 1998
	Soldiers Home	2006	19.5	18.5	Setback completed just prior to 2006 flood
	Calistoga	2014	18.3	17.1	Levee notched but not fully removed
	South Fork	2014	15.8	15.2	Levee notched but not fully removed; substantial side channel constructed
Carbon River	Fennel Creek	2013	13.6	13.1	Levee largely intact, overflow channels constructed
	Ski Park Bluff	1990-2006	7.8	6.6	Eroded during major floods since 1990, completely washed out by 2006
	Fish Ladder	< 1990	6.1	5.9	Removal or erosion of small extent of existing levee
	South Prairie Fork	1990-2009	5.5	5.3	Removal or erosion of small extent of existing levee

In contrast, recent work around the region has indicated sediment loads may be substantially modulated by the storage and release of valley-floor sediment deposits over decadal to millennial timescales (Collins and others, 2019; Anderson and Jaeger, 2021; Scott and Collins, 2021). This may be particularly true for coarse sand and gravel that make up the channel bed in most regional rivers. Conversely, sizable amounts of sediment from rock falls and debris flows on the flanks of Mount Rainier have tended to be deposited high in the watersheds and

remobilized only slowly (Anderson and Shean, 2021). These findings suggest that sediment storage may buffer or decouple coarse sediment delivery to the lower watershed from contemporary variations in upland sediment supply on the flanks of Mount Rainier. However, research in this realm is far from conclusive, and a practical understanding of if, how, and when sediment inputs from the upper watershed influence bedload transport rates in the lower watershed remains to be developed.

Developing a watershed-scale understanding of coarse sediment delivery and transport is an important step towards understanding how changing flood hydrology (Mastin and others, 2016; Tohver and others, 2014) and glacier retreat (Nylen, 2004; Beason and others, 2023) may impact sediment delivery and deposition in the lower Puyallup River watershed. Thus far, efforts to assess coarse sediment have been limited by the difficulty of estimating or measuring sediment delivery or transport rates, particularly in terms of sand and gravel. However, advances in high-resolution topographic mapping, including both aerial lidar and semi-automated photogrammetric methods (Structure from Motion (SfM); Fonstad and others, 2013; Anderson and Shean, 2021; Knuth and others, 2023; Schwat and others, 2023), now provide opportunities to assess erosion and deposition rates across the study area, including recently deglaciated areas on Mount Rainier and the major upland river valleys.

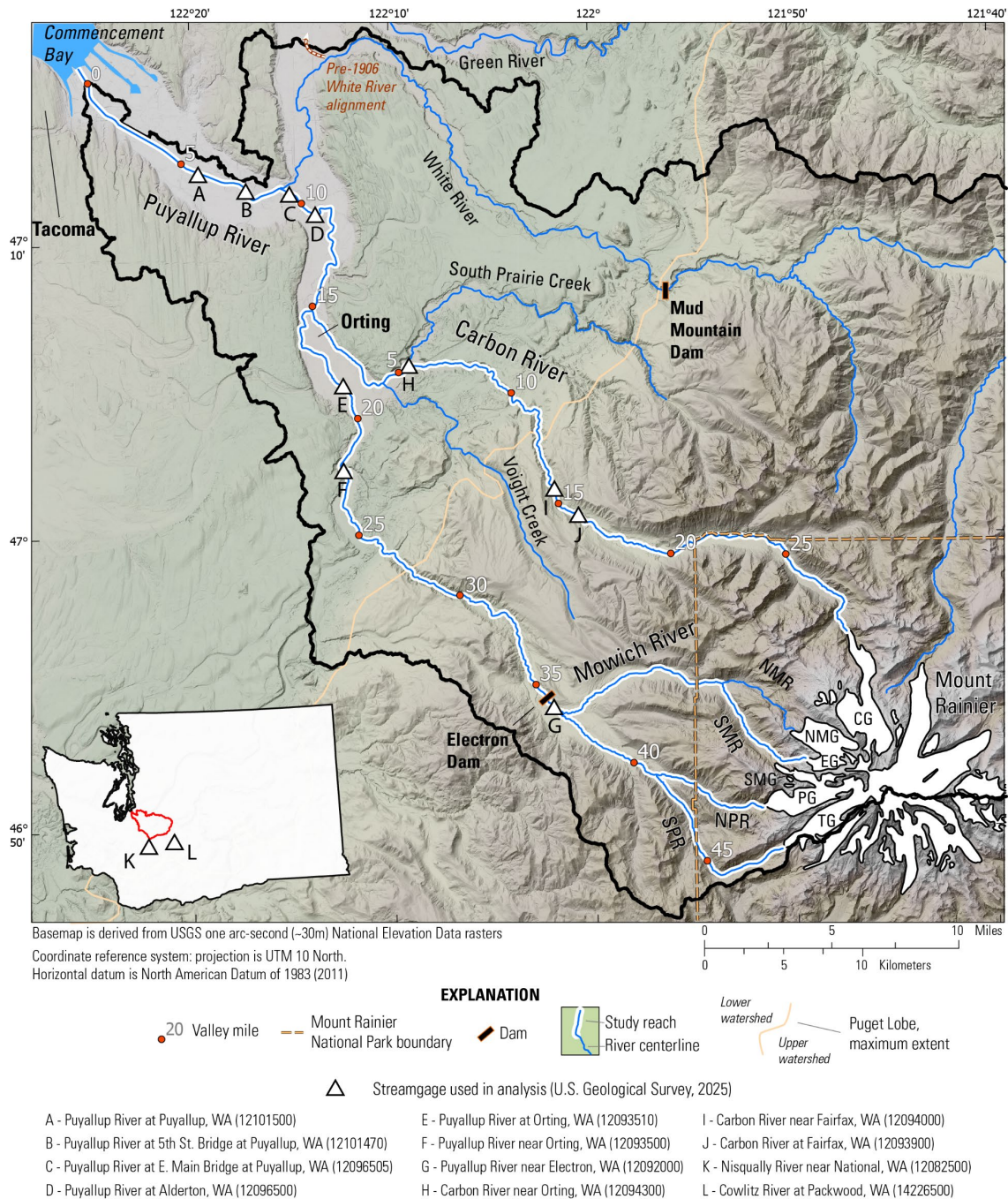


Figure 1. Overview map of Puyallup River watershed. Primary study reaches are indicated by white border around river lines. The Puget Sound lowlands are defined as areas previously covered by the Puget lobe, to the northwest side of maximum extent line. The maximum extents of the Puget lobe also correspond to the divide between the lower and upper Puyallup River watersheds as defined in this report. Basemap is

derived from one arc-second National Elevation Data (U.S. Geological Survey, 2024). National Glacier extents extracted from 1:100,000 geological mapping (Washington Geological Survey, 2022). CG – Carbon Glacier; EG – Edmunds Glacier; NMG – North Mowich Glacier; NMR – North Mowich River; NPR – North Puyallup River; PG – Puyallup Glacier; SMG – South Mowich Glacier; SMR – South Mowich River; SPR – South Puyallup River; TG – Tahoma Glacier.

Purpose and Scope

The primary purpose of this report is to improve understanding of sediment delivery and deposition in the lower reaches of the Puyallup River watershed, with a focus on the deposition of sand and gravel. This was accomplished through documentation of erosion and deposition rates over the past several decades; assessments of controls on those rates, their spatial patterns, and variability over time; and considerations of how channels may be expected to change over the next several decades. This work was motivated by flood hazard management concerns in the lower Puyallup River watershed. The scope of this study is limited to the Puyallup and Carbon Rivers and does not include the White River, as similar analyses for the White River were completed in a previous study (Anderson and Jaeger, 2021).

Table 2. Summary of major analyses by report section. [VM – Valley mile]

Report section	Analyses presented	Spatial extent	Data inputs
Modern channel change in the lower Puyallup and Carbon River watersheds	Topographic change based on differencing of repeat aerial lidar	Puyallup River, VM 4-26; Carbon River, VM 0-9	2004, 2011, 2020 aerial lidar (Table 3)
	Comparison of 2004-20 change in levee setback reaches against adjacent reaches	Puyallup River, VM 9-26	2004, 2011, 2020 aerial lidar (Table 3)
	Relative changes in floodway cross sectional area in levee setback reaches, 2004-20	Puyallup River, VM 9-26	2004, 2011, 2020 aerial lidar (Table 3)
	Assessment of bias in previously-published 1984-2009 cross section analyses	Puyallup River, VM 19-26	1984-2009 repeat cross sections (Czuba and others, 2010)
	Compilation of deposition rates in the lower Puyallup River, 1976/77-2020	Puyallup River, VM 9-20	1976/77-84 channel change and sediment removal (Prych, 1988) 1984-2009 channel change and sediment removal (Czuba and others, 2010) 2004, 2011, 2020 aerial lidar (Table 3)
	Assessment of sediment transport capacity versus deposition rates, 1976/77-2020	Puyallup River, VM 22	Empirical bedload-discharge rating (Czuba and others, 2012a) Daily discharge at USGS 12093500, 12092000, 12094000, 12082500, 14226500 (U.S. Geological Survey, 2025)
Sediment delivery and channel change in the upper Puyallup River watershed	Topographic change, various intervals between 1991 and 2022	Upper Puyallup River watershed	1991/2 photogrammetric DEMs (Anderson, 2025) 2002, 2008, 2011 and 2022 aerial lidar (Table 3)
	Changes in stage-discharge relations, 1930s to 2022	Upper Puyallup River watershed; watersheds adjacent to study area.	Streamflow measurements at USGS 12092000, 12093900, 12094000, 12082500, 14226500 (U.S. Geological Survey, 2025)
Integrated topographic change and watershed sediment budgets	Synthesis of observed topographic change, ~2002/4-20/22	Entire study area	Topographic differencing presented in this report
	Watershed sediment budgets, ~2004-2020	Entire study area	Topographic differencing presented in this report Sub-glacial erosion rates (Mills, 1978) Glacier extents on Mount Rainier (Beason and others, 2023) Non-glacial tributary sediment load estimates (Nelson, 1974; Czuba and others, 2012b)
Long-term channel change in the lower Puyallup River watershed	Changes in stage-discharge relations, 1914-2022	Puyallup River, VM 6, 11 and 22	Streamflow measurements at USGS 12093500, 12096500, and 12101500 (U.S. Geological Survey, 2025)
	Planform and vertical change, 1907-2009/11	Puyallup River, VM 0-12	1907 survey sheets (Chittenden, 1907; Anderson and Jaeger, 2020) 2009 cross sections (Czuba and others, 2010) 2011 lidar (Table 3)
	Estimated bedload transport capacity in 21st century, based on model-forecast daily discharge estimates.	Puyallup River, VM 22	Empirical bedload-discharge rating (Czuba and others, 2012a) Model-forecast daily discharges at USGS 12093500, 1950-2100 (Chegwidden and others, 2019)

The work presented in this report covers two broad objectives. The first objective was to provide an updated synthesis of deposition and erosion rates across the lower Puyallup River watershed, combining results from prior studies (Prych, 1988; Czuba and others, 2010) with new

information provided by repeat aerial lidar collected between 2004 and 2020. Particular attention was given to sediment storage trends in reaches where levees have been eroded, removed, or set back over the past several decades, addressing the question of whether such modifications were likely to provide persistent flood protection benefits.

The second objective was to improve understanding of the controls on sand and gravel delivery and deposition rates in the lower Puyallup River watershed. This objective involved considerations of sediment input and routing processes operating throughout the watershed, influenced by both watershed history and contemporary disturbances. A better understanding of those controls is a precondition for any projections of what sediment delivery and deposition rates may look like over the 21st century. Analyses addressing this second objective primarily involved documenting modern sources and sinks of sediment throughout the watershed over two roughly decadal periods, based on repeat high-resolution topographic surveys. Results from topographic differencing in both the upper and lower watershed were then combined with approximate sediment transport estimates to construct period-specific sediment budgets for the entire watershed.

Additional analyses addressing this second objective included documentation of vertical and planform channel change in the lower watershed over the past century, motivated by recognition that watershed reorganization, channel straightening, and dredging over the 20th century may continue to be major controls on channel change in these watersheds (Anderson and Jaeger, 2021). Finally, estimated changes in local flood hydrology through 2100 (Chegwidden and others, 2019) were used to estimate how changes in flood hydrology alone would be expected to impact bedload sediment transport capacity in the lower watershed independent of any concurrent changes in sediment supply. This overall scope largely mirrors what has been

presented in prior U.S. Geological Survey (USGS) reports over the past decades (Prych, 1988; Sikonia, 1990; Czuba and others, 2010; 2012a), extending observations through the early 2020s.

This report is organized into five main analysis sections, each containing a suite of related analyses (Table 2). These sections include, in sequential order:

1. Assessments of sediment erosion and deposition through the lower Puyallup River watershed, summarizing new observations from repeat aerial lidar collected between 2004 and 2020 and previously published assessments based on repeat cross sections.
2. Analyses of erosion and deposition through the upper Puyallup River watershed, including both the major river valleys and the flanks of Mount Rainier. Analyses are primarily based on repeat topographic surveys collected between 1991 and 2022. Long-term local channel elevation trends are also inferred from several long-term USGS streamgages.
3. Construction of watershed-scale sediment budgets, combining results from repeat topographic analyses presented in the previous two sections with measurement-based estimates of sediment transport and literature-based estimates of sediment inputs from non-glacial tributaries and sub-glacial erosion.
4. Analyses of long-term (~100 year) channel change, based on a combination of 1907 surveys covering the lower 12 valley miles of the Puyallup River and long-term streamgage data at three locations along the lower Puyallup River.
5. An assessment of how forecasted changes in flood hydrology would be expected to change bedload transport capacity in the lower Puyallup River.

Methods and results are presented for each section. Those five sections are followed by a summary of key results and a discussion of those results and their implications for flood hazard management in the lower watershed. Given the breadth of analyses presented (Table 2), the results do not all cohere into a single narrative takeaway. However, all results presented here advance understanding of recent channel change in the lower Puyallup River, their causes, and likely trajectories in the coming decades.

This work makes use of data collected between 1907 and 2022, though most new analyses are based on repeat topographic datasets collected between 2002 and 2022. Aerial lidar collected between 2008 and 2011 sub-divides this 20-year interval into early and late periods. For the analyses of repeat topographic change presented in this report and the sediment budgets they inform, a nomenclature of an early (2002/4 to 2008/11) and late (2008/11 to 2020/22) period is used throughout. While the start and end dates of these early and late periods vary across the watershed as a function of when topographic data were collected, the early period includes a large (~0.01 annual exceedance probability) November 2006 storm in all areas, while the late period was marked by active, but less extreme, flood hydrology.

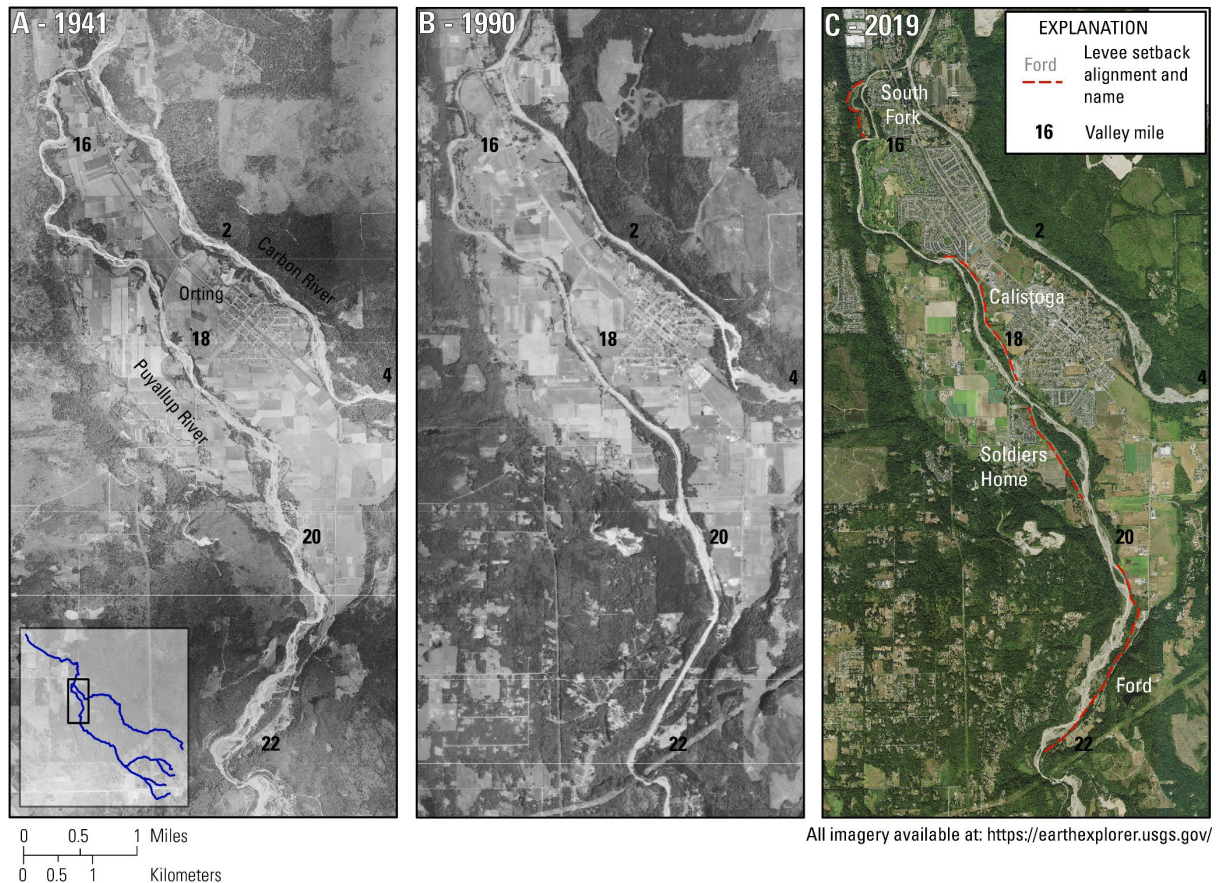


Figure 2. Aerial imagery of the Puyallup and Carbon Rivers near Orting, Washington in A) 1941, B) 1990, and C) 2019. Inset in A shows imagery extents overlain on primary study reaches from Figure 1. The 1941 imagery shows the rivers prior to most major channelization efforts within the imagery extents; 1990 imagery represents maximum channelization. 2019 imagery shows the river after multiple levee setback projects had been completed, and levee systems upstream of VM 20 had been lost to erosion.

Description of Study Area

The Puyallup River drains a 990 square mile (mi^2) watershed in western Washington State, which begins at the summit of Mount Rainier (14,410 ft) and flows down to sea level at

Commencement Bay, part of Puget Sound (Figure 1; U.S. Geological Survey, 2024). The Puyallup River and its major tributaries—the White, Carbon, and Mowich Rivers – traverse this 14,410 ft of elevation change over distances ranging from 50 to 90 miles. The watershed is underlain by a mix of Tertiary volcanic and sedimentary rocks (Washington Geological Survey, 2022), while Mount Rainier was formed by Quaternary andesitic and dacitic eruptions that overlie Tertiary volcanic material (Fiske and others, 1964; Reid and others, 2001). Much of the Puyallup River watershed is mantled by unconsolidated sediment from the late Pleistocene and Holocene, including continental glacier deposits emplaced by the Puget lobe of the Cordilleran ice sheet and both glacier and lahar deposits sourced from Mount Rainier (Crandell, 1963; 1969; 1971; Crandell and Miller, 1974; Booth, 1994; Vallance and Scott, 1997). Notable lahars in the watershed include the 500-year-old Electron Mudflow, which deposited material down the full length of the Puyallup River (Crandell, 1963); and the larger 5,600-year-old Osceola Mudflow, which primarily traveled down the White River but also emplaced material in the modern valleys of South Prairie Creek, the Carbon River, and the Puyallup River (Crandell, 1971; Vallance and Scott, 1997).

The upper Puyallup River watershed includes six distinct glaciers that drain into five headwater river systems (Figure 1). These include the Carbon Glacier, draining into the Carbon River; the North Mowich Glacier, draining into the North Mowich River; the Edmunds and South Mowich Glaciers, both of which drain into the South Mowich River; the Puyallup Glacier, which drains into the North Puyallup River; and the Tahoma Glacier, which drains into the South Puyallup River (Figure 1). Glaciers on Mount Rainier have generally been retreating since the mid-19th century (Sigafoos and Hendricks, 1972), though climate variability related to the Pacific Decadal Oscillation (Mantua and Hare, 2002) resulted in mountain-wide glacier re-advances

starting in the 1950s. Those advances persisted into the 1970s for south-facing glaciers and into the 1990s for north-facing glaciers (Nylen, 2004). All the glaciated headwaters and varying extents of the upper river valleys are within the boundaries of Mount Rainier National Park, established in 1899 (16 U.S.C. §§ 91-110b; Figure 1).

The Carbon and Puyallup Rivers both pass through a regionally consistent series of valley types formed as a result of continental glaciation and subsequent landscape adjustments after glacier retreat around 16,500 years ago (Collins and Montgomery, 2011). These include, in upstream to downstream order: broad mountain valleys carved by alpine glaciers in the upper watershed; a narrow bedrock gorge at the mountain front (the upstream edges of these gorges are located near VM 30 along the Puyallup River and VM 15 along the Carbon River; Figure 1); ‘post-glacial’ valleys, where rivers have incised into continental glacial deposits; and ‘glacial’ valleys, where deposition from river-borne sediment and lahars has progressively filled in the fjord-like channels of Puget Sound. The ‘post-glacial’ and ‘glacial’ terminology follows Collins and Montgomery (2011). The transition between post-glacial and glacial valleys occurs near VM 20 on the Puyallup River and VM 5 on the Carbon River, where both enter onto the broad valley floor near Orting, Washington (Figure 1). In this report, the downstream extent of the bedrock gorges along the Puyallup and Carbon Rivers are used to divide the watershed into upper and lower extents; this breakpoint also corresponds to the maximum extent of the Puget lobe (Figure 1).

Streamflow in the study reaches is sustained by a mix of rainfall, snowmelt through the spring and early summer, and glacier melt through late summer. High flows are associated with rainfall events through the fall and winter, with the largest peaks occurring during rain-on-snow “atmospheric river” events (McCabe and others, 2007; Konrad and Dettinger, 2017). The

Electron Dam, located on the upper Puyallup River and constructed in 1904, is the only dam within the primary study area (Figure 1). The Electron Dam is a run-of-the-river diversion structure used for power generation and does not materially impact long-term streamflow or sediment transport. Downstream of VM 9, streamflow and sediment transport on the lower Puyallup River is influenced by Mud Mountain Dam, located on the White River (Figure 1). Mud Mountain Dam was completed in 1948 with the primary goal of reducing peak flows on the lower Puyallup River by desynchronizing water inputs from the White River (Czuba and others, 2010). Sediment is allowed to pass the dam between storm systems through outlets located at or near the pre-dam channel bed elevation. As a result, the dam has not fundamentally cut off sediment delivery from the upper White River watershed to the lower White and Puyallup Rivers (Anderson and Jaeger, 2021).

Prior to 1906, the White River turned north near Auburn and was a major tributary of the Green River (Figure 1; Dragovich and others, 1994). In 1906, a flood shifted the White River to the south, making it a tributary of the Puyallup River. This shift, or avulsion, was made permanent with the construction of a barrier wall near the avulsion node in the 1910s. The lower extents of the White and Puyallup Rivers were then extensively straightened, leveed, and dredged through the early 20th century (Herrera Environmental Consultants, 2010). Additional straightening and levee construction occurred farther upstream on the Puyallup, Carbon, and White Rivers throughout the 1950s and 1960s (Figure 2).

River management through the 1970s and 1980s primarily involved the removal of sediment and vegetation to maintain flood conveyance (Sikonia, 1990; Czuba and others, 2010). Concerns about the environmental impacts of those actions, coupled with reductions in river management funding, led to the end of vegetation removal in the mid-1980s. Sediment removal

tapered through the 1990s and ultimately ceased in 1997 (Czuba and others, 2010). Since the late 1990s, flood hazard management in the watershed has primarily focused on the removal or setback of levees (Table 2; refer to Smith and others (2017) for a general overview of levee setbacks as a management tool). Most levee modifications, including both planned setback projects and losses to river erosion, have occurred along the Puyallup River upstream of the Carbon River confluence (VM 15). Upstream of VM 19, the progressive loss of levee confinement since the 1990s has been followed by a return to the wide and dynamic planform conditions characteristic of the Puyallup River in the 1940s (Figure 2). Between VM 15 and 19, levee setback projects have been more localized, and banks have often been left with some degree of artificial protection. Consequently, there has been less dramatic change in the planform character of the Puyallup River downstream of VM 19 relative to 1990s conditions (Figure 2).

In the Carbon River, the most significant recent change in levee structures has been the loss of the Ski Park Bluff levee system, which was progressively eroded by major floods between 1990 and 2006 (Table 2). This has allowed the river to resume erosion of 300-ft tall glacial bluffs located behind that levee system. Other recent levee losses or removals along the Carbon River have been relatively minor.

Sediment Dynamics in the Puyallup River Watershed

Rivers draining Mount Rainier are characterized by high sediment loads and broad, braided, and dynamic channel planforms (Czuba and others, 2012a). High sediment delivery and transport rates in these rivers result from the combination of a steep landscape, widely mantled by unconsolidated sediment, with active glaciers and high precipitation rates. Sediment yields (load divided by drainage area) from rivers draining Mount Rainier are often an order of magnitude higher than from adjacent forested watersheds (Czuba and others, 2012b).

The accessibility of these dynamic river systems, and their associated management hazards, has resulted in a large body of research around sediment delivery, transport, and channel change on or downstream of Mount Rainier (Fahnestock, 1963; Nelson, 1974; Mills, 1976; Nelson, 1978; Dunne, 1986; Driedger and Fountain, 1989; Sikonia, 1990; Walder and Driedger, 1994; Beason, 2007; Copeland, 2009; Czuba and others, 2010, 2012a, 2012b; Anderson and Pitlick, 2014; Legg and others, 2014; Anderson and Jaeger, 2021; Anderson and Shean, 2021; Ahammad and others, 2021; Turley and others, 2021). It is beyond the scope of this report to fully summarize this body of work; Czuba and others (2012a) and Turley and others (2021) provide good descriptions of general sediment delivery processes, with Turley and others (2021) focusing specifically on upland processes on Mount Rainier.

Long-term sediment delivery from Mount Rainier occurs through a combination of mass-wasting processes—lahars, rockfalls, and debris flows—and glacial processes, which include both sub-glacial erosion and the advection of supra- and en-glacial sediment. Lahars are the largest of the mass-wasting processes, mobilizing 50–1,000 million yd^3 in individual events, but are rare (Vallance and Scott, 1997). Major rockfalls (\sim 10 million yd^3) have occurred over the historical record, though most documented rockfall events have been smaller (Crandell and Fahlenstock, 1965). Debris flows, mobilizing on the order of 0.1–1.0 million yd^3 per event, are the most common type of mass-wasting process, with dozens of events documented over the past decades (Driedger and Fountain, 1989; Walder and Driedger, 1994; Copeland, 2009; Legg and others, 2014). Debris flows most commonly occur in the late summer and fall, triggered either by heavy rain or the rapid release of sub-glacially stored water (outburst floods; Walder and Driedger, 1994).

Much the recent sediment-related research on Mount Rainier has focused on whether glacier retreat and changes in precipitation patterns have increased sediment delivery rates from its flanks or are likely to do so in the near future (Beason, 2007; Czuba and others, 2012a; Copeland, 2009; Anderson and Pitlick, 2014; Beason and others, 2014; Legg and others, 2014; Anderson and Jaeger, 2021; Anderson and Shean, 2021). This concern is grounded in the concept of a paraglacial sediment response, in which glacier retreat leads to a period of increased sediment delivery due to the exposure of unstable glacial deposits. This process may be accelerated by a projected increase in the frequency or intensity of rain at elevation through the 21st century (Salathé and others, 2014). Beason (2007) and Beason and others (2014) suggested that rivers within Mount Rainier National Park have been aggrading in response to recent glacier retreat and an inferred increase in sediment delivery, though the data supporting these findings are relatively sparse. Estimates of change based on high-resolution topographic datasets have generally found that, downstream of distinct zones of debris flow deposition, upland rivers draining Mount Rainier have generally been stable or eroding (Anderson and Pitlick, 2014; Anderson and Jaeger, 2021).

The most robust estimates of how sediment delivery has varied over time from upland rivers draining comes from sedimentation studies in Alder Lake, which traps nearly all sediment transported by the Nisqually River (Czuba and others, 2012b; the Nisqually River watershed is directly south of the Puyallup River watershed and drains the south flank of Mount Rainier). Sedimentation rates in Alder Lake were lower from 1956–85 and relatively higher from 1945–56 and 1985–2011, demonstrating variability that includes a recent increase, though no long-term secular trend. Post-1985 increases in Alder Lake sedimentation rates coincide with increases in active channel width generally observed on upland rivers draining Mount Rainier from 1994 to

2009 (Czuba and others, 2012a). The changes in sedimentation rates and channel width both track trends in flood hydrology, which was relatively quiescent through mid- and late-20th century and more active starting in the 1990s (Mastin and others, 2016).

Flood Hydrology from 2002/04 to 2020/22

While this report includes datasets and results spanning the past century, most new analyses focus on observations from 2002/4–08/11 (‘early period’) and 2008/11–20/22, (‘late period’). These periods are defined by the timing of aerial lidar data collections used to assess topographic change in the Puyallup River watershed. The exact start and end dates for the two periods vary by several years across the full study area, reflecting differences in when lidar was collected for a given area.

The early study period includes major high flows in water years (WY) 2007 and 2009 (Figure 3). A water year is defined as a 12-month period from October 1st to the following September 30th and is named for the year in which it ends. The WY 2007 high flow (November 6, 2006) was the flood of record at the Puyallup River at Orting, WA (USGS 12093500) and Carbon River near Fairfax, WA (USGS 12094000; U.S. Geological Survey, 2025) streamgages and the second-largest peak on record at the Puyallup River at Alderton, WA (USGS 12096500) streamgage (Figure 4). Recurrence intervals for the 2006 peak were at or above the 0.01 annual exceedance probability (AEP) flow, often referred to as a 100-year flood, at all three sites. There were then two high flows in WY 2009, one in November of 2008 and one in January of 2009. The January 2009 high flow was the flood of record for the Puyallup River at Alderton, WA streamgage.

There were multiple significant high flows over the late period, including 5 to 6 events with peaks equivalent to 0.1–0.04 AEP flows (10- to –25-year recurrence intervals; Figure 3). When compared against full periods of record at these sites, which extend back to the 1930s or 1910s, the full 2002–22 study period represents a relatively active period of high flows for the region (Figure 4).

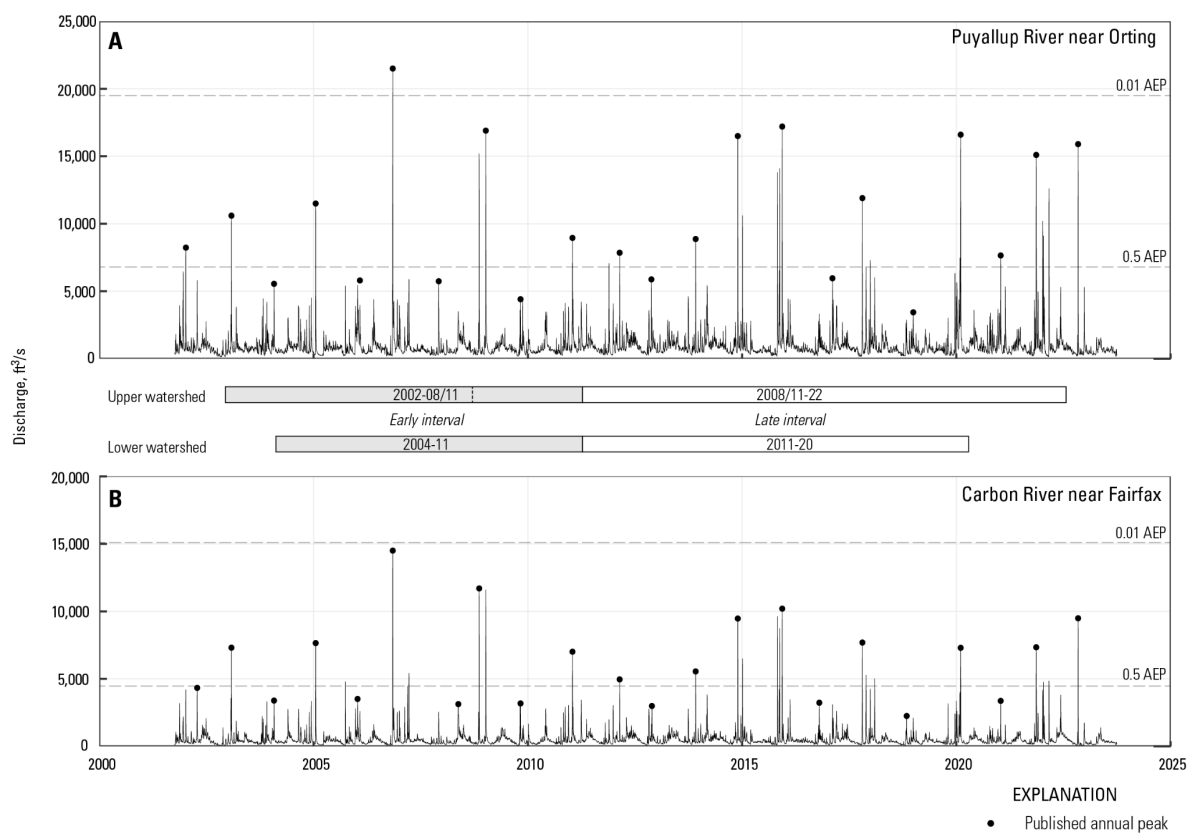


Figure 3. Discharge records over the primary study periods covered by repeat aerial lidar at A) the Puyallup River near Orting, WA, (USGS 12093500) and B) the Carbon River near Fairfax, WA (USGS 12094000);

U.S. Geological Survey, 2025). Published annual peak values for each water year shown as black dots.

Timing of major lidar collections and sub-periods used in this study in the upper and lower watersheds shown between panels. Annual exceedance probability (AEP) values based on calculations by Mastin and others (2016).

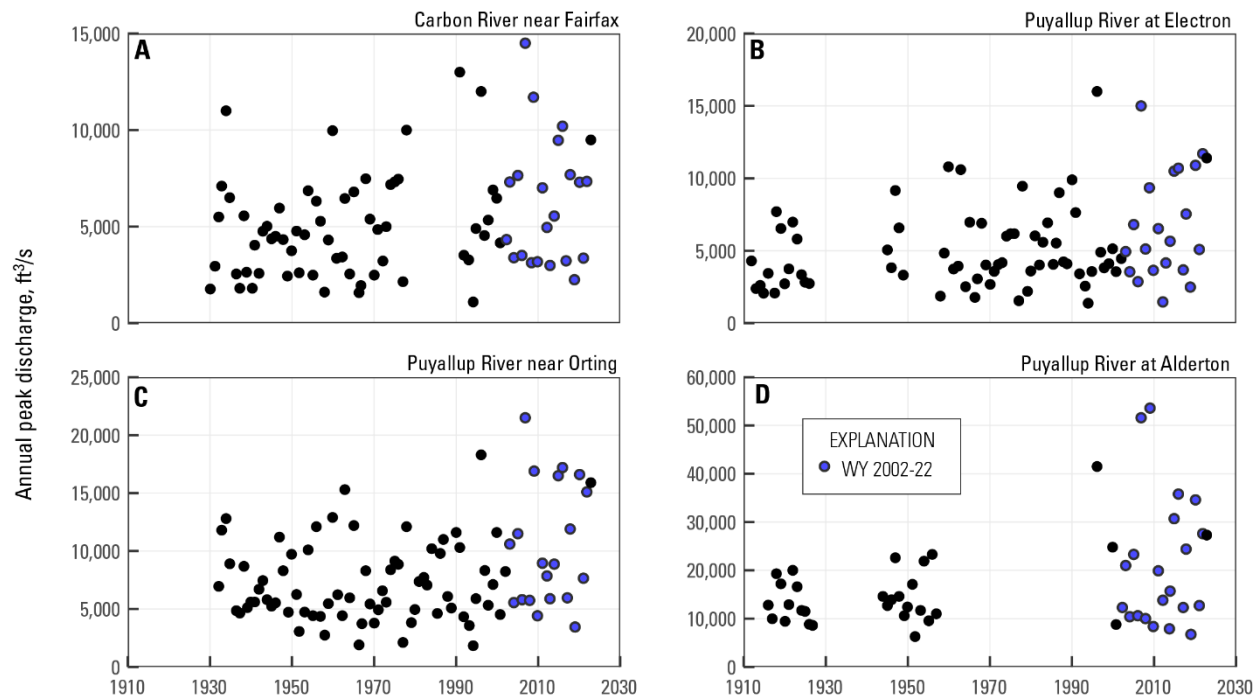


Figure 4. Annual peak discharge records for A) the Carbon River near Fairfax, WA (USGS 12094000), B) the Puyallup River at Electron, WA (USGS 12092000), C) the Puyallup River near Orting, WA (USGS 12093500) and D) the Puyallup River at Alderton, WA (USGS 12096500; U.S. Geological Survey, 2025).

Recent Channel Change in the Lower Puyallup and Carbon River Watersheds

Channel change in the lower Puyallup River watershed has previously been assessed using repeat cross section surveys collected in 1976/77, 1984, and 2009 (Prych, 1988; Czuba and others, 2010). In this report, aerial lidar surveys collected in 2004, 2011, and 2020 were used to

assess channel change through the lower Puyallup and Carbon River watersheds (Table 2, Table 3). Particular attention was given to assessments of erosion and deposition occurring in reaches of the lower Puyallup River where levees have recently been removed or set back (Table 1), addressing whether these levee modifications are likely to provide persistent flood conveyance benefits. A methodologic issue with previously published estimates of change during 1984–2009 (Czuba and others, 2010), which likely overstated deposition observed in levee setback reaches on the Puyallup River upstream of VM 19, is discussed. Finally, lidar-based channel change estimates were combined with results from prior studies to assess sediment deposition rates along the Puyallup River since 1977 and the degree to which flood hydrology alone can explain observed variations in those deposition rates.

Channel change was also estimated based on comparisons of 2009 cross section survey collected by the USGS (Czuba and others, 2010) and in 2023 by David Evans and Associates (Anderson, 2025). However, the results from that analysis were primarily used as a cross-validation of results based on repeat aerial lidar, and so are presented in Appendix A. Observed change from repeat aerial lidar was also compared against channel change estimated from one-dimensional sediment transport modeling presented in Czuba and others (2010), but was likewise primarily used as a methodologic cross-comparison and so is also presented in Appendix A.

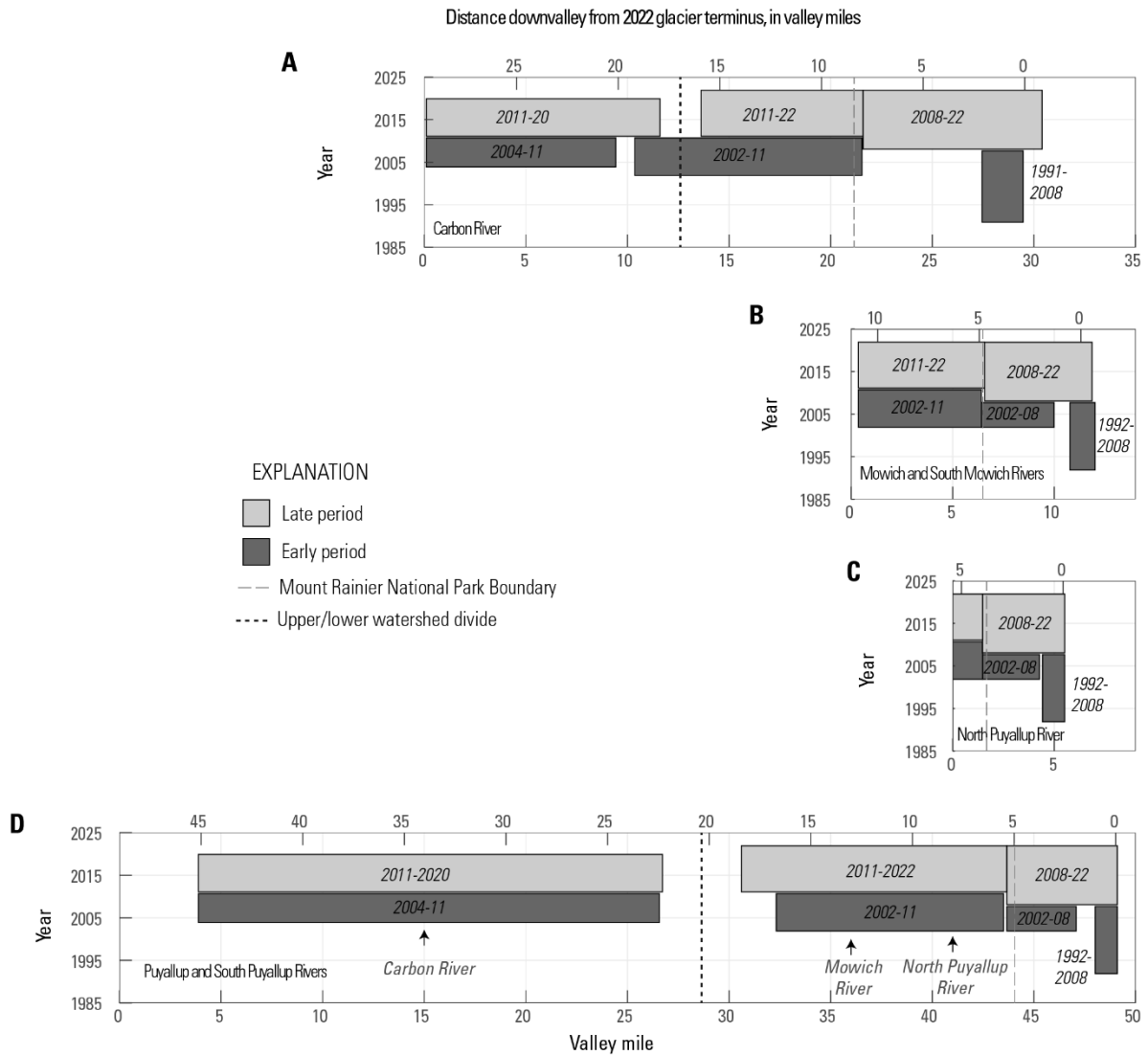


Figure 5. Longitudinal extents of repeat topographic change analyses in the Puyallup River watershed, showing specific extents in the A) Carbon River, B) Mowich and South Mowich Rivers, C) North Puyallup River, and D) Puyallup and South Puyallup Rivers. Bottom x-axes indicate valley mile from river-specific zero points (11th St. bridge in the Puyallup River; confluence with the Puyallup River for all others; Figure 1). Top x-axes indicate distances downstream from the river-specific glacier termini (VM-DG). Panels are aligned so that the left side of panels A, B, and C align with the location of their respective confluences with the Puyallup River in panel D.

Methods for Assessing Topographic Change Using Repeat Aerial Lidar

Aerial lidar was collected over the lower Puyallup River watershed in 2004, 2010/11, and 2020 (Figure 5; Table 3). All lidar data were accessed from the Washington State Department of Natural Resources lidar repository (Table 3). For the 2010/11 collection, most of the lower Puyallup River watershed was covered in the February 2011 collection block and so referred to as the ‘2011 lidar.’

Table 3. Summary of aerial lidar datasets used to assess change in the Puyallup River watershed. [pt – point; ft – feet]

Study area	Lidar reference year	Collection date range	Average ground point density, pt/ft ²	Raster grid size, ft	Source Reference
Lower Puyallup River watershed	2004	2/5/2004 - 3/8/2004	0.10	6.6	Washington Geological Survey, 2005
	2011	12/3/2010 - 2/9/2011	0.17	3.3	Washington Geological Survey, 2011
	2020	4/10/2020 - 4/13/2020	0.34	3.3	Washington Geological Survey, 2020
Upper Puyallup River watershed	2002	December 2002	0.08	6.6	Washington Geological Survey, 2003
	2008	September-October 2008	0.08	3.3	Washington Geological Survey, 2009
	2011	9/3/2011 - 9/6/2011	0.17	3.3	Washington Geological Survey, 2011
	2022	7/24/2022	0.58-0.85	3.3	Washington Geological Survey, 2023a; 2023b

All lidar surveys were collected using near-infrared (NIR) sensors, which provide water surface elevations at the time of the survey but not any bathymetric data. For each survey, raster digital elevation models (DEMs) aligned to a common grid were created from classified point clouds using a triangulated irregular network (TIN) to raster process, using all points classified as either ground or water. This avoided the smoothed post-processed (‘hydroflattened’) water surface present in most of the publicly available raster products. Raster resolution was 6.6 ft for the 2004 data, and 3.3 ft for the 2011 and 2020 datasets. For 2004–11 differencing, the 2011

raster was aggregated from 3.3 ft to 6.6 ft resolution prior to analysis to match 2004 data resolution (Table 3).

Given two DEMs, topographic change is assessed by subtraction of the earlier DEM from the later DEM, resulting in a DEM of difference (DoD). Obtaining accurate estimates of reach-scale net elevation or volumetric change requires identifying and correcting systematic relative errors that may exist between the two surveys (Anderson, 2019). This process of aligning one DEM to another is referred to as co-registration. Because the goal is to assess differences between DEMs, as opposed to elevations referenced to an external datum, the choice of which DEM in a given pair is taken as the reference surface, and which DEM is adjusted to best match that reference, is arbitrary.

Horizontal offsets between lidar surveys were identified and corrected based on systematic relations between land surface slope, aspect, and apparent change in areas of stable topography (Nuth and Kääb, 2011). Smooth and level stable surfaces in or near the river corridors were then used to define and correct systematic vertical offsets. Those stable surfaces were primarily roads and parking areas but also included some levee crests and stable surfaces with little to no vegetation within the river corridors. Local vertical offsets were estimated within sequential 1,600 ft segments measured along the valley centerline, producing a correction that varied along the length of the valley. This approach allows the correction to capture the typical structure of vertical offsets observed in these datasets, which tended to vary smoothly over distances of several thousand feet. After correcting horizontal and vertical offsets, DoDs were recreated and visually inspected for systematic offsets correlated with vegetation structure (Anderson and others, 2019). No such issues were identified.

Accounting for Cross-Survey Differences in Discharge

The NIR lidar surveys used in this study provide measures of water surface elevation at the time of the survey, as opposed to the submerged channel bed elevation. Reach-scale change estimates based on naïve differencing of the DEMs derived from those NIR lidar surveys would represent the sum of changes in sediment storage and changes in water storage. Because the purpose of this report is to assess changes in sediment storage alone, apparent due to changing water storage alone represent a source of bias.

This bias was addressed by using hydraulic modeling to synthetically raise water surface elevations in DEMs to elevations expected if the survey had been acquired at some higher discharge conditions. For each DEM-pair to be differenced, water surface elevations in the lower-discharge survey were raised to expected elevations at the discharge of the higher-discharge survey, effectively normalizing the DEMs to a common discharge. The underlying assumption, discussed more below, is that reach-scale water storage volume is primarily a function of discharge, such that changes in water storage volume after correcting both DEMs to a common discharge should be close to zero. The measured change from differencing of the discharge-normalized DEMs should then provide an unbiased measure of the net sediment storage change, including the aggregate effect of changes occurring in submerged areas (Figure 6). This same conceptual approach to DEM differencing along rivers was used in Anderson and others (2019) and Anderson and Jaeger (2021). However, the methods for estimating the

appropriate water surface elevation correction used in this report have been revised since those earlier efforts and are described here in detail.

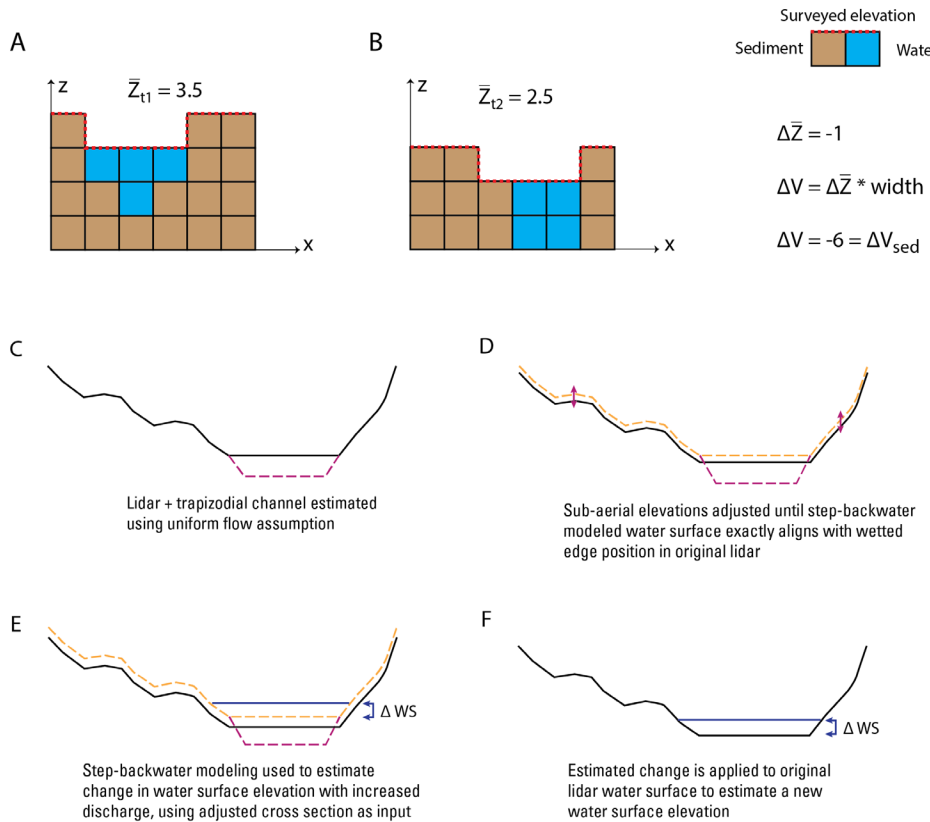


Figure 6. Conceptual basis and practical application of the 'discharge normalization' process used for lidar differencing. A) Two-dimensional landscape composed of unit-area blocks of either sediment or water, captured in a hypothetical near-infrared (NIR) lidar survey (red dashed line). B) The same landscape at some later time, after erosion and channel migration have occurred, captured in a second NIR lidar survey. Calculations to the right demonstrate that because the volume of water held in the landscapes was the same in both surveys, lidar differencing provides an accurate and complete measure of sediment storage change despite the absence of submerged channel elevations in the survey data. C) – F) provide visual representations of the four-step modeling approach described in the "General Step-Backwater Methods for

Correcting Water Surface Elevations" sub-section. ΔZ – elevation change; ΔV – volume change; ΔWS – water surface elevation change.

Conceptual Basis for Discharge Correction Approach

The conceptual basis for this 'discharge normalization' process starts with the observation that if a given analysis area contained only sediment and water, and the volume of water was constant over time, any overall net volumetric change observed in repeat topographic surveys could only be due to changes in the volume of stored sediment (Figure 6A, B). This is just an expression of mass balance and holds true regardless of how the local configuration of sediment and water changed between surveys. Consequently, subject to the assumption of constant water volume, repeat NIR lidar can provide complete and unbiased reach-scale estimates of sediment storage change, including the net effect of changes in areas that were submerged in one or both surveys, without direct information about elevations in submerged areas.

There is no way to directly measure water storage volumes from a NIR lidar survey. Operationalizing this approach then rests on the assumption that if two NIR lidar surveys were collected at identical discharges, the volume of water held in surficial channels over reach scales would tend to be very similar for the two surveys. This is equivalent to an assumption that there were no systematic and substantial changes in reach-average channel roughness or residual pool depth between the surveys. Finally, while repeat surveys are unlikely to be collected at identical discharges, lidar surveys contain sufficient information (channel width, channel slope, bank geometry) to estimate how local water surface elevations would be expected to change with increasing discharge. Hydraulic modeling can then be used to synthetically raise the water surface in the lower-discharge survey to the elevations expected if it had been collected at the

same discharge as the higher-discharge survey. Differencing of these the ‘discharge-normalized’ surveys should then provide complete reach-scale estimates of sediment storage change, including the net effect of change in submerged areas (Figure 6). This approach is conceptually analogous to the use of changing stage-discharge relations at streamgages to infer changing bed elevations (for example, James, 1991) applied at reach scale. Assumptions of stable roughness and residual pool depth over time are considered reasonable for the study area, given that low-flow channels in the lower Puyallup River watershed are generally shallow, planar, and composed of mobile gravel with size distributions that have not changed substantially over time (Czuba and others, 2010),

General Step-Backwater Methods for Correcting Water Surface Elevations

In this report, water surfaces in the lidar DEMs were raised using step-backwater modeling techniques (Chow, 1959). Step-backwater modeling provides a robust method of estimating water surface profiles in open channels and represents an improvement over previous water surface elevation corrections estimated based on stage-discharge relations at USGS streamgages (Anderson and others, 2019) or uniform flow calculations at regular cross sections (Anderson and Jaeger, 2021).

For a given lidar dataset, estimating expected water surface elevations at a higher-than-surveyed discharge via hydraulic modeling involves two general steps: first, channel width and slope information obtained from the lidar are combined with discharge information at the time of the survey (obtained from nearby USGS streamgages) and used to estimate the effective hydraulic geometry of the submerged channel. That effective hydraulic geometry is represented here by a trapezoidal channel with a depth that passes the known discharge at the observed water surface elevation. That synthetic channel is then merged with the exposed bank geometry from

the lidar, and the resulting cross section is used in step-backwater calculations at the higher discharge of interest.

In theory, step-backwater modeling could be used for both steps (for example, Gessese and others, 2011). However, initial attempts to estimate hydraulic geometry using step-backwater methods were found to be numerically unstable. An alternate approach was then developed for the purpose of this work, involving four steps (Figure 6C-F): first, initial estimates of hydraulic geometry were made at regular cross sections using a uniform-flow assumption (Chow, 1959) informed by the known width, water surface slope, and discharge. Second, step-backwater calculations were used to estimate water surface elevation at the known discharge of the lidar survey, using the submerged channel geometry estimated from the previous step. To account for minor difference between modeled and observed water surface elevations, the cross section was iteratively shifted up or down until modeled and ‘observed’ (observed + shift) water surfaces matched. This ensured that the initial step-backwater estimate of water surface elevation exactly preserved the known wetted top-width and the relative vertical position of the water surface within the cross section. Third, step-backwater modeling was used to estimate the expected water surface elevation at a higher discharge, using the cross section generated in the previous step. Finally, the estimated increase in water surface elevation was applied to the original lidar surface and used to create a continuous estimate of the raised water surface elevation. This calculation was done at sequential cross sections and the results used to create a continuous estimate of the raised water surface elevation along the river corridor. All DEM cells lower than the estimated surface were replaced with the new water surface elevation. Because the step-backwater modeling was used to estimate a *change* in water surface elevation, which is then used to adjust to the original lidar water surface, the cross section offsets introduced in the third step do not

propagate into the final estimate of raised water surface elevation. This multi-step approach was found to provide numerically stable results.

Application to the Puyallup River Watershed

This ‘discharge normalization’ process was used for all DEM-pairs in all reaches of the lower Puyallup River watershed except for the Puyallup River downstream of VM 4. Downstream of VM 4, water surface elevations were tidally influenced, introducing an additional and substantial control on water storage volumes not accounted for in this normalization approach. No DEM differencing results are then presented for the Puyallup River downstream of VM 4. Information about recent channel change in those lower reaches is available based on 2009–23 repeat cross section surveys (Appendix A; Figure A1).

All uniform flow and step-backwater calculations were done in Python (Anderson, 2025). Hydraulic methods and computational approaches were taken directly from the U.S. Army Corps of Engineers HEC-RAS hydraulic reference manual (Brunner, 2020; ‘1D Steady Flow Water Surface Profiles,’ within the ‘Theoretical Basis for One-Dimensional and Two-Dimensional Hydrodynamic Calculations). Outputs from the Python scripts were verified against output from HEC-RAS using identical test inputs.

Vector inputs required to define the hydraulic modeling domain and geometry include polygons defining the wetted channel area, channel centerlines, regular cross sections cut roughly perpendicular to those centerlines, and information about local discharge at the time of each lidar survey. Wetted channel areas were defined using a combination of automated delineation based on lidar point classifications and manual delineation. Channel centerlines were then drawn up those wetted channel areas, and regular cross sections cut perpendicular to those

centerlines at 165 ft intervals. Cross sections were manually reviewed and modified to ensure that they fully covered all relevant channel areas and were oriented perpendicular to the direction of local flow.

Timestamps in the lidar point cloud data were used to obtain the time of collection at a given location, and USGS streamflow records throughout the lower watershed used to estimate discharge at those locations and times (Table 4). Discharge was averaged over reaches defined by both major tributary inflows and major blocks of lidar acquisition. Downstream boundary conditions for step-backwater modeling were defined using normal depth calculations, with friction slopes estimated from water surface slopes estimated from the lidar. Manning's coefficient of roughness (n) was calibrated through comparisons of observed changes in water surface elevation between initial and target discharges at USGS streamgages against model-estimated increases at the locations of those gages (Table 5). Distinct calibration tests were performed for each lidar DEM to be corrected, using stage-discharge records near in time to when the lidar was collected. The resulting n values were low (0.020 to 0.030) relative to typical values used in flood modeling (Brunner, 2020). This may indicate a distinction between roughness values for the low flows considered here, which are fully contained within relatively smooth inner channels, and roughness values for bankfull flows interacting with banks and vegetation. Regardless, the estimated water surface elevations, and final estimates of topographic change, were not particularly sensitive to changes in assumed n values (Table 5).

Direct validation that this discharge-normalization approach would require topobathymetric data to have been collected at the same time as the NIR lidar collections. No such repeat topobathymetric datasets exist in the Puyallup River watershed. However, coincident repeat NIR and topobathymetric data exist along the Nooksack River, located in northwest

Washington, over a six-mile reach that is comparable in width, slope, and planform characteristics to much of the lower Puyallup and Carbon Rivers. Over that reach of the Nooksack River, estimated mean elevation change based on discharge-normalized NIR lidar agreed with estimates from repeat topobathymetric surveys within 0.04 ft, validating that the general approach can work in settings like the Puyallup and Carbon Rivers (Figure B2, B3; refer to appendix B for details).

Additional validation specifically in the Puyallup River watershed is provided by comparisons of 2011–20 channel change results from repeat aerial lidar against change based on comparison of 2009 and 2023 repeat cross sections (Appendix A). While the mismatches in survey timing make this an imperfect methodologic check, there is good agreement on the direction and scale of observed change, both at the scale of individual cross sections and over reach averages (Figure A1, Figure A2).

Table 4. Summary of ‘discharge normalization’ process inputs, discharge sources, and outputs. Sub-reaches are defined based on unique combinations of discharge in both surveys (U.S. Geological Survey,

2025) and Manning's coefficient of roughness (n) values. [DS - downstream; ft - feet; s - second; US - upstream; VM - valley mile]

River	Reach extent		Lower discharge survey			Higher discharge survey			Discharge source (USGS site number)	Manning's n	Mean modeled water surface elevation change, ft	Mean estimated channel depth (lower discharge), ft	Modeled mean channel velocity (lower discharge), ft/s
	DS VM	US VM	Reference year	Survey Date	Discharge, ft ³ /s	Reference year	Survey Date	Discharge, ft ³ /s					
Puyallup River, 2004 to 2011	4.02	4.80	2004	2/15/2004	2,230	2011	12/6/2010	2,809	12101500	0.020	0.38	3.5	3.8
	4.83	6.83	2004	2/15/2004	2,230	2011	12/5/2010	2,993	12101500	0.020	0.54	3.9	3.7
	6.87	8.47	2004	2/15/2004	2,230	2011	12/4/2010	3,354	12101500	0.020	0.75	4.0	4.1
	8.50	9.04	2004	2/21/2004	2,222	2011	12/4/2010	3,354	12101500	0.020	0.74	4.1	4.6
	9.10	10.35	2004	2/21/2004	1,258	2011	12/4/2010	1,769	12096500	0.020	0.42	3.1	4.2
	10.37	14.54	2004	2/21/2004	1,258	2011	2/9/2011	1,997	12096500	0.020	0.61	3.0	4.7
	14.57	15.12	2004	2/22/2004	1,330	2011	2/9/2011	1,997	12096500	0.020	0.62	3.0	6.2
	15.19	16.74	2004	2/21/2004	501	2011	12/4/2010	669	12093500	0.025	0.27	1.8	3.9
	16.77	18.32	2004	2/22/2004	501	2011	2/9/2011	862	12093500	0.025	0.52	2.1	4.6
	18.35	19.38	2004	2/14/2004	514	2011	2/9/2011	862	12093500	0.025	0.54	1.7	5.3
	19.41	19.63	2004	2/14/2004	514	2011	2/9/2011	862	12093500	0.030	0.54	1.6	4.9
Puyallup River, 2011 to 2020	19.66	21.17	2004	2/22/2004	484	2011	2/9/2011	862	12093500	0.030	0.48	1.3	4.6
	21.20	24.41	2004	2/14/2004	475	2011	2/9/2011	862	12093500	0.030	0.59	1.5	5.3
	24.43	26.42	2004	3/8/2004	483	2011	2/9/2011	862	12093500	0.030	0.58	1.4	5.4
	4.02	4.80	2020	4/10/2020	2,235	2011	12/6/2010	2,809	12101500	0.020	0.36	3.1	3.7
	4.83	4.98	2020	4/10/2020	2,235	2011	12/5/2010	2,993	12101500	0.020	0.37	3.7	3.0
	5.01	6.83	2020	4/13/2020	2,217	2011	12/5/2010	2,993	12101500	0.020	0.52	3.9	3.4
	6.86	9.08	2020	4/13/2020	2,217	2011	12/4/2010	3,354	12101500	0.020	0.71	3.9	4.0
	9.11	10.35	2020	4/13/2020	1,156	2011	12/4/2010	1,769	12096500	0.020	0.53	2.9	4.3
	10.37	15.13	2020	4/13/2020	1,156	2011	2/9/2011	1,997	12096500	0.020	0.72	2.8	4.5
	15.17	16.74	2020	4/13/2020	471	2011	12/4/2010	669	12093500	0.025	0.38	2.1	4.2
	16.77	19.37	2020	4/13/2020	471	2011	2/9/2011	862	12093500	0.025	0.52	1.8	4.1
	19.40	26.56	2020	4/13/2020	471	2011	2/9/2011	862	12093500	0.030	0.56	1.4	4.8
Carbon River, 2004 to 2011	0.13	3.08	2004	2/22/2004	454	2011	2/9/2011	812	12094000 + 12095000	0.025	0.54	1.9	4.4
	3.11	5.38	2004	2/20/2004	454	2011	2/9/2011	812	12094000 + 12095000	0.030	0.52	1.5	4.6
	5.41	6.00	2004	2/20/2004	247	2011	2/9/2011	465	12094000	0.030	0.43	1.0	4.3
	6.04	7.78	2004	2/12/2004	247	2011	2/10/2011	433	12094000	0.030	0.36	1.0	4.4
	7.81	10.39	2004	2/12/2004	247	2011	4/29/2011	339	12094000	0.030	0.22	1.1	4.6
Carbon River, 2011 to 2020	0.09	3.07	2020	4/13/2020	422	2011	2/9/2011	812	12094000 + 12095000	0.025	0.54	1.6	3.7
	3.09	5.39	2020	4/13/2020	422	2011	2/9/2011	812	12094000 + 12095000	0.030	0.53	1.4	4.1
	5.43	6.03	2020	4/13/2020	267	2011	2/9/2011	465	12094000	0.030	0.43	1.2	4.3
	6.06	7.80	2020	4/13/2020	267	2011	2/10/2011	433	12094000	0.030	0.32	1.1	4.4
	7.83	9.94	2020	4/13/2020	267	2011	4/29/2011	339	12094000	0.030	0.17	1.1	4.5

Table 5. Calibration of Manning's coefficient of roughness (n) based on observed changes in stage at USGS streamgages (U.S. Geological Survey, 2025). [ft – feet; s – second]

USGS site number	Lidar reference year	Initial discharge, ft ³ /s	Target discharge, ft ³ /s	Observed stage difference, ft	Modeled stage difference, ft (n value)	As used	lower n	higher n
12101500	2004	2,230	2,993	0.69	0.65 (0.020)	0.54 (0.015)	0.75 (0.025)	
12101500	2020	2,217	2,993	0.71	0.63 (0.020)	0.53 (0.015)	0.70 (0.025)	
12101470	2020	2,217	3,354	0.98	0.84 (0.020)	0.69 (0.015)	0.95 (0.025)	
12096505	2020	1,156	1,769	0.92	0.95 (0.020)	1.14 (0.015)	0.94 (0.025)	
12096500	2020	1,156	1,997	0.65	0.61 (0.020)	0.56 (0.015)	0.65 (0.025)	
12093500	2020	471	862	0.48	0.50 (0.030)	0.50 (0.025)	0.45 (0.035)	
12093500	2004	475	862	0.63	0.62 (0.030)	0.64 (0.025)	0.63 (0.035)	

Quantifying Mean Elevation and Volumetric Channel Change

After correcting for horizontal, vertical, and discharge-related offsets, final DoDs were created (Anderson, 2025). Analysis extents for change analysis were manually delineated to encompass all change inferred to be the result of fluvial or mass wasting processes, based on spatial patterns and magnitude of change and local setting context. Human-caused changes where material was either removed or added to the river corridor, such as manual levee modifications or excavation of side channels, were excluded from the analysis.

Change estimated from the DoDs was summarized in regular 820-ft lengths along the valley centerline. Gross erosion (sum of all DoDs grid cells with negative change) and gross deposition (sum of all DoD grid cells with positive) were calculated after applying a uniform

threshold of ± 0.50 ft, reducing positive bias introduced by random errors in areas of little or no change (Wheaton and others, 2010). The uniform threshold of 0.50 ft was defined based on assessments of representative scales of local random errors observed across the various DoDs. Net change (the sum of all DoD grid cells) was estimated based on DoDs without the application of a threshold, as random errors do not introduce bias into estimates of net change (Anderson, 2019).

In the Puyallup River, change was further sub-divided between change occurring within the floodway, where deposition would tend to reduce flood conveyance, and change occurring in overbank areas, where deposition would not reduce that conveyance. ‘Floodway’ is used here to denote the area bounded by natural banks or levees through which high flows are intended to pass without causing structural damage. The floodway was manually defined based on the locations of levee crests or natural banks and bluffs and is not identical to the ‘regulatory floodway’ defined by the Federal Emergency Management Agency (FEMA; 44 CFR § 59.1). Because bank erosion and levee modifications altered the floodway extents over time, unique floodway extents were delineated in each lidar survey. For a given differencing interval, the union of the floodway extents from the two differenced surveys was used to define the ‘floodway’ area of interest.

In the Carbon River, change was sub-divided between areas impacted by bluff dynamics, encompassing both erosion of prominent glacial bluffs and associated proximal downslope deposition, and all other fluvially caused change. The two distinct partitioning schemes used for the two river systems are based on differences in the key relevant geomorphic processes observed in the two systems.

Uncertainty in mean elevation change estimates were calculated assuming a spatially uniform systematic error of ± 0.16 ft, taken to represent 95-percent confidence intervals (Anderson, 2019). This value is based on prior uncertainty assessments using similar datasets in similar river systems (Anderson, 2019; Anderson and others, 2019; Anderson and Jaeger, 2021), and represents potential mean errors over reach scales. Because the error is modeled as a spatially uniform vertical offset, uncertainties around volumetric change estimates are obtained by multiplying ± 0.16 ft by the area of analysis. The final raster DoDs and tabular summaries of change described here are available in a USGS data release (Anderson, 2025).

Assessing Changes in Floodway Cross-Sectional Area

A key goal of levee setbacks is to increase local flood conveyance via an increase in the cross-sectional area of the floodway (Smith and others, 2017). Conversely, sediment deposition within the floodway would tend to reduce cross-sectional area and, by extension, flood conveyance. Consequently, the lidar datasets were used to assess floodway cross-sectional areas over time for the lower Puyallup River, which provides a measure of the relative magnitude of those two offsetting processes.

Changes in floodway cross-sectional area are an imperfect proxy for flood conveyance changes, since it does not account for changes in roughness or local flow depth. However, changes in the mean elevation of the floodway have tended to result in similar changes in water surface elevations at high flows (Sikonia, 1990; Czuba and others, 2010), supporting the use of mean changes in cross section geometry alone as a rough guide to conveyance changes. This analysis was only done for the Puyallup River, where there were multiple setback projects and more concern regarding sediment deposition (Figure 1; Czuba and others, 2010).

The floodway cross-sectional area was defined as the area bounded by the lidar surface and the minimum local bank height. ‘Banks’ here correspond to the floodway boundaries defined earlier. This cross-sectional area is incomplete, because it does not include the areas below the water surface elevation at the time of the lidar surveys. However, because the cross-sectional area of those low-flow channels are generally a small fraction of total floodway cross-sectional area, and because the discharge-normalization process used to correct the various DEMs should result in a similar effective volume of water storage in those channels in each survey, this missing area should not substantially impact assessments of relative change over time.

For all recent levee setback projects in the lower Puyallup River, the first post-project lidar data collection occurred five to six years after project completion. As a result, estimated changes in floodway cross-sectional area over the project completion intervals represent a combination of project-related changes in bank location and sediment erosion and deposition that occurred both before and after that project. In order to both better capture the initial cross-sectional area at the time of project completion, and to provide a more intuitive impression of changes in cross-sectional area over time, an attempt was made to separate out direct project-related impacts from progressive fluvial change.

Separating out the direct impacts of changing levee positions from fluvial processes was accomplished based on the erosion and deposition volumes observed in the repeat lidar. The observed net erosion or deposition was partitioned into pre-project and post-project volumes based on estimates of the relative amount of sediment transport that occurred in the two periods. For example, if there was net deposition of 10,000 yd³ over the full repeat lidar interval, and transport calculations indicate that 20 percent of total sediment transport over that time interval occurred before the setback project completion date and 80 percent occurred after, it was

assumed that 2,000 yd^3 deposited prior to the project and 8,000 yd^3 were deposited after. Sediment transport rates were estimated based on discharge records and limited sediment transport data collected at the Puyallup River near Orting and the Puyallup River at Orting; refer to appendix C for details of sediment transport estimates.

Once partitioned between the two periods, net volumetric changes were divided by the valley length of the relevant setback project to get change in yd^3/yd , which equates to a change in average cross-sectional area. The estimated ‘pre-project’ area change was then added to cross-sectional area calculated in the lidar dataset preceding the setback project, resulting in an estimate of cross-sectional area just prior to the start of the levee setback project. The ‘post-project’ area change was then subtracted from cross-sectional area calculated from the first lidar data postdating the setback project, resulting in an estimate of the cross-sectional area just after project completion. The difference between those two extrapolated values represents an estimate of the quasi-instantaneous change in floodway cross-sectional area resulting from the levee setback project itself.

Observed Channel Change in the Lower Puyallup River, 2004–20

Sediment storage changes along the lower Puyallup River (VM 4-26) showed consistent spatial patterns over the 2004–11 and 2011–20 intervals, with net erosion upstream of approximately VM 20 and net deposition downstream (Figure 7–9, Table 6). The transition between erosion and deposition was relatively abrupt. From 2004 to 2020, a total of $540,000 \pm 150,000 \text{ yd}^3$ of sediment was eroded over the six miles upstream of VM 20 and $1,330,000 \pm 200,000 \text{ yd}^3$ was deposited downstream of VM 20. This amounted to a decrease in mean elevation of about $0.52 \pm 0.16 \text{ ft}$ upstream of VM 20 and an increase in mean elevation of $1.06 \pm 0.16 \text{ ft}$ downstream of VM 20.

Substantial overbank deposition was only observed over the 2004–11 interval, primarily downstream of VM 17 (Figure 7). Overbank deposition accounted for approximately 30 percent of total 2004–20 deposition downstream of VM 20 (Table 6). The remaining 70 percent of deposited material accumulated within the floodway.

Table 6. Volumetric and mean elevation change in the lower Puyallup River watershed based on repeat aerial lidar, 2004–2020. For total change: Blue – significant net erosion; Red – significant net deposition; Black – indeterminant. [D/S - downstream; ft - feet; U/S - upstream; V/M - valley mile; yd - yards; yr - year]

Reach description	U/S VM	D/S VM	Zone	2004 to 2011			2011 to 2020		
				Volume, yd ³	Rate, yd ³ /yr	mean, ft	Volume, yd ³	Rate, yd ³ /yr	mean, ft
Mountain front to onset of deposition	26.56 (26.74)*	20.05 (19.27)	Floodway	-400,000 ± 139,000	-57,400 ± 20,000	-0.47 ± 0.16	-171,100 ± 144,000	-18,600 ± 15,700	-0.19 ± 0.16
			Overbank	20,400 ± 11,400	2,900 ± 1,600	0.3 ± 0.16	7,200 ± 7,100	800 ± 800	0.17 ± 0.16
			Total	-380,000 ± 151,000	-54,500 ± 21,600	-0.41 ± 0.16	-163,800 ± 151,100	-17,800 ± 16,500	-0.18 ± 0.16
Onset of deposition to Carbon River	20.04 (19.26)	15.23	Floodway	282,000 ± 58,000	40,700 ± 8,400	0.79 ± 0.16	252,200 ± 48,800	27,200 ± 5,200	0.85 ± 0.16
			Overbank	121,000 ± 15,000	17,700 ± 2,200	1.3 ± 0.16	1,300 ± 400	100 ± 0	0.66 ± 0.16
			Total	403,000 ± 74,000	58,300 ± 10,600	0.9 ± 0.16	253,500 ± 49,000	27,300 ± 5,400	0.85 ± 0.16
Carbon River to Fennel Creek	15.22	13.68	Floodway	156,000 ± 16,000	22,400 ± 2,400	1.58 ± 0.16	43,800 ± 16,400	4,700 ± 1,800	0.44 ± 0.16
			Overbank	57,000 ± 9,000	8,200 ± 1,300	1.04 ± 0.16	0 ± 0	0 ± 0	0.09 ± 0.16
			Total	214,000 ± 25,000	30,600 ± 3,700	1.38 ± 0.16	43,800 ± 16,500	4,700 ± 1,800	0.44 ± 0.16
Fennel Creek To White River	13.67	9.17	Floodway	57,000 ± 37,000	8,200 ± 5,400	0.25 ± 0.16	81,200 ± 38,300	8,800 ± 4,200	0.35 ± 0.16
			Overbank	179,000 ± 24,000	25,800 ± 3,500	1.21 ± 0.16	1,700 ± 1,400	100 ± 100	0.18 ± 0.16
			Total	236,000 ± 62,000	34,000 ± 8,900	0.63 ± 0.16	82,800 ± 39,800	9,000 ± 4,300	0.34 ± 0.16
D/S of White River	9.16	4.36	Floodway	26,000 ± 32,000	3,900 ± 4,700	0.13 ± 0.16	71,500 ± 38,300	7,600 ± 4,100	0.31 ± 0.16
			Overbank	400 ± 100	0 ± 0	0.78 ± 0.16	0 ± 0	0 ± 0	-0.19 ± 0.16
			Total	27,000 ± 32,000	3,900 ± 4,700	0.14 ± 0.16	71,500 ± 38,500	7,600 ± 4,100	0.31 ± 0.16

*Reach extents differed between 2004–11 and 2011–20 differencing; top valley mile values are for 2004–11, values in parentheses are for 2011–20

During 2004–11, almost all floodway deposition occurred between VM 20 and VM 13.5, with particularly high deposition rates along the Soldiers Home levee setback reach (~VM 19) and just downstream of the Carbon River confluence (VM 15 to 13.5; Figure 7). Floodway deposition rates then dropped abruptly near VM 13.5 to essentially zero, with little to no net deposition occurring downstream of VM 13.5.

During 2011-20, most floodway deposition occurred between VM 15 and 19. While deposition rates then dropped abruptly downstream of the Carbon River confluence (VM 15), they remained non-zero, and about 35 percent of all 2011–20 floodway deposition occurred downstream of the Carbon River confluence (Figure 7).

Upstream of VM 20, erosion rates were nearly three times higher from 2004 to 2011 ($-55,000 \pm 22,000 \text{ yd}^3/\text{yr}$) than from 2011 to 2020 ($-18,000 \pm 16,500 \text{ yd}^3/\text{yr}$). Over both intervals, net erosion was the result of lateral bank erosion exceeding deposition across lower bare-gravel surfaces, as opposed to uniform downcutting across the entire active channel (Figure 9). Erosion of remnant levee structures totaled $-17,500 \pm 3,500 \text{ yd}^3/\text{yr}$ during 2004–11, representing about 30 percent of all 2004–20 erosion that occurred upstream of VM 20. No substantial erosion of remnant levee structures was observed during 2011–20.

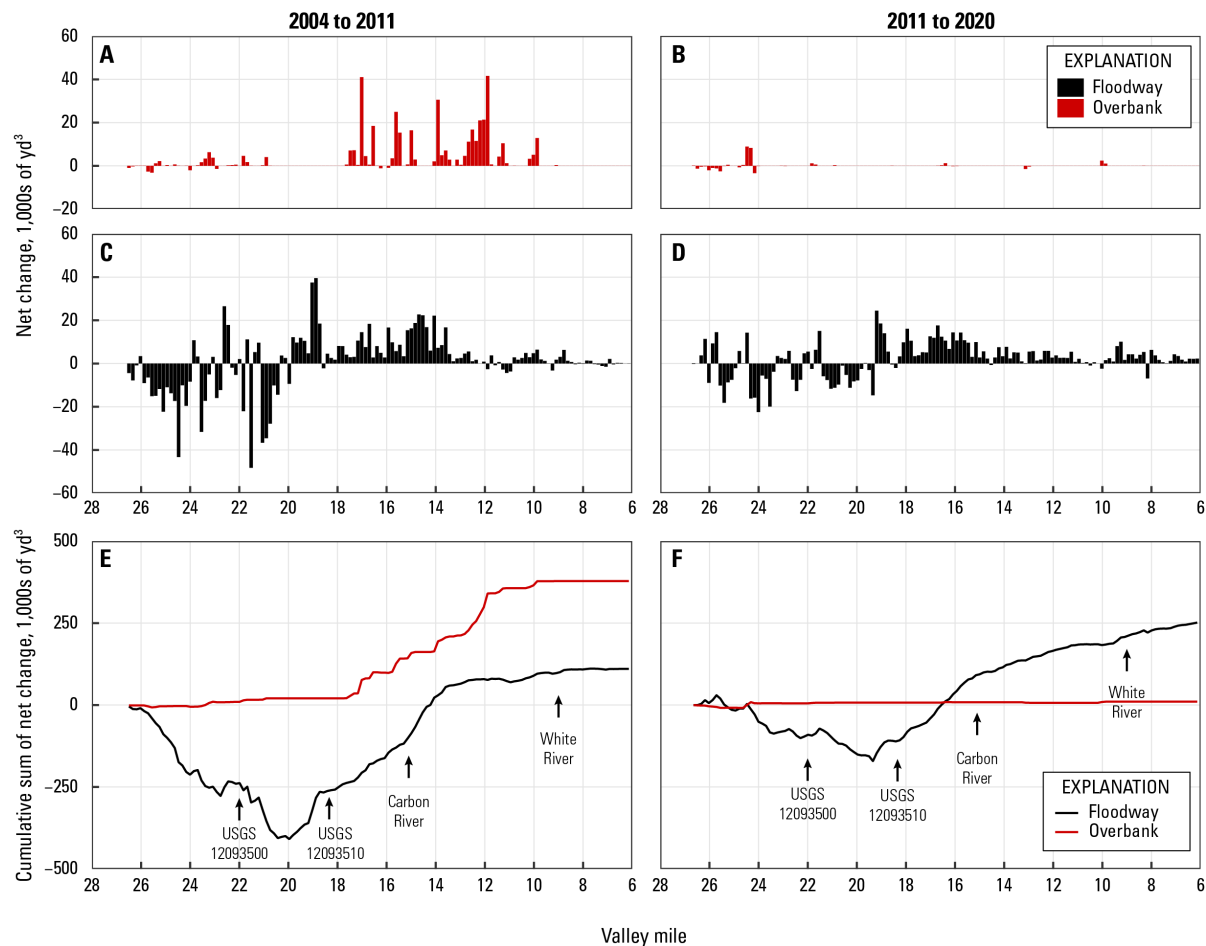


Figure 7. Summary of volumetric change on the Puyallup River, showing local net volumetric change in the overbank area from (A) 2004 to 2011 and (B) 2011 to 2020; in the floodway from (C) 2004 to 2011 and (D) 2011 to 2020; and the cumulative sum, moving downstream, of volumes from both areas from (E) 2004 to 2011 and (F) 2011 to 2020. Plots are oriented with upstream to the left.

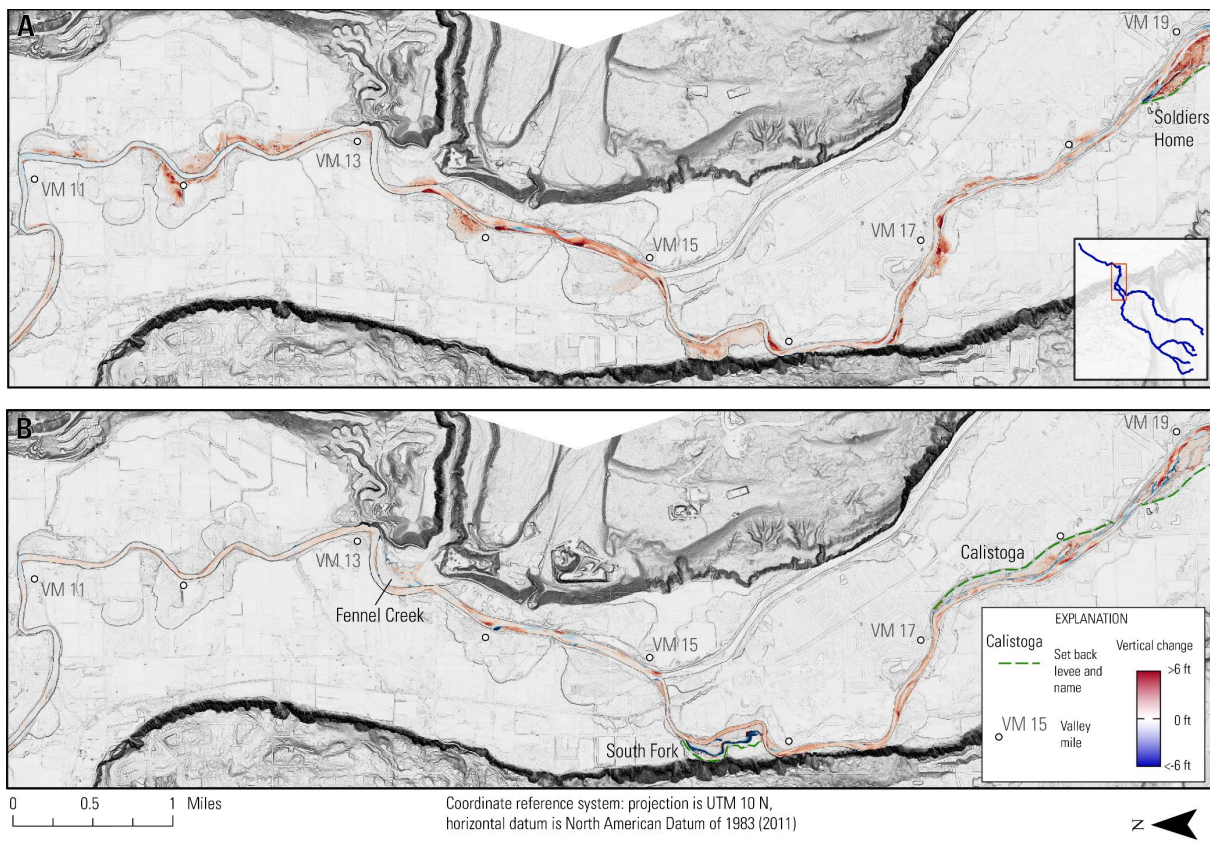


Figure 8. Change in elevation in the Puyallup River between valley mile (VM) 11 and 19 from (A) 2004 to 2011 and (B) 2011 to 2020, based on differencing of aerial lidar. Positive values (red) represent deposition; negative values (blue) represent erosion. Inset in A shows figure extents overlain on study area streamlines. Basemaps derived from 2011 (A) and 2020 (B) aerial lidar provided by the Washington Geological Survey (2011; 2020).

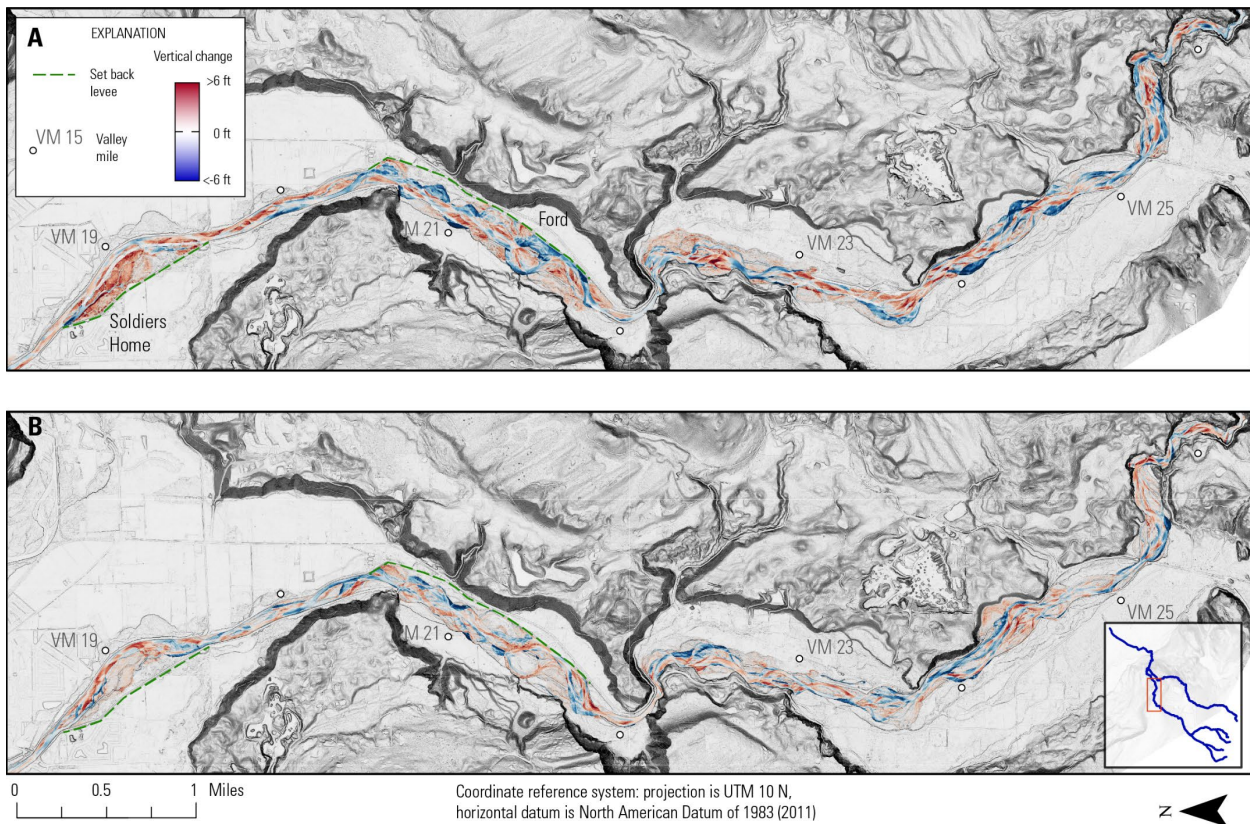


Figure 9. Change in elevation in the Puyallup River between valley mile (VM) 19 and 26 from (A) 2004 to 2011 and (B) 2011 to 2020, based on differencing of aerial lidar. Positive values (red) represent deposition; negative values (blue) represent erosion. Inset in B shows figure extents overlain on study area streamlines. Basemaps derived from 2011 (A) and 2020 (B) aerial lidar provided by the Washington Geological Survey (2011; 2020).

Rates of Change Along Levee Setback Projects

From 2004 to 2011, floodway deposition rates (cubic yards per mile per year, $yd^3/mi/yr$) along the Soldiers Home levee setback project were over four times higher than adjacent reaches with no levee modifications (Figure 10A). Most deposition in the Soldiers Home levee setback reach occurred across a large, river-left forested surface that was reconnected to the main channel as a result of the setback project (refer to Figure 9A, near VM 19). However, because the

setback project also substantially increased the width of the floodway relative to adjacent leveed reaches, and so the total area over which sediment could deposition, the mean elevation change across the Soldiers Home levee setback reach was similar to adjacent unmodified reaches (Figure 10B).

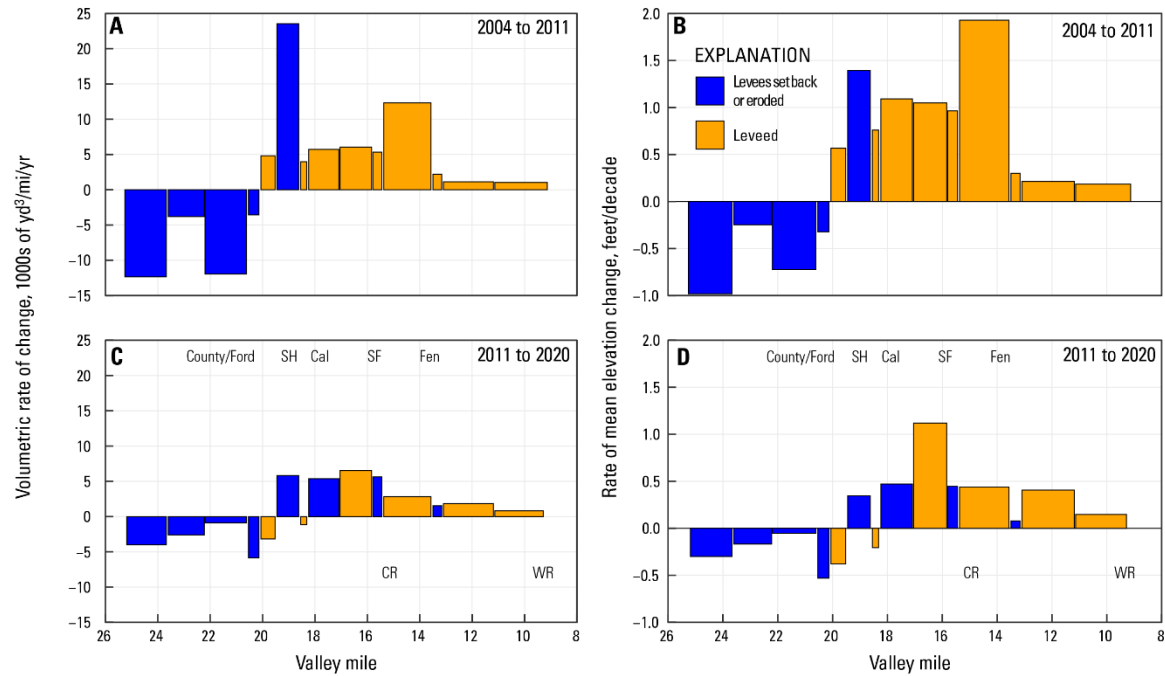


Figure 10. Reach-average volumetric rate of change (A) and rate of mean elevation changes (B) along the lower Puyallup River, from 2004 to 2011. (C) and (D) are the same for the 2011–20 interval. Reaches were defined by the extents of different levee setback projects, with additional breaks placed at locations of significant change in rates or direction of volumetric change or major changes in valley character. Mean elevation changes were calculated using the full bank-to-bank extents as the area basis, as opposed to just areas experiencing detectable geomorphic change. SH – Soldiers Home; Cal – Calistoga; SF – South Fork; Fen; Fennel Creek; CR – Carbon River confluence; WR – White River confluence.

By 2014, three additional levee setback projects were completed in the Puyallup River downstream of VM 20 (Table 1). From 2011 to 2020, floodway deposition rates in the four

setback project reaches downstream of VM 20 were generally comparable to deposition rates in adjacent unmodified reaches (Figure 10C), though results for the Soldiers Home setback were somewhat ambiguous. While 2011-20 deposition rates for the Soldiers Home setback reach were similar to those in both setback and leveed reaches between VM 18 and 15, net erosion was observed in the sub-reaches immediately upstream and downstream. However, the sub-reach just downstream of the Soldiers Home levee setback reach is only 200 yds long, while the upstream sub-reach is part of the spatially coherent net erosion observed between VM 20 and 26; it is unclear whether these represent valid comparison reaches. Mean elevation changes over the 2011–20 interval were generally lower in setback reaches than the leveed reaches, again due to the increased floodway width created by those setback projects (Figure 10D).

Upstream of VM 20, a nearly continuous system of narrow, straight levees was progressively eroded away during major floods of the 1990s and early 2000s (Figure 2). Sediment storage trends over those reaches have been consistently negative since 2004 (Figure 7, Figure 10).

Changes in Floodway Cross-sectional Area

Downstream of VM 20, changes in floodway cross-sectional area over time show the local increases associated with setback projects amid a general decreasing trend associated with sediment deposition (Figure 11A). Results are primarily presented in terms of relative or fractional change in values since 2004, providing a measure that can be roughly interpreted as relative change in bankfull flood conveyance. In relative terms, loss of cross-sectional area due to deposition was most substantial in the narrow reaches near VM 17 and in the reaches just downstream of the Carbon River confluence (VM 15; Figure 11).

In the Soldiers Home levee setback reach, initial construction in 2006 increased the average floodway cross-sectional area to 2.8 times the area of the 2004 river corridor (Figure 12A). Deposition through 2020 then reduced that cross-sectional area to about 2.3 times larger than 2004 conditions. Simple linear extrapolation of average deposition rates since 2006 implies that the mean cross-sectional area would return to 2004 values in about 2050; this extends to 2090 if the lower 2011-20 deposition rates are used for extrapolation.

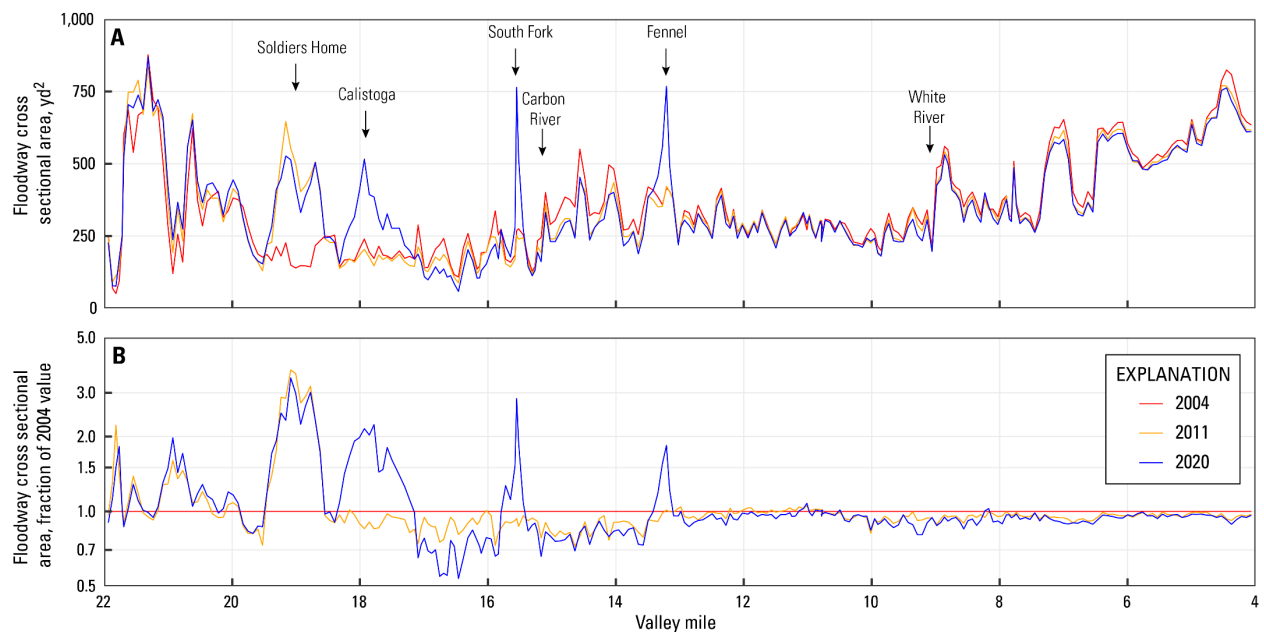


Figure 11. Changes in floodway cross-sectional area between 2004 and 2020 of the Puyallup River, WA, with A) absolute values and B) values as a fraction of 2004 conditions, log-scale. Annotations in (A) indicate locations of the levee setback projects and major river confluences. [yd^2 , square yards]

The initial increases in mean cross-sectional area associated with the Calistoga and South Fork levee setback projects were relatively smaller (~60–70 percent above 2004 values; Figure 12) and, for both projects, extrapolation of recent deposition rates would imply a return to 2004 cross-sectional areas around 2055-60. Similar calculations were not done for the Fennel Creek

project, which involved relatively minor notching of levees and some modification to floodplain topography to reduce fish stranding.

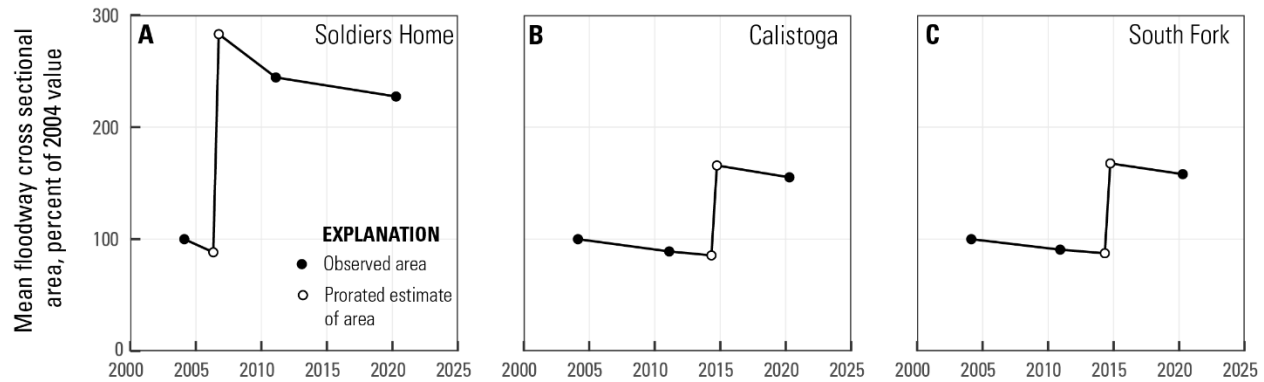


Figure 12. Changes in mean floodway cross-sectional area averaged over recent levee setback projects completed in the lower Puyallup River, WA, including A) the Soldiers Home levee setback; B) the Calistoga levee setback; and C) the South Fork levee setback (Figure 1, Table 2).

Observed Channel Change in the Lower Carbon River, 2004–20

From 2004 to 2020, the most prominent geomorphic change along the Carbon River was erosion of the 300-ft high glacial bluffs located on river-right between VM 6.8 and 8 (Figure 13–15, Figure 14, Figure 15 Table 7). In total, $550,000 \pm 9,000 \text{ yd}^3$ were eroded from these bluffs, with three quarters of that erosion occurring between 2004 and 2011. Net erosion of the active channel between VM 6.5 and 9.3 also acted as a net sediment source over both differencing intervals, supplying $180,000 \pm 45,000 \text{ yd}^3$ from 2004 to 2020. Minor bluff erosion downstream of VM 6.5 supplied an additional $50,000 \pm 1,000 \text{ yd}^3$ of material over the 2004–20 study interval.

Downstream of VM 6.5, sediment storage changes within the active channel were variable in space and time (Figure 13; Table 7). From 2004 to 2011, $200,000 \pm 65,000 \text{ yd}^3$ were deposited between VM 3.5 and 6.5, while net change downstream of VM 3.5 was close to 0.

From 2011 to 2020, $130,000 \pm 70,000 \text{ yd}^3$ were eroded between VM 2.6 and 6.5, removing about two-thirds of the volume that accumulated in the prior period. There was then net deposition of $80,000 \pm 20,000 \text{ yd}^3$ between VM 0 and 2.6. Qualitatively, these changes downstream of VM 6.5 can be interpreted as an initial deposition of sediment in the upper half of the reach, which was partially remobilized to either the lower half of the reach or out into the Puyallup River.

Table 7. Volumetric and mean elevation change on Carbon River reaches based on repeat aerial lidar, 2004-20. For total change: Blue – significant net erosion; Red – significant net deposition; Black – indeterminant. [D/S - downstream; ft - feet; U/S - upstream; V/M - valley mile; yd - yards; yr - year]

Reach description	U/S VM	D/S VM	Zone	2004 to 2011			2011 to 2020		
				Volume, yd^3	Rate, yd^3/yr	mean, ft	Volume, yd^3	Rate, yd^3/yr	mean, ft
Ski park bluff	9.31	6.53	Bluff	$-412,200 \pm 4,700$	$-58,700 \pm 700$	-14.21 ± 0.16	$-141,400 \pm 2,700$	$-15,400 \pm 300$	-8.37 ± 0.16
			Channel	$-114,400 \pm 36,600$	$-16,000 \pm 5,100$	-0.51 ± 0.16	$-64,700 \pm 35,100$	$-7,100 \pm 3,800$	-0.30 ± 0.16
			Total	$-526,600 \pm 41,300$	$-74,700 \pm 5,900$	-2.09 ± 0.16	$-206,100 \pm 37,800$	$-22,500 \pm 4,200$	-0.90 ± 0.16
Middle Carbon River	6.52	3.58 (2.65)*	Bluff	$-16,600 \pm 400$	$-2,400 \pm 0$	-7.78 ± 0.16	$-24,300 \pm 700$	$-2,600 \pm 100$	-6.37 ± 0.16
			Channel	$199,100 \pm 65,500$	$28,500 \pm 9,400$	0.5 ± 0.16	$-128,600 \pm 70,600$	$-14,000 \pm 7,700$	-0.30 ± 0.16
			Total	$182,300 \pm 65,900$	$26,200 \pm 9,400$	0.45 ± 0.16	$-152,900 \pm 71,300$	$-16,600 \pm 7,700$	-0.35 ± 0.16
Lower Carbon River	3.57 (2.64)*	0.00	Bluff	0 ± 0	0 ± 0	0 ± 0.16	$-9,800 \pm 100$	$-1,000 \pm 0$	-15.85 ± 0.16
			Channel	$4,100 \pm 38,300$	$700 \pm 5,500$	0.02 ± 0.16	$77,400 \pm 19,900$	$8,400 \pm 2,200$	0.64 ± 0.16
			Total	$4,100 \pm 38,300$	$700 \pm 5,500$	0.02 ± 0.16	$67,600 \pm 20,000$	$7,300 \pm 2,200$	0.55 ± 0.16

*Reach extents differed between 2004-11 and 2011-20 differencing; top valley mile values are for 2004-11, values in parentheses are for 2011-20

Integrated from 2004 to 2020, there was net deposition of sediment in most reaches of the Carbon River downstream of VM 6.5, totaling $150,000 \pm 100,000 \text{ yd}^3$. This amounted to a mean elevation increase of $0.24 \pm 0.16 \text{ ft}$ over those 6.5 miles. Deposition downstream of VM 6.5 accounted for about 15-20 percent of the $780,000 \pm 60,000 \text{ yd}^3$ eroded from bluffs and active channel surfaces along the Carbon River between VM 6.5 and 9.3. The remaining $630,000 \pm 150,000 \text{ yd}^3$ was exported downstream to the Puyallup River.

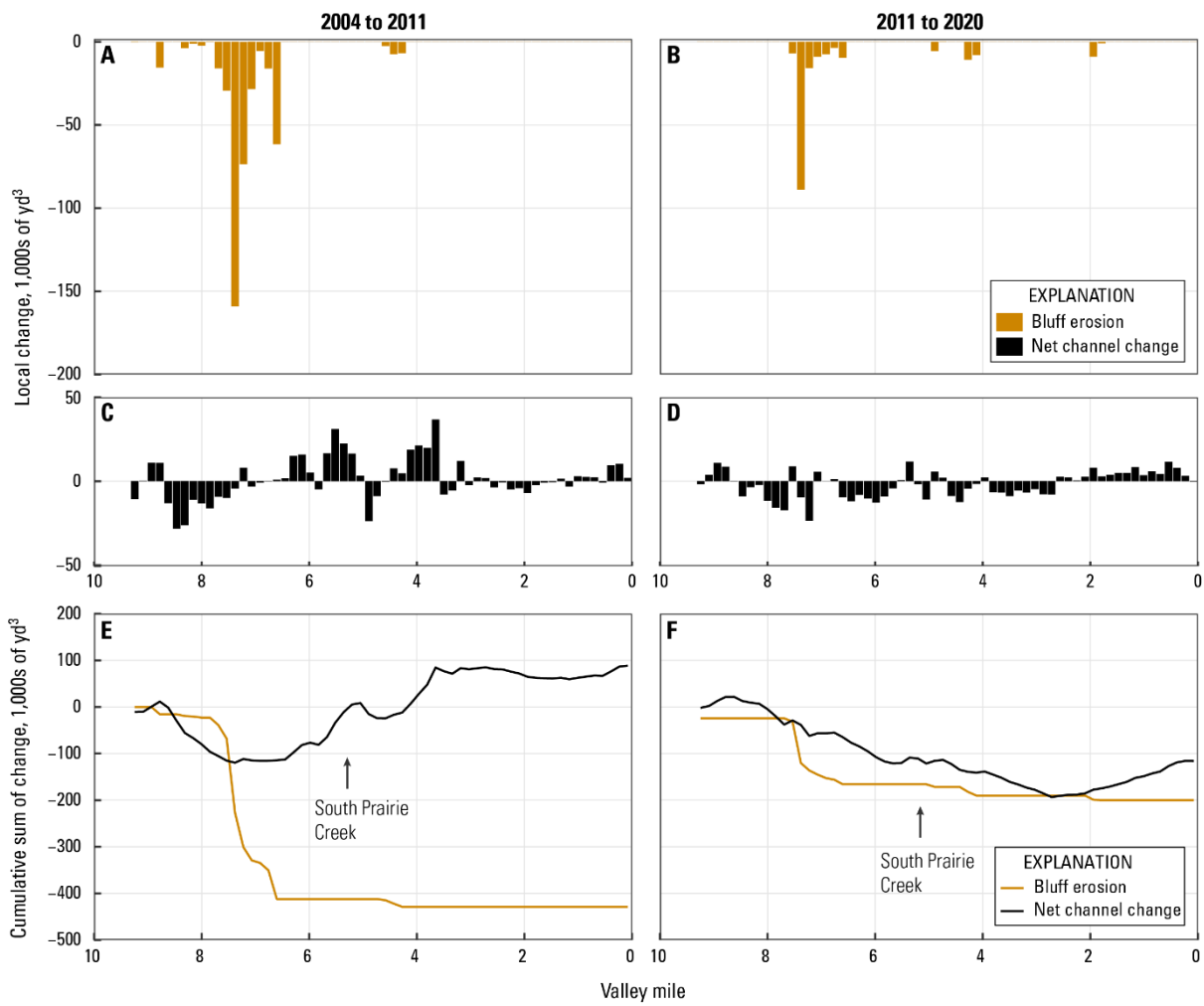


Figure 13. Summary of volumetric change on the Carbon River, showing bluff erosion volumes from (A) 2004 to 2011 and (B) 2011 to 2020; net channel change, excluding bluff erosion, from (C) 2004 to 2011 and (D) 2011 to 2020; and the cumulative sum, moving downstream, of those volumes from (E) 2004 to 2011 and (F) 2011 to 2020. Valley miles are plotted from upstream (VM 10) to downstream (VM 0).

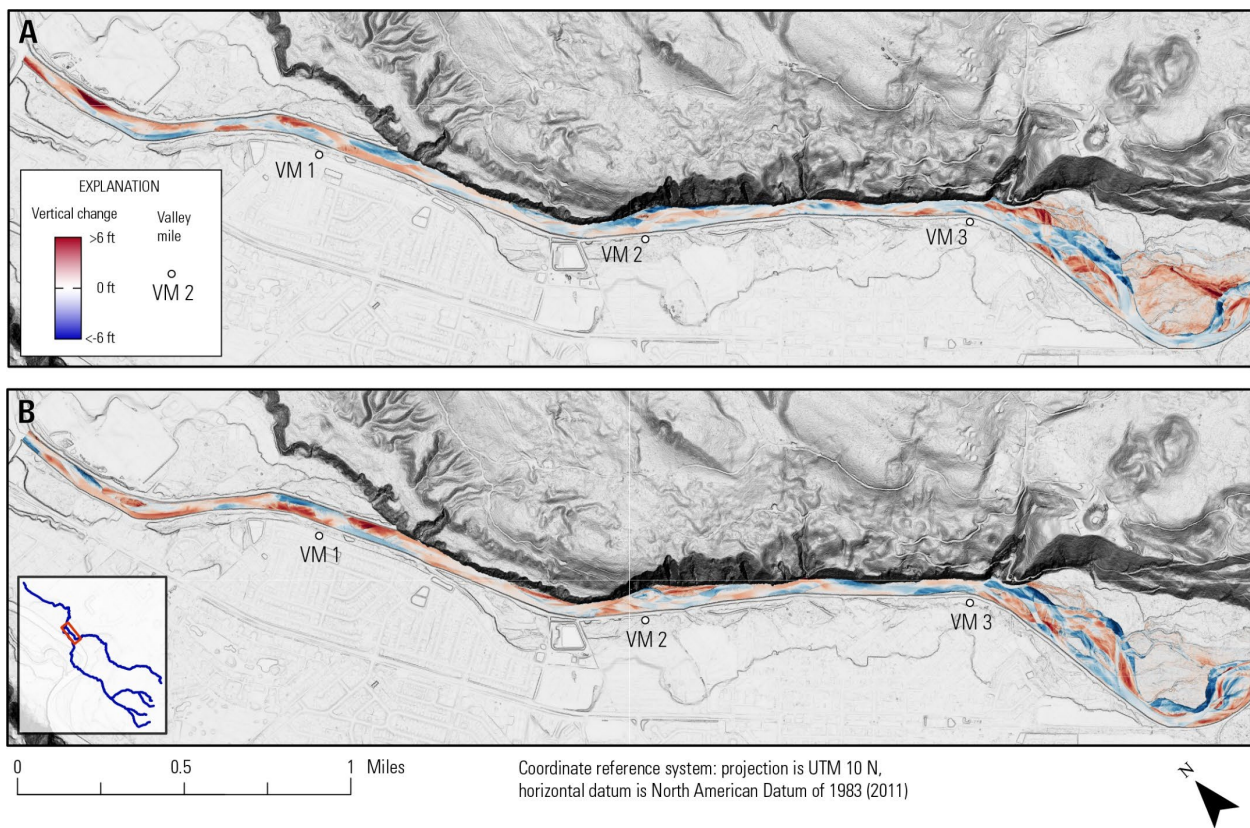


Figure 14. Change in elevation in the Carbon River based on differencing of aerial lidar between valley mile (VM) 0 and 4 from (A) 2004 to 2011 and (B) 2011 to 2020. Positive values (red) represent deposition; negative values (blue) represent erosion. Inset in B shows figure extents overlain on study area streamlines. Basemaps derived from 2011 (A) and 2020 (B) aerial lidar provided by the Washington Geological Survey (2011; 2020).

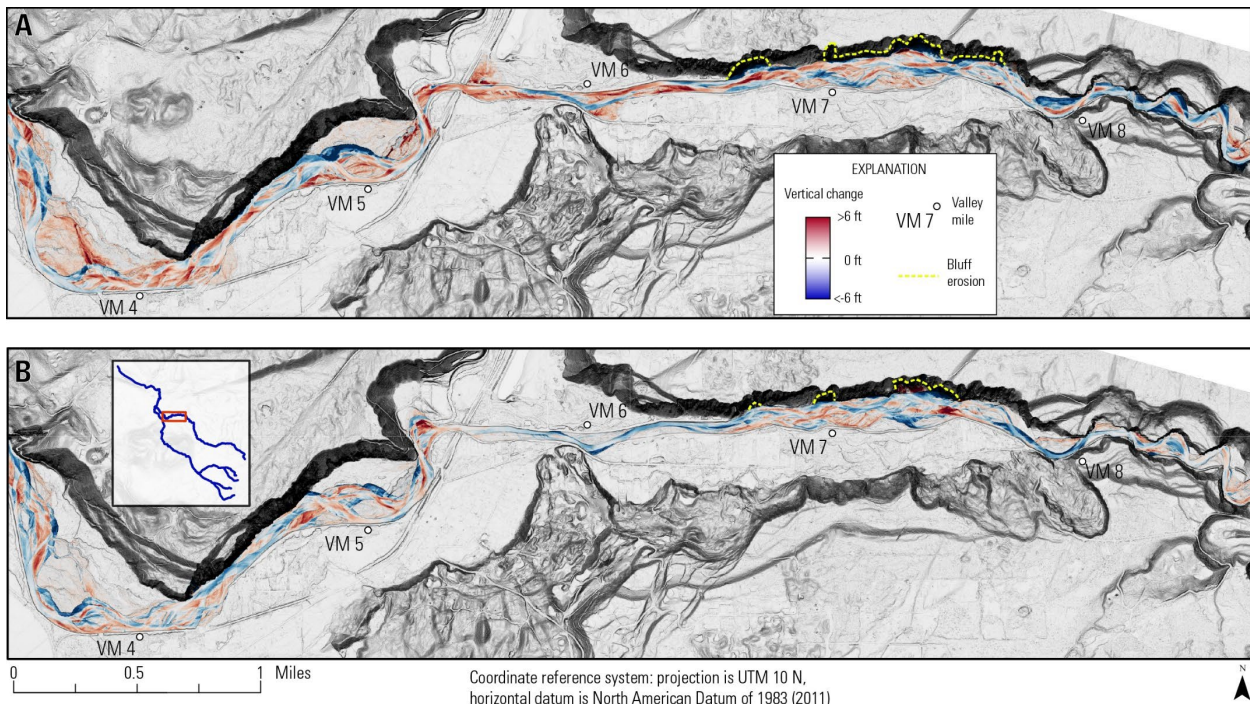


Figure 15. Change in elevation in the Carbon River based on differencing of aerial lidar between valley mile (VM) 3 and 8.5 from (A) 2004 to 2011 and (B) 2011 to 2020. Positive values (red) represent deposition; negative values (blue) represent erosion. Inset in B shows figure extents overlain on study area streamlines. The upslope extents of bluff erosion are shown with blue dashed lines for better visibility. Basemaps derived from 2011 (A) and 2020 (B) aerial lidar provided by the Washington Geological Survey (2011; 2020).

Biases in 1984–2009 Repeat Cross Section Analyses

Czuba and others (2010) reported that from 1984 to 2009, the Puyallup River from VM 19 to 22 aggraded between 3 and 8 feet. This represented some of the most substantial aggradation observed across the lower Puyallup River watershed. This zone of aggradation overlapped with all major levee modifications at the time of that report, including the Soldiers Home levee setback, the Ford levee setback and the washout of the County levee system (Table

1). Consequently, Czuba and others (2010) concluded that the loss of levee confinement, by allowing flow to spread and slow, likely increased deposition. However, a review of the 1984–2009 cross section data conducted as part of this study, indicated that published 1984–2009 channel change estimates between VM 19 and 22 were likely biased high by a methodologic issue.

Survey data from 1984 typically only covered the 250–300 ft between levees that existed at that time, and did not cover the full extent of the 2009 active channel (Figure 16). At a given section, Czuba and others (2010) addressed this mismatch either by calculating mean elevations over different lateral extents in different survey years or sub-setting the 2009 data to a width similar to that of the 1984 survey. Both approaches effectively omit change that occurred beyond the limits of the 1984 survey and do not provide a valid estimate of the true mean elevation change across the active channel. Between VM 19 and 22, the areas omitted from comparison were almost exclusively vegetated surfaces in 1984 that were transformed into bare gravel or wetted channel areas through bank erosion, and so areas where local elevation change would tend to be negative. Systematically omitting this bank erosion would then tend to bias local mean elevation change estimates high.

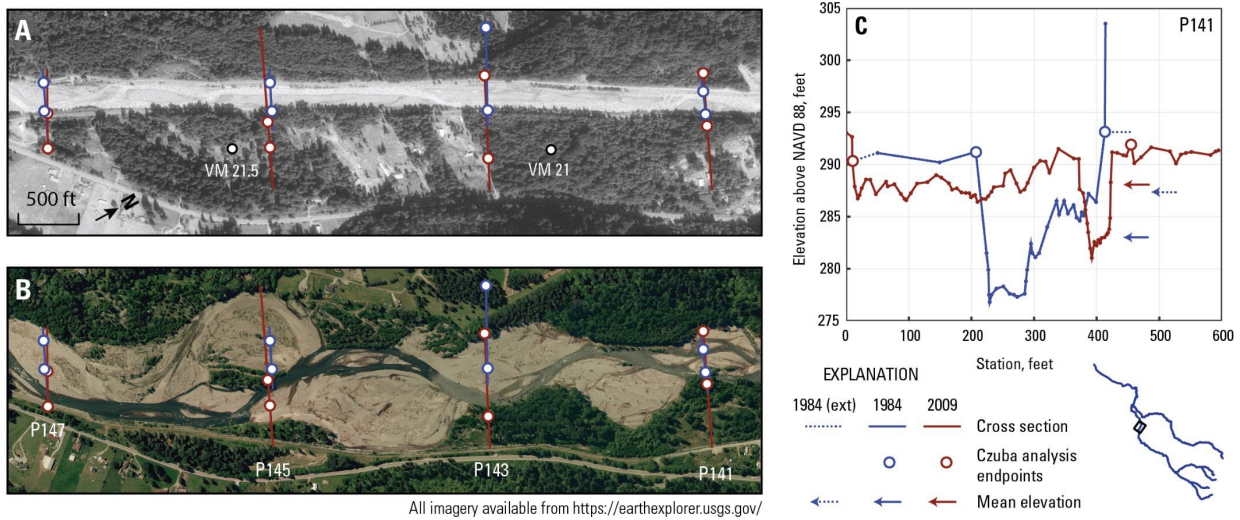


Figure 16. Examples of different lateral extents of analysis used to assess 1984–2009 elevation change along the Puyallup River in Czuba and others (2010). A) Survey extents from 1984 and 2009 overlain on 1990 aerial imagery. Levees in 1990 imagery were unchanged from 1984 survey conditions. Circles indicate the approximate endpoints between which Czuba and others (2010) calculated mean elevations in a given survey year. B) The same survey data overlain on 2009 imagery. C) Cross section data for P141. Solid arrows indicate mean elevations as estimated in Czuba and others (2010); the dashed blue arrow indicates a re-calculated mean elevation for the 1984 data using the same lateral extents as the 2009 estimate. This involved minor extrapolation of 1984 data on both sides (dashed lines).

Data at cross section P141 provides a concrete example of this issue. Czuba and others (2010) reported 5.0 ft of aggradation at this section. This result was based on a comparison of the mean elevation of a 200-ft swath of the 1984 section against the mean elevation of a 450-ft swath of the 2009 section (Figure 16C; Anderson, 2025). However, 1984 survey data extending beyond the river-left levee, which was not used in the original comparison, show several feet of net lowering over a width of several hundred feet. Extending the analysis to include that river-left change reduces the mean elevation change to 0.7 ft. Fully accounting for bank erosion on the

river-right bank, which aerial imagery indicates occurred but cannot be estimated with the available survey data, would further shift the estimate of change down.

The example at P141 demonstrates the general nature and potential magnitude of this issue. Unfortunately, there were almost no other cases where the available 1984 data upstream of VM 19 allowed for a simple recalculation of 1984–2009 mean elevation change (Anderson, 2025). However, qualitative assessments of survey data and imagery suggest that similar omissions likely overestimated deposition at many sections upstream of VM 19. While the true magnitude and direction of changes are unknown, the substantial deposition reported by Czuba and others (2010) between VM 19 and 22 on the Puyallup River is almost certainly overstated.

Incomplete survey overlap was less of an issue on the Puyallup River downstream of VM 19 and along the lower Carbon River, where river corridors have remained more confined. The biases described here are then considered unlikely to have substantially impacted 1984–2009 mean elevation change estimates downstream of VM 19 on the Puyallup River or along the lower Carbon River.

Synthesis of Observed Deposition Rates for the Lower Puyallup River, 1976–2020

Between prior analyses of repeat cross sections (Prych, 1988; Czuba and others, 2010) and the analyses of repeat aerial lidar presented in this report (Table 6), channel change in the lower Puyallup River has been assessed over four different intervals between 1976 and 2020. In this section, these various channel change analyses are compiled to provide an overview of long-term trends in deposition rates. The analysis focused on floodway deposition rates along the Puyallup River from VM 20 down to the confluence of the White River (VM 9). This encompassed the reaches that were consistently depositional in post-2004 repeat lidar surveys

(Figure 7), covers the major zones of historical gravel extraction (Prych, 1988), and limits the analysis to deposition related to sediment inputs from the Carbon and Puyallup Rivers, excluding the White River. This section also assesses whether historical variations in deposition rates can be explained by historical variations in flood hydrology and sediment transport capacity alone. This provides a test of Czuba and others (2012a) inference that, given the abundant supply of sediment available for transport, variations in flood hydrology were likely to be the dominant control on deposition rates in the lower Puyallup River.

Sources of Volumetric Deposition Information

Volumetric deposition over a given interval was estimated as the sum of measured floodway channel change and the documented sediment removal (Table 8). Sediment removal rates were compiled from annual volumes of extraction reported in Prych (1988) and Czuba and others (2010). Prior to 1984, sediment removal volumes presented in Czuba and others (2010) were obtained directly from tables in Prych (1988). From 1984 on, Czuba and others report values based on information provided by Pierce County, Washington. There were substantial disagreements between the 1984 and 1985 extraction values reported in Prych (1988) and those reported in Czuba and others (2010). A review of the underlying gravel removal information from Pierce County indicates that the relatively higher 1984 value reported by Czuba and others (2010) was a product of incorrectly treating maximum permitted removal volumes as actual removal volumes, while the relatively lower value in 1985 are based on missing information about extraction volumes for several permitted operations. The 1984–85 extraction volumes from Prych (1988) were considered more reliable and used for this analysis. Post-1985 volumes were taken from Czuba and others (2010), though instances of known extraction operations with no known extraction volume were common, such that these volumes are likely biased low. Private

gravel extractions also occurred along the Puyallup River between VM 9 and 22 over the 1976/77–84 period (Prych, 1988) but extraction volumes are unknown. Extraction rate estimates for 1976/77–84 are then also likely biased low.

Prych's (1988) analysis of 1976/77–84 repeat cross sections on the Puyallup River found no reaches with significant change in a consistent direction, and the average of reported mean elevation changes was -0.01 ft. Net sediment storage change over this interval was then assumed to be zero, and deposition was estimated solely from reported sediment removal volumes. Total extraction volume over this interval was estimated as the sum of annual extractions from 1978 to 1983, using the same years described in Prych (1988).

Volumetric deposition based on 2004–11 repeat lidar was subtracted from 1984–2009 change estimated from repeat cross sections, and the result was interpreted as an estimate of net deposition from 1984–2004. This nominally misattribution change that occurred between the summer of 2009 and April 2011 to the 20-year interval prior to 2004. However, given that this was a relatively short period with no major high flows (Figure 3), the impact of this misattribution is presumed to be small.

Table 8. Summary of sediment deposition rates along the Puyallup River floodway, valley mile (VM) 9 to VM 20. [yd³/yr – cubic yards per year]

Start	End	Measured floodway deposition, yd ³ /yr	Source	Note	Sediment removal, yd ³ /yr	Source	Note
1976/77	1984	0	Prych, 1988	Assumed exactly zero based on lack of spatially coherent change, mean reported mean elevation change of 0.01 ft	38,300	Prych, 1988	Based on average annual extraction rates from 1978 to 1983; does not account for private gravel extraction
1984	2004	35,500	Czuba and others, 2010; this report	Calculated as 1984–2009 net change minus 2004–2011 net change	12,300	Prych, 1988 (1984–85); Czuba and others, 2010 (1986–1997)	Minimum estimate; missing extraction volumes for multiple documented removal efforts.
2004	2011	72,600	This report, Table 6	Floodway deposition only	0	Czuba and others, 2010	-
2011	2020	41,300	This report, Table 6	Floodway deposition only	0	N/A	-

Methods of Characterizing Bedload Transport Capacity

To assess whether flood hydrology alone could explain observed variations in deposition rates, the empirical bedload-discharge power law relation presented in Figure 27 of Czuba and others (2012a) was applied to daily discharge records from the Puyallup River at Orting, WA (USGS 1209300; U.S. Geological Survey, 2025) streamgage to estimate mean annual loads over the four distinct intervals for which deposition estimates were available (Table 8). Czuba and others (2012a) fit that power-law relation to a compilation of 10 bedload measurements made across the White, Carbon, and Puyallup Rivers between 1986 and 2011. The resulting sediment load estimates were interpreted here as approximate estimates of bedload transport capacity, as opposed to true estimates of sediment load, and primarily provide a means of summarizing discharge records in a way that captures the non-linear relation between discharge and bedload transport. Annual transport capacity values were normalized by the mean annual value from 1984 to 2004.

To provide context and comparisons to results at the Puyallup River near Orting, WA streamgage, this same bedload transport capacity analysis was repeated for other gages around Mount Rainier, including the Puyallup River at Electron, WA (USGS 12092000), the Carbon River near Fairfax, WA (USGS 12094000), the Nisqually River at National, WA (USGS 12082500), and the Cowlitz River near Packwood, WA (USGS 14226500; U.S. Geological Survey, 2025; Figure 1), using the same power-law bedload-discharge relation at all sites. Note that the Nisqually and Cowlitz River streamgages are outside of our formal study area.

Deposition Rates in the Lower Puyallup River and Relations to Bedload Transport Capacity

Floodway deposition occurred along the lower Puyallup River over all four assessed intervals between 1976 and 2020, with an overall average rate of 48,500 yd³/yr (Figure 17; table 8). This average is likely biased low due to incomplete gravel extraction records over the first two intervals. Period-average deposition rates ranged from 38,300 to 72,600 yd³/yr, with the highest deposition rates occurring over the 2004–11 interval. Given that gravel extraction and channel monitoring initiated in the 1970s was a response to a perceived loss of flood conveyance due to sediment deposition (Prych, 1988), it seems plausible that deposition was occurring prior to 1976 as well.

Average annual bedload transport capacity at the Puyallup River near Orting, WA streamgage was close or (by definition) equal to the 1984–2004 mean (normalized value of 1) over the two analysis intervals between 1977 and 2004, and then increased about 40 percent over both the 2004–11 and 2011–20 intervals (Figure 18). Results from the Puyallup River at Electron, WA essentially the same trends. Results from the Carbon, Nisqually, and Cowlitz Rivers show similar results through the 2004–11 period but, in contrast to the two Puyallup River streamgages, normalized bedload transport capacity at all three of those sites dropped back to around 1.0 over the 2011–20 interval (Figure 18).

These results indicate that variations in deposition rates along the lower Puyallup River generally tracked variations in average sediment transport capacity in the Puyallup River through 2011, in that both quantities were fairly steady prior to 2004 and then increased on the order of 30–50 percent from 2004–11. The two quantities then diverged over the 2011–20 interval, when deposition rates dropped while average sediment transport capacity along both gages on the Puyallup River remained high (Figure 17, Figure 18). However, the observed drop in 2011–20

deposition rates along the Puyallup River corresponds to a similar-scale reduction in average sediment transport capacity observed in the Carbon River and other neighboring watersheds (Figure 18). These observations suggest two possible explanations.

The first explanation is that localized weather events over the 2011–20 interval led to more high flows and higher average bedload transport capacity in the Puyallup River than in adjacent watersheds. At the same time, other factors governing deposition rates (for example, sediment supply) reduced 2011–20 deposition rates independent of flood hydrology. The other possibility is that discharge records at both streamgages on the Puyallup River overestimated the magnitude of moderate and high flows from 2011–20, and that actual variations in sediment transport capacity were similar to those of adjacent watersheds. In this scenario, variations in flood hydrology would provide a succinct explanation for sediment deposition rates in the lower Puyallup River over all four intervals since 1976. At present, it is not possible to distinguish between these possibilities.

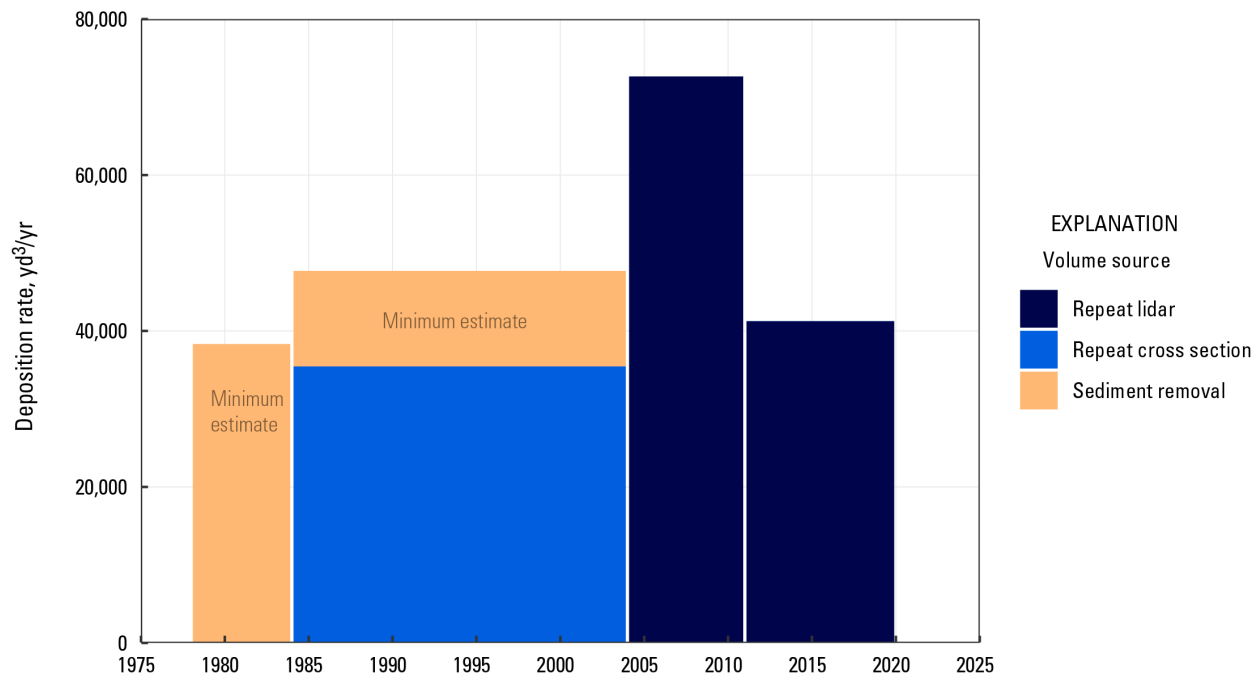


Figure 17. Floodway deposition rates along the Puyallup River, Washington, between valley mile 20 and the White River confluence (valley mile 9). Sediment removal estimates from the first two intervals are likely minimum estimates. Sediment removal volumes based on data in Prych (1988) and Czuba and others (2010); 1984–2004 channel change derived from analyses presented in Czuba and others (2010).

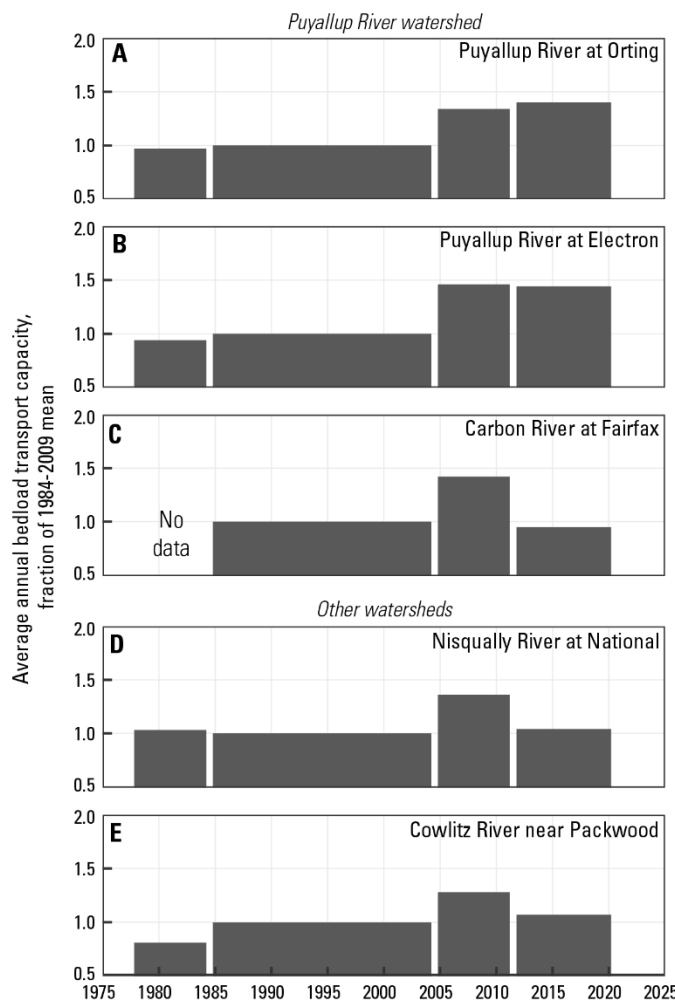


Figure 18. Trends in average annual bedload transport capacity at USGS streamgages on rivers draining Mount Rainier, including A) the Puyallup River near Orting, WA (USGS 12093500), B) the Puyallup River at Electron, WA (USGS 12092000), C) the Carbon River at Fairfax, WA (USGS 12094000), D) the Nisqually River at National, WA (USGS 12082500), and E) the Cowlitz River at Packwood, WA (USGS 14226500; U.S. Geological Survey, 2025). Bedload transport capacity was estimated by applying the empirical power-law relation between discharge and bedload transport presented in Czuba and others (2012a) to daily discharge records at each site.

Sediment Delivery and Channel Change in the Upper Puyallup River

Watershed

Sediment transport in the lower Puyallup River watershed is strongly influenced by the presence of Mount Rainier. Concerns about changing sediment supply in the Puyallup River watershed have tended to focus on changing sediment inputs from Mount Rainier (Czuba and others, 2012a) as glaciers continue to retreat and precipitation at elevation becomes increasingly likely to fall as rain. Concerns about headwater sediment inputs were likely elevated by a large November 2006 rainstorm, during which debris flows, flooding, and river bank erosion caused widespread damage to infrastructure around Mount Rainier National Park. This was followed by reports that rivers within Mount Rainier National Park have generally been aggrading over the past century, and at increasingly fast rates, a process attributed to contemporary glacier retreat and an inferred increase in coarse sediment delivery (Beason, 2007; Beason and others, 2014).

These concerns—that glacier retreat, by exposing unstable sediment, has or will increase coarse sediment delivery to downstream rivers and result in downstream channel aggradation—are grounded in well-established geomorphic concepts, including those of a paraglacial sediment response (Ballantyne, 2002) and river response to changing sediment or water inputs (Lane, 1954). Substantial glacier retreat has unambiguously occurred around Mount Rainier (Nylen, 2004; Beason and others, 2023), and most documented debris flows have initiated in recently deglaciated areas and mobilized unstable glacial sediment (Copeland, 2009; Legg and others, 2014). However, it remains difficult to assess whether coarse sediment delivery from Mount Rainier has increased appreciably in recent decades (Anderson and Shean, 2022). It is also unclear how tightly coupled deposition rates in the lower Puyallup River watershed are to

variations in headwater coarse sediment delivery (Czuba and others, 2012a; Anderson and Jaeger, 2021). To a large degree, both difficulties stem from the difficulty of directly measuring sediment delivery, transport, and channel change over sufficient periods of time and space.

The objective of this section is to expand the observational record of sediment delivery and channel change in the upper Puyallup River watershed, from the flanks of Mount Rainier down to the narrow bedrock canyons marking the transition to the lower watershed (Figure 1, Figure 19). The work presented here is primarily based on observed topographic change from 2002 to 2022, divided into two sub-intervals based on 2008 and 2011 aerial lidar datasets (Figure 5). However, in the recently deglaciated headwaters, the earliest topographic data were derived from aerial imagery from the early 1990s instead of 2002 lidar.

The period evaluated for this study is too short to determine long-term trends in headwater erosion rates. Repeat topographic surveys are also unable to quantify sediment delivery from sub-glacial erosion and so do not provide complete estimates of headwater sediment delivery. However, the early period of differencing brackets the November 2006 storm, which was associated with the largest mountain-wide pulse of debris flows of at least the past 60 years (Anderson and Shean, 2021). The late period then brackets the subsequent channel and headwater responses over 11–14 years of less extreme, albeit still active, hydroclimatic conditions (Figure 3; Anderson and Shean 2021). The available data also provided a good accounting of erosion through recently deglaciated areas and concurrent downstream channel adjustments. The analyses presented here then provide relatively comprehensive view of the key process areas typically implicated in a climate-driven change in sediment delivery, over a period marked by an exceptional rain event and associated debris flow response. Observations from repeat topographic surveys over the past several decades were supplemented by assessments of

long-term trends in stage-discharge relations at multiple streamgages on upland rivers draining Mount Rainier, including records both within the upper Puyallup River watershed and from adjacent watersheds.

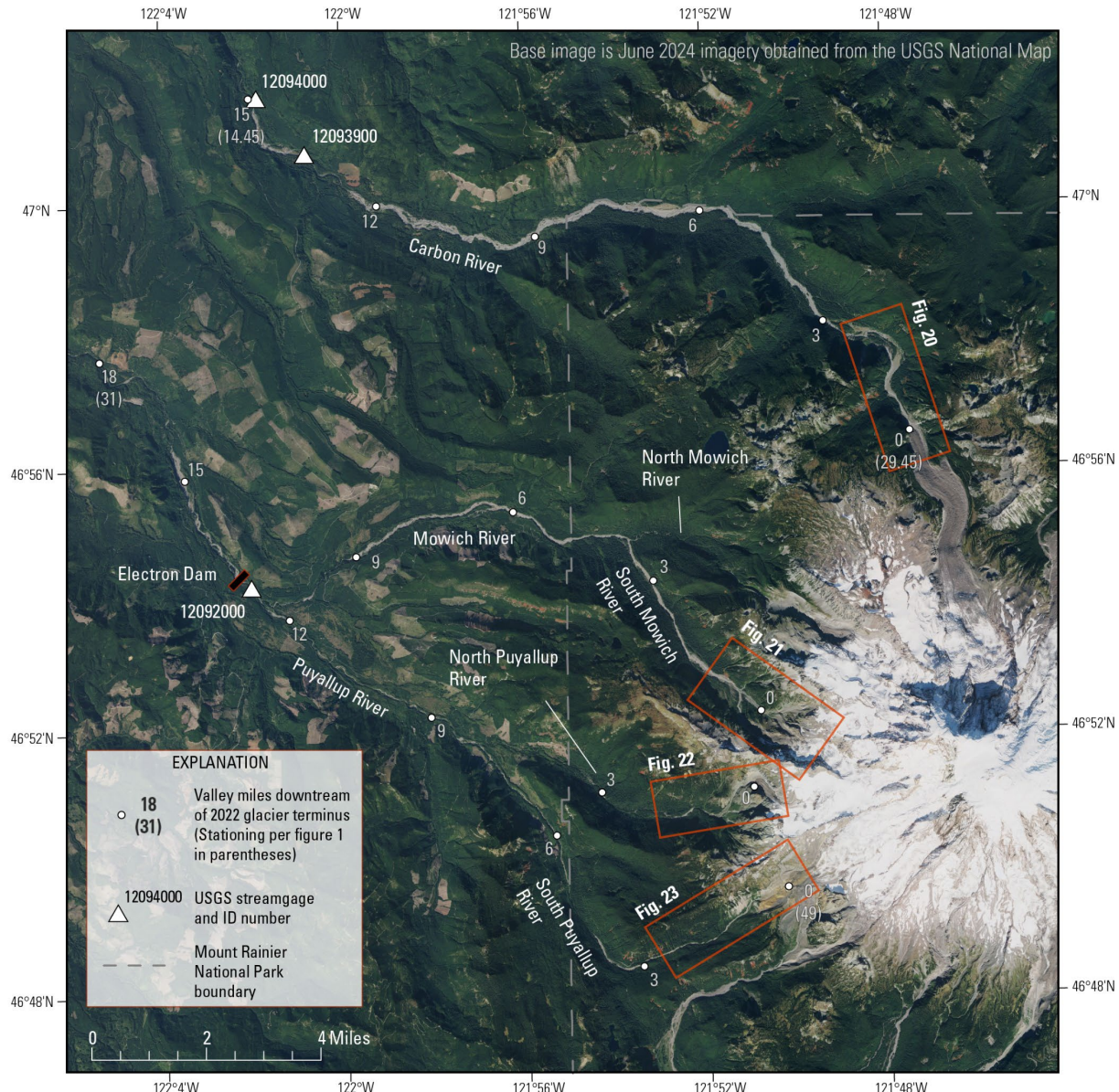


Figure 19. Aerial imagery of the upper Puyallup River watershed and headwaters on Mount Rainier.

Upper Watershed Topographic Data Sources and Change Analysis Methods

High resolution topographic surveys of the upper Puyallup River watershed primarily consist of aerial lidar datasets collected in 2002, 2008, 2011, and 2022 (Figure 5; Table 3). Additional topographic data were derived from 1991 and 1992 aerial imagery (Nolan and others, 2017) using structure-from-motion photogrammetry techniques (Fonstad and others, 2013). Those photogrammetric DEMs and processing summary reports are available in a USGS data release (Anderson, 2025).

Methods of co-registration and analysis for repeat aerial lidar in the upper watershed were largely the same as those described for repeat topography in the lower Puyallup River watershed (“Methods for Assessing Topographic Change Using Repeat Aerial Lidar”), with the exception that no discharge corrections were applied. Discharge corrections were omitted because the wetted channels in upper watershed reaches were generally small relative to the geomorphically active extents of the valley floor, such that differences in discharge were considered unlikely to substantially influence the results. Processing and co-registration of photogrammetric DEMs followed methods described in Anderson and Shean (2021).

As in the lower watershed, change results were summarized down the length of individual river valleys. In addition to assessing longitudinal patterns of geomorphic change, results in the upper Puyallup River watershed were also stratified by the height above the local water surface, or relative elevation. This provided an efficient means of parsing out sediment storage changes from lower surfaces within the active channel, such as gravel bars and the wetted channel itself, from higher overbank or bluff surfaces. Relative elevation rasters were calculated by creating regular cross sections along a given valley centerline; identifying the minimum elevation of the wetted channel for each cross section and assigning it to that cross

section; interpolating between those attributed cross sections to create a spatially continuous estimate of the low-flow water surface elevation, covering the width of the valley floor; and subtracting that interpolated surface from the original DEM. For each differencing interval, relative elevations from the earlier of the two differenced DEMs was used to stratify the results. Vertically stratified results were summarized only for reaches dominated by fluvial change, excluding debris flow-dominated zones of the headwaters that lack distinct active channel, floodplain, and/or bluff landforms.

As in the lower watershed, uncertainty in change estimates derived entirely from aerial lidar data was taken to be ± 0.16 ft, based on prior assessments in similar settings (Anderson and Jaeger, 2021). Uncertainties in analyses involving 1990s photogrammetric DEMs were estimated to be ± 0.66 ft based on assessments of the same data types in multiple basins around Mount Rainier (Anderson and Shean, 2021). Uncertainty bounds represent 95 confidence limits on potential mean errors over reach scales.

Data from 1991, 1992, and 2002 were used to define an ‘early’ surface, though there were gaps between the downstream limits of 1990s data and the upstream extents of 2002 data in most watersheds. Data from 2008 and 2011 were used to define a gapless ‘mid’ surface. Data from 2022 provided a single complete ‘late’ surface. The fact that the datasets making up the ‘early’ surface were collected 10–11 years apart nominally complicates interpretation of the results. However, aerial imagery and prior analyses of neighboring watersheds (Anderson and Shean, 2021) indicate that geomorphic activity on the flanks of Mount Rainier was relatively low from the early 1990s through about 2002 and then increased after 2003, culminating in the November 2006 storm. Erosion rates based on 1991/2–2008 differencing are then taken to be primarily the result of change from roughly 2003 to 2006, such that differencing from 1991/2–

2008 in the headwaters and from 2002–08 in the channels downstream are considered comparable.

The North Mowich River, emanating from the North Mowich Glacier, was not included in the following analyses because it was not covered in the 2002 lidar dataset or early 1990s imagery. While there is a large area of steep, exposed sediment below the North Mowich Glacier, the river itself is relatively short (~3.5 miles) and often so narrow that the channel is not visible through forest cover in modern satellite imagery (Figure 19). Aerial imagery showed no indications of major disturbances along the river valley associated with the November 2006 storm. The omission of the North Mowich River from this analysis is then considered unlikely to bias the watershed-scale results and interpretations of this study.

Methods for Assessing Changes in Stage-Discharge Relations

Data collected as part of routine USGS streamgaging can be used to infer changes in local channel geometry (James, 1991; Juracek and Fitzpatrick, 2009; Czuba and others, 2010). While these results are necessarily limited to the locations of USGS streamgages, the approach provides one of the few means of assessing long-term trends in channel geometry with relatively high temporal resolution (approximately every 6–12 weeks).

Channel geometry changes were inferred using stage-discharge data obtained from regular streamflow measurements. Methods follow those presented in Anderson and Konrad (2019) and are summarized here. The general method involves defining a baseline or average stage-discharge relation and then calculating the difference between measured stage and expected stage per that baseline stage-discharge relation. The result is a sequence of ‘stage offsets’ that, when plotted over time, describe relative changes in stage-discharge relations.

Increasing values over time (that is, stage for a given discharge is getting progressively higher) are typically interpreted as indicating channel aggradation, and decreasing values as channel incision, though stage-discharge relations can also be influenced by changes in channel width and roughness. These methods were applied to the three long-term USGS streamgages in the upper Carbon and Puyallup Rivers (USGS 12092000, 12093900, and 12094000; Figure 1; U.S. Geological Survey, 2025), with periods of record extending back to the early or mid-20th century. Trends from long-term streamgages on the upper Cowlitz and Nisqually Rivers (USGS 12082500 and 14226500; U.S. Geological Survey, 2025), both of which drain substantial glacier-covered areas on Mount Rainier and have records extending back to 1940s or earlier, were also assessed to provide a broader view of long-term elevation trends in upland rivers draining Mount Rainier.

For this work, baseline stage-discharge relations were defined using locally weighted regression (LOESS; Cleveland and Devlin, 1988) curves fit to all discharge measurement data collected in WYs 2011–20 at a given streamgage, using a LOESS smoothing parameter of 0.9. Stage offsets were calculated for all measurements made below the site-specific 95th percentile daily mean flow. This focuses the analysis to measurements made when flow was likely contained within the main channel and not impacted by overbank hydraulics.

On the Carbon River, the streamgaging record is split between two sites located about 1.5 miles apart. Measurements were made at the downstream site (Carbon River near Fairfax, WA; USGS 12094000) from 1929 to 1965 and then again from 1992 through present, and at the upstream site (Carbon River at Fairfax, WA; USGS 12093900) between 1965 and 1992. When the downstream site was re-established in 1992, the local datum was unchanged, but the stage sensor was located about 350 ft downstream of the pre-1965 location. The available lidar was

used to estimate the water surface elevation change over those 350 ft, which was found to be ~4.3 ft. Stage from post-1992 measurements were then shifted up by this amount to estimate the expected stage at the pre-1965 stage sensor located upstream. For the Carbon River at Fairfax, WA, baseline stage-discharge relations were defined using measurements from WYs 1965–70, since no measurements exist in the WYs 2011–20 baseline period used for other streamgages.

Observed Geomorphic Change in the Upper Puyallup River Watershed

Geomorphic changes observed in the upper Puyallup River watershed between 1991/2002 and 2022 were similar across the four distinct study rivers and headwater areas, though the patterns differed between the two periods assessed. Results are then presented in two sections, the first covering observations from the early (1991/2002 to 2008/11) period, and the second over the late (2008/11 to 2022) period. Results based on stratification of change by relative elevations are then summarized over both periods in a third section.

Early Period—1991/2002 to 2008/11

Between the early 1990s and 2008, substantial erosion occurred in the upper extents of all four proglacial watersheds (Figure 20–23; Table 9). This erosion was almost certainly the result of debris flows (Walder and Driedger, 1994; Scott and others, 1995; Legg and others, 2014). Most erosion occurred via incision of large gully-like channels along the primary valley floors, with smaller amounts of erosion occurring in gullies cut into lateral moraines. In the Carbon River, headwater erosion was only documented indirectly in the form of a large deposit of material emplaced about a half mile down-valley of the 2008 glacier terminus (Figure 20A). The source of this deposit was either obscured by the glacier or located up-valley of the available data.

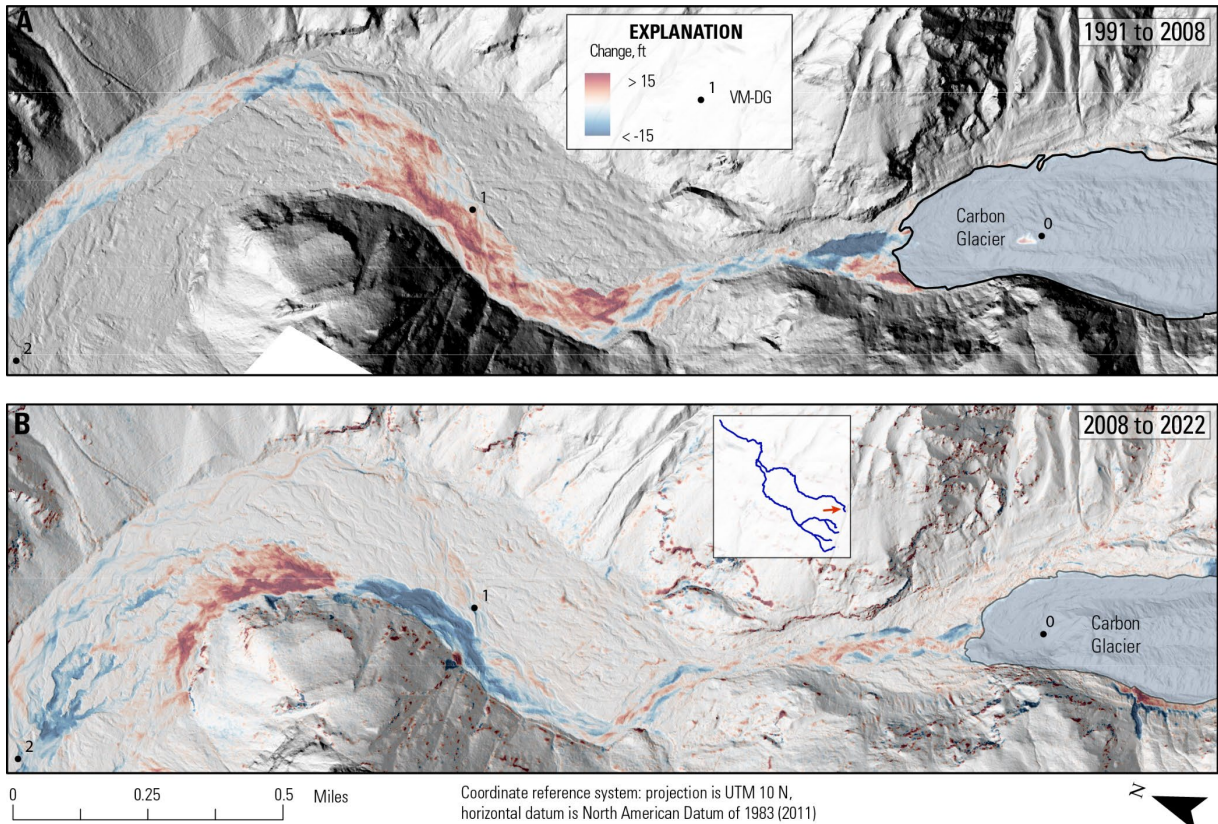


Figure 20. Geomorphic change in the Carbon River headwaters based on differencing of high-resolution topography from A) “early period” 1991–2008 and B) “late period” 2008–2022. Areas where geomorphic change is the result of ice mass changes are shown with transparent overlay. Basemaps are derived from 2008 (A) and 2022 (B) aerial lidar provided by the Washington Geological Survey (2009; 2023b). VM-DG – Valley miles downstream of 2022 glacier terminus.

Measurable debris flow erosion in the South Mowich, North Puyallup, and South Puyallup River headwaters totaled 1.7 ± 0.1 million yd^3 , with about 60 percent of that total coming from the South Mowich River headwaters (Figure 21A; Table 9). Using the volume of debris flow deposition observed in the Carbon River (Figure 20A) as a minimum estimate of

source area erosion, total headwater debris flow erosion across the four watersheds was at least 2.1 million yd^3 .

In all four watersheds, much of the early-period erosion was likely the result of the November 2006 storm, though aerial imagery indicates that sizable debris flows occurred in most of the study watersheds sometime after 2003 but before the summer of 2006. A similar cluster of debris flow events between 2003 and the summer of 2006 were observed in other headwater basins around Mount Rainier (Anderson and Shean, 2021).

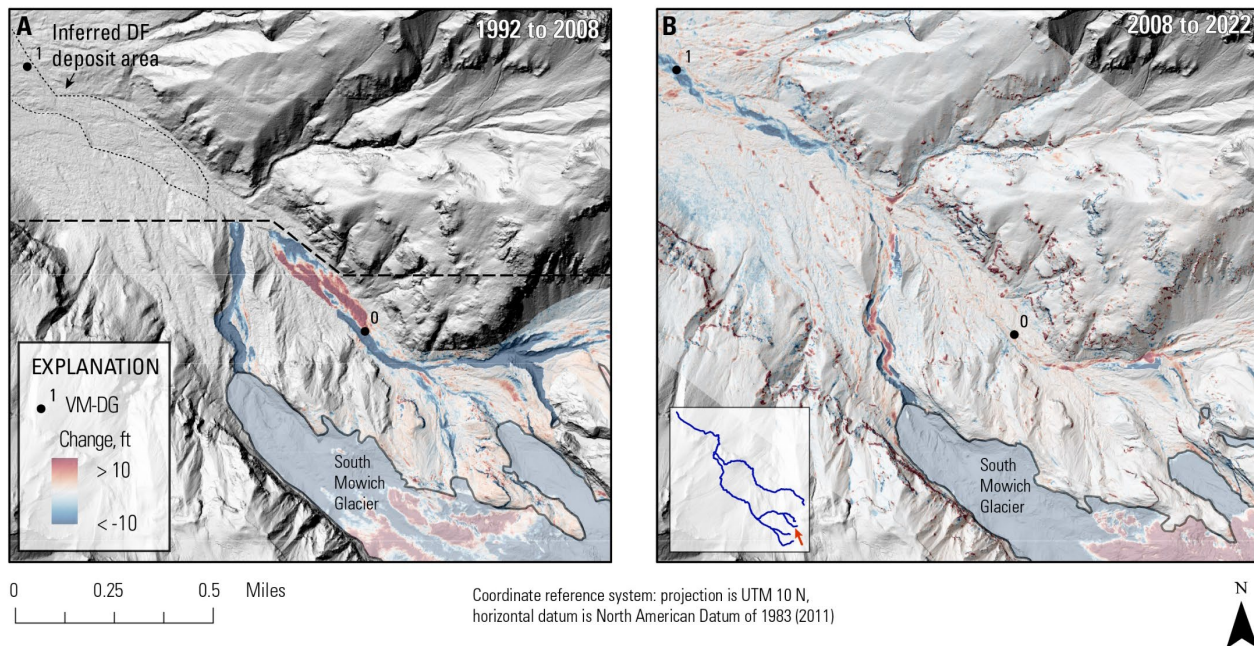


Figure 21. Geomorphic change in the South Mowich River headwaters based on differencing of high-resolution topography during A) 1992–2008 and B) 2008–2022. Areas where geomorphic change is obscured by ice mass changes are shown with transparent overlay. Dashed line in A shows the down-valley limits of 1991 data coverage. Basemaps are derived from 2008 (A) and 2022 (B) aerial lidar provided by the Washington Geological Survey (2009; 2023b). VM-DG - Valley miles downstream of 2022 glacier terminus.

The debris flows of the early 2000s formed distinct deposits in the Carbon, North Puyallup, and South Puyallup River valleys, with well-defined downstream limits located 1 to 2 miles down-valley of 2022 glacier termini (Figure 20A, Figure 22A, Figure 23A). Some deposition was also observed within the available data extents of the South Mowich River, though aerial imagery, valley geometry, and subsequent patterns of 2008-22 change all suggest that the primary depositional zone was in the data gap between 1992 and 2002 datasets (Figure 21A). Aggregated across the four watersheds, observed debris flow deposition totaled 0.9 ± 0.1 million yd^3 , though incomplete accounting of deposition in the South Mowich River makes this a lower bound on the true value (Table 9).

Table 9. Summary of topographic change results in the upper Puyallup River watershed. [DEM- digital elevation model; ft - feet; yd³ - cubic yards].

River	Period	Start DEM Year	End DEM Year	Process Zone	Reach extents, miles downstream of 2022 glacier terminus		Volumetric change, yd ³	Mean elevation change, ft
					Start	End		
Carbon River	Early	1991	2008	Debris flow erosion			No data	
		1991	2008	Debris flow deposition	0.7	1.48	406,000 ± 42,000	6.28 ± 0.66
		2002	2008/11	River valley erosion	8.16	19.19	-314,000 ± 175,000	-0.3 ± 0.16
Carbon River	Late	2008	2022	Proglacial	-0.85	0.54	-17,000 ± 5,000	-0.59 ± 0.16
		2008	2022	Erosion of debris flow deposits	0.54	1.32	-222,000 ± 12,000	-2.97 ± 0.16
		2008	2022	Re-deposition of debris flow deposit material	1.32	1.79	168,000 ± 14,000	1.97 ± 0.16
		2008/11	2022	River valley deposition	1.79	11.26	129,000 ± 256,000	0.08 ± 0.16
		2011	2022	River valley erosion	11.26	15.93	-97,000 ± 71,000	-0.22 ± 0.16
South Mowich and Mowich Rivers	Early	1992	2008	Debris flow erosion	-0.7	0.54	1,073,000 ± 46,000	-15.32 ± 0.66
		1992	2008	Debris flow deposition (incomplete)	0.2	0.54	151,000 ± 20,000	4.83 ± 0.66
		2002	2008/11	River valley erosion	3.96	10.95	-315,000 ± 106,000	-0.49 ± 0.16
South Mowich and Mowich Rivers	Late	2008	2022	Proglacial	-0.54	0.54	-52,000 ± 12,000	-0.72 ± 0.16
		2008	2022	Erosion of debris flow deposits	0.54	1.17	-103,000 ± 8,000	-2.2 ± 0.16
		2008	2022	Re-deposition of debris flow deposit material	1.17	1.94	90,000 ± 16,000	0.94 ± 0.16
		2008	2022	River valley deposition	1.94	6.91	87,000 ± 88,000	0.16 ± 0.16
		2011	2022	River valley erosion	6.91	10.95	-174,000 ± 47,000	-0.61 ± 0.16
North Puyallup River	Early	1992	2008	Debris flow erosion	-0.08	1.01	-459,000 ± 31,000	-9.63 ± 0.16
		2002	2008	Debris flow deposition	1.17	1.94	244,000 ± 9,000	4.39 ± 0.16
		2002	2008/11	River valley erosion	2.1	5.52	-122,000 ± 27,000	-0.75 ± 0.16
North Puyallup River	Late	2008	2022	Proglacial	-0.08	0.85	10,000 ± 3,000	0.64 ± 0.16
		2008	2022	Erosion of debris flow deposits	1.17	1.63	-36,000 ± 3,000	-2.33 ± 0.16
		2008	2022	Re-deposition of debris flow deposit material	1.63	2.25	51,000 ± 6,000	1.3 ± 0.16
		2008	2022	River valley deposition	2.25	3.65	11,000 ± 6,000	0.31 ± 0.16
		2011	2022	River valley erosion	3.96	5.52	-28,000 ± 6,000	-0.71 ± 0.16
South Puyallup and Puyallup Rivers	Early	1992	2008	Debris flow erosion	-0.08	1.01	-190,000 ± 20,000	-6.37 ± 0.16
		2002	2008	Debris flow deposition	1.94	2.41	56,000 ± 3,000	2.77 ± 0.16
		2002	2008/11	River valley erosion	2.41	16.7	-550,000 ± 137,000	-0.66 ± 0.16
South Puyallup and Puyallup Rivers	Late	2008	2022	Proglacial	-0.08	2.1	-32,000 ± 11,000	-0.47 ± 0.16
		2008	2022	Erosion of debris flow deposits	2.1	2.41	-18,000 ± 2,000	-1.41 ± 0.16
		2008	2022	Re-deposition, River valley deposition mix	2.41	4.12	40,000 ± 16,000	0.42 ± 0.16
		2011	2022	River valley erosion	4.12	18.41	-480,000 ± 111,000	-0.71 ± 0.16

In the North Puyallup River, where gaps between 1990s and 2002 datasets were smallest, measured debris flow deposition accounted for about 50 percent of up-valley erosion (Figure 22A; Table 9). In the South Puyallup River, measured deposition accounted for about 30 percent of up-valley erosion, though neither source area nor the deposit were fully captured in the available data (Figure 23A).

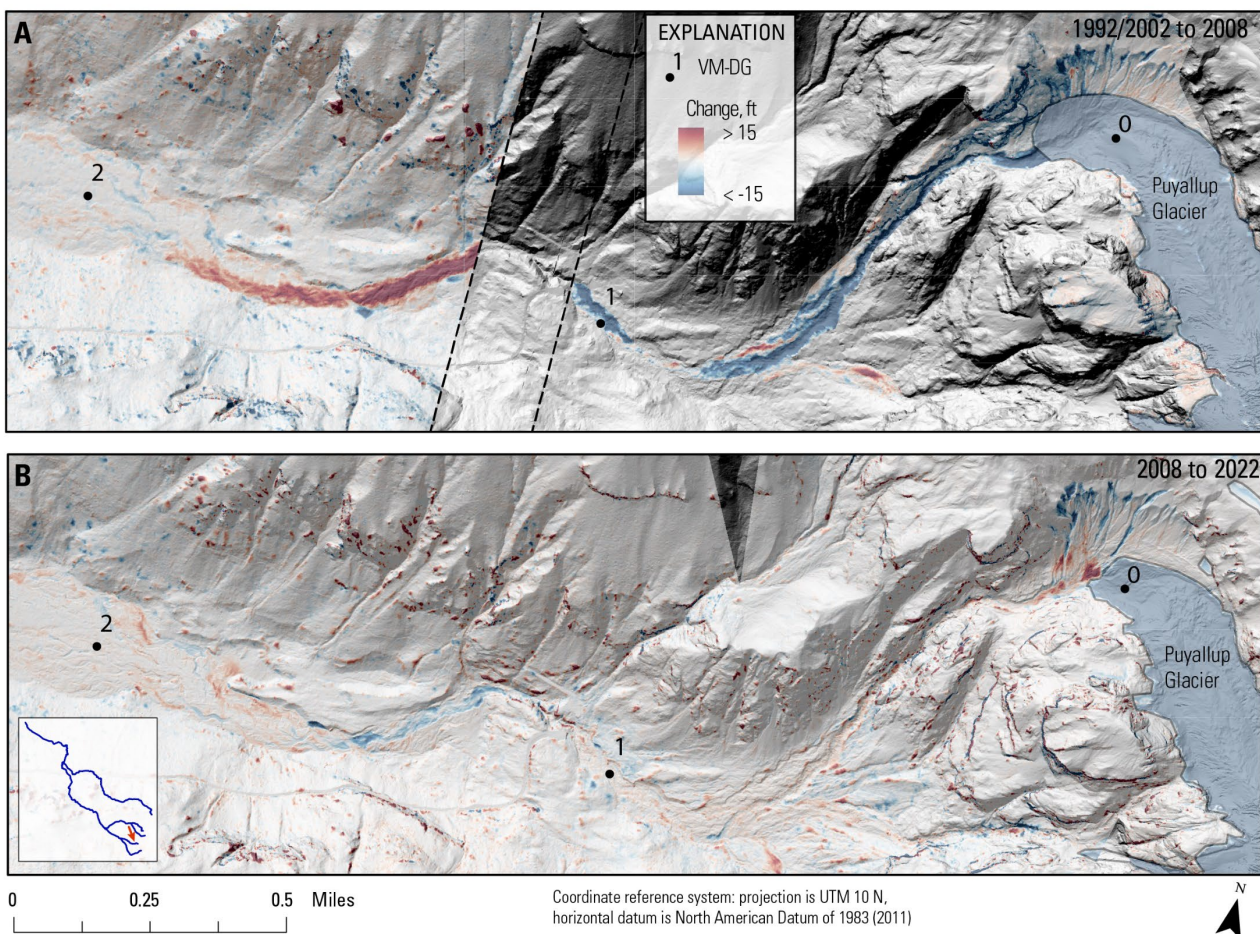


Figure 22. Geomorphic change in the North Puyallup River headwaters based on differencing of high-resolution topography from A) 1992 or 2002 to 2008 and B) 2008 to 2022. Areas where geomorphic change is the result of ice mass changes are shown with transparent overlay. In A, change on the left side of the dashed lines is from 2002 to 2008, and change on the right side is from 1992 to 2008. Basemaps are

derived from 2008 (A) and 2022 (B) aerial lidar provided by the Washington Geological Survey (2009, 2023b). VM-DG – Valley miles downstream of 2022 glacier terminus.

Down-valley of the debris flow deposits, 2002–08/11 sediment storage change along the four main river valleys was overall negative (net erosion), with local erosion rates generally increasing farther downstream (Figure 24). Net erosion along the four valleys totaled 1.3 ± 0.5 million yd^3 (Table 9), equivalent to about $160,000 \pm 55,000 \text{ yd}^3/\text{yr}$. A large fraction of this volume was supplied by the Puyallup River downstream of the North Puyallup River confluence, primarily because erosion occurred over such a long length of the river (Figure 24). Erosion rates per unit valley distance were similar across the four rivers, averaging between 4,600 to 5,600 $\text{yd}^3/\text{mi}/\text{yr}$ along the Mowich, North Puyallup, and combined South Puyallup and Puyallup Rivers, and about 3,300 $\text{yd}^3/\text{mi}/\text{yr}$ along the Carbon River. Mean elevation change averaged over the eroding river valleys ranged from -0.50 ± 0.16 to $-0.75 \pm 0.16 \text{ ft}$ for the Mowich, North Puyallup, and combined South Puyallup and Puyallup Rivers, and $-0.30 \pm 0.16 \text{ ft}$ for the Carbon River (Table 9).

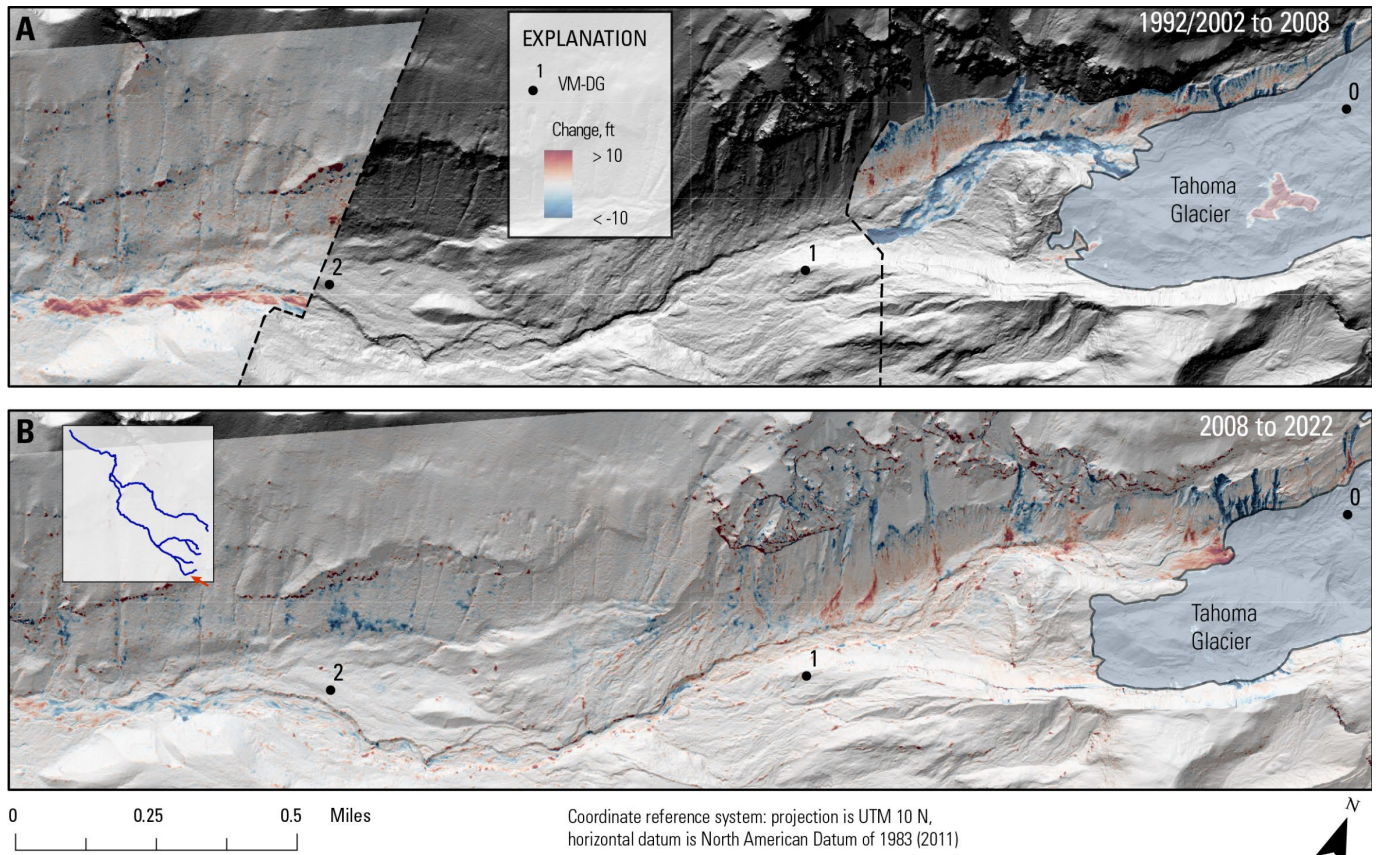


Figure 23. Geomorphic change in the South Puyallup River headwaters based on differencing of high-resolution topography from A) 1992/2002 to 2008 and B) 2008 to 2022. Areas where elevation changes are partially or entirely due to snow and ice mass changes are shown with transparent overlay. In A, change more than two miles downstream from the 2022 glacier terminus (VM-DG 2) is from 2002 to 2008, while change upstream of roughly VM-DG 1 is from 1992 to 2008. Basemaps are derived from 2008 (A) and 2022 (B) aerial lidar provided by the Washington Geological Survey (2009; 2023b). VM-DG – Valley miles downstream of 2022 glacier terminus.

Late period—2008/11 to 2022

From 2008/11 to 2022, spatial patterns of channel change were similar across all four rivers. That shared pattern, in upstream to downstream order, included: relatively modest geomorphic change in the headwaters, with small to negligible net erosion; erosion of early 2000s debris flow deposits, followed by re-deposition of an equivalent volume of material within about a half mile downstream; a reach of modest aggradation, extending several miles downstream of the debris flow deposits; and a transition to substantial net erosion to the downstream limits of the upper watershed (Figure 20B, Figure 21B, Figure 22B, Figure 23B, Figure 24; Table 9).

In the North Puyallup and South Puyallup Rivers, 2008–22 change in the headwaters primarily involved gully erosion down lateral moraines, focused near areas of recent glacier retreat (Figure 22B and Figure 23B). Eroded material tended to accumulate along the lower slopes of the valley walls or within the primary valley floor. In both systems, there was minimal detectable geomorphic change along the first 1 to 2 miles of the rivers downstream of the glacier termini. In the South Mowich and Carbon Rivers, change in the headwaters involved more extensive collapse of lateral moraines or gully walls (Figure 20B, Figure 21B). Large fractions of the mobilized material accumulated in the proximal valley floor or along the flanks of the glaciers, though there was measurable net erosion in both watersheds (Table 9). Significant geomorphic change was observed along both rivers starting right at glacier termini.

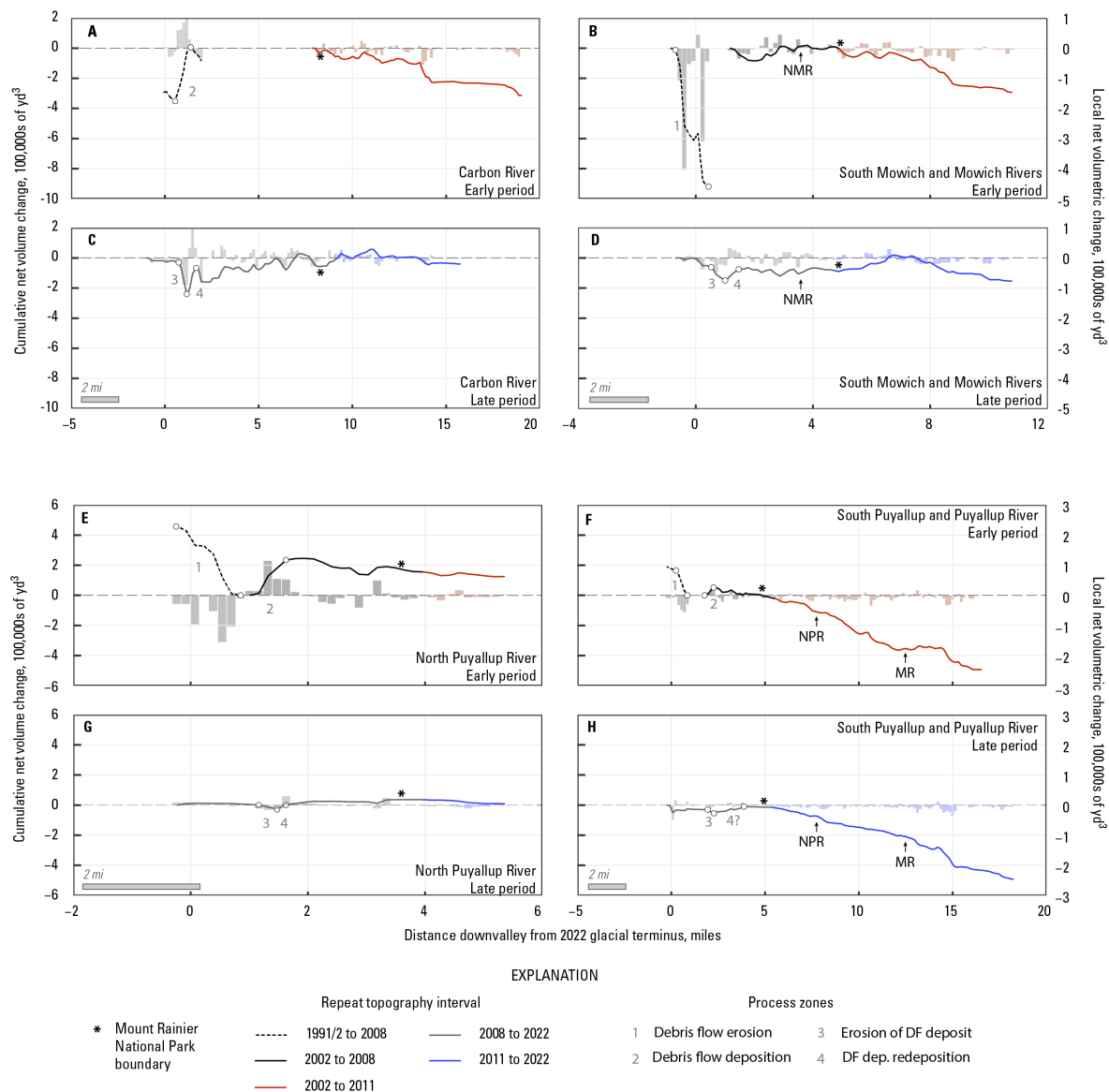


Figure 24. Volumetric change in the upper Puyallup River watershed across rivers and periods based on differencing of high-resolution topography. A) Carbon River, early period. B) South Mowich and Mowich Rivers, early period. C) Carbon River, late period. D) South Mowich and Mowich Rivers, late period. E) North Puyallup River, early period. F) South Puyallup and Puyallup Rivers, early period. G) North Puyallup River, late period. H) South Puyallup and Puyallup Rivers, late period. Extents of the major process zones discussed in the main text are indicated. Note that horizontal scale of plots vary between rivers. DF – Debris flow; MR – Mowich River; NMR – North Mowich River; NPR – North Puyallup River.

In all four rivers, net erosion occurred where the rivers traversed early 2000s debris flow deposits. Erosion into these debris flow deposits marked either the onset (in space) of significant fluvial reworking of the active channel or, in the Carbon and South Mowich Rivers, a significant increase in rates of reworking. An equivalent volume of material then typically deposited over the next half-mile downstream (Figure 24; Table 9). In the North Puyallup and South Puyallup Rivers, erosion through the debris flow deposits remobilized 15 and 30 percent, respectively, of the originally emplaced deposit volume (Table 9). While the initial deposit volume was unknown for the South Mowich River, observed erosion through the inferred deposits amounted to about 10 percent of 1992–2008 source area erosion. Relative re-mobilization of debris flow deposit material was most substantial in the Carbon River, where 55 percent of the 1991–2008 debris flow deposit volume was re-mobilized during 2008–2022 (Table 9). About 75 percent of the remobilized material was then re-deposited within half a mile down-valley, forming a broad deposit along the west side of the valley (Figure 20B).

Down-valley of this local redistribution of debris flow material, all four rivers contained reaches with modest net deposition (Figure 24; Table 9). These aggrading reaches were between 2 to 10 miles in length. Net deposition totaled across the four rivers was $270,000 \pm 370,000 \text{ yd}^3$. Mean elevation change specifically within these aggrading reaches was relatively larger along the narrow South Puyallup and North Puyallup Rivers (0.31 ± 0.16 and $0.42 \pm 0.16 \text{ ft}$, respectively) and relatively smaller and within uncertainty in the wider Carbon and Mowich Rivers (0.08 ± 0.16 and $0.16 \pm 0.16 \text{ ft}$, respectively).

Downstream of the aggrading reaches, net erosion was observed in all four rivers down to the downstream limits of available data (Figure 24; Table 9). Aggregated over the four rivers, net

erosion in these reaches totaled $780,000 \pm 240,000 \text{ yd}^3$, or about $70,000 \pm 20,000 \text{ yd}^3/\text{yr}$. Most of that material originated from the Puyallup River (63 percent) and the Mowich River (22 percent; Table 9). Erosion rates normalized by valley length were relatively lower in the North Puyallup and Carbon Rivers (1,630 and 1,900 $\text{yd}^3/\text{mi/yr}$, respectively) and relatively higher for the combined South Puyallup and Puyallup Rivers and Mowich River (3,100 and 4,000 $\text{yd}^3/\text{mi/yr}$, respectively).

Channel Change by Relative Elevation

Volumetric change stratified by relative elevation was summarized for each river and period, with 2008/11–22 change further split between upstream reaches that experienced net deposition and downstream reaches that experienced net erosion (Figure 24). Results show a consistent pattern of net deposition on lower surfaces and net erosion of higher surfaces observed in all rivers valleys, sub-reaches, and period (Figure 25). The consistency of this pattern likely indicates the common underlying process of sediment deposition on gravel bars driving lateral channel migration and bank erosion (Church, 2006; Wheaton and others, 2013). In all reaches, most deposition occurred on surfaces that were initially less than 1.5 ft above the local water surface elevation, while most net erosion occurred along surfaces initially 3–12 ft above the local water surface elevation. The overall net erosion observed in many reaches of the upper Puyallup River watershed was thus the result of rivers eroding more material from banks and bluffs than was deposited over lower parts of the active channel, as opposed to uniform downcutting across the width of the active channel.

In the early period (2002–08/11), erosion of surfaces with greater than 16 ft relative elevation, broadly considered to represent bluff erosion, was an appreciable source of sediment in all rivers, though net changes after excluding that bluff erosion would still have been negative

in all four rivers (Figure 25). Bluff erosion was a relatively minor source of sediment over the late period (2008/11–22) in all four rivers.

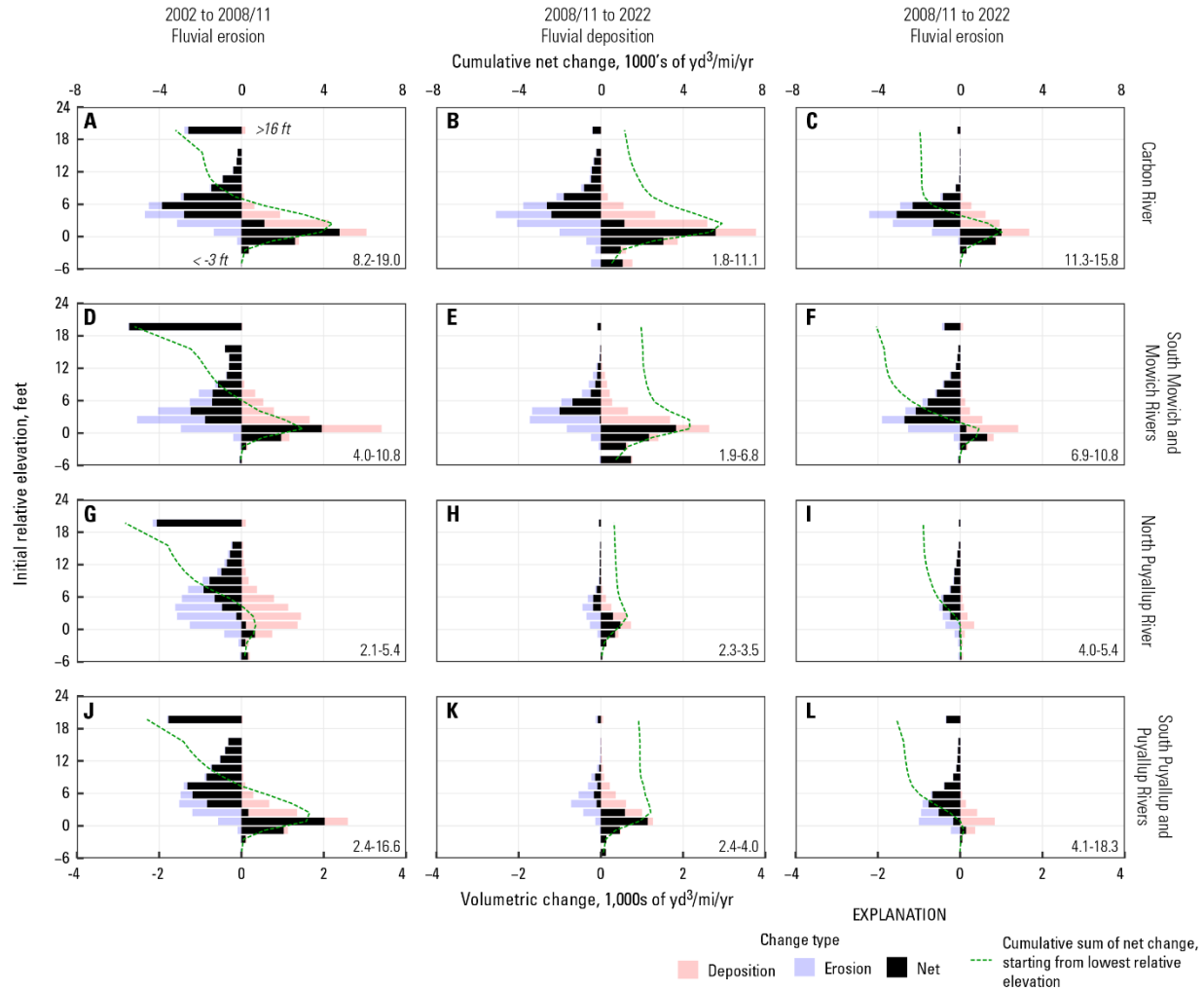


Figure 25. Volumetric change in the upper Puyallup River watershed stratified by surface height above the adjacent water surface (relative elevation) in the earlier of the differenced digital elevation models (DEMs; Table 3). Results are split into time intervals and sub-reaches with consistent directions of change, including 2002–08/11, when all rivers were predominately eroding along their full extents (A, D, G, J); reaches where, from 2008/11 to 2022, most reaches saw net depositional (B, E, H, K), and reaches from

2008/11 to 2022 where change was predominately net erosive (C, F, I, L). Numbers in lower right of each panel indicate the longitudinal extents being summarized, referencing valley miles down-valley of 2022 glacier termini (VM-DG; Figure 19).

Stage-Discharge Changes in Upland Rivers

Changes in stage-discharge relations, a proxy for local bed elevation change, at five gages draining Mount Rainier demonstrate the dynamic nature of these upland channels, with total variations of 3–4 ft over the past 60–90 years (Figure 26). Those changes involve a complex mix of long-term trends and abrupt shifts; for the purpose of this report, the general long-term trends are of most interest. Note that the Cowlitz and Nisqually Rivers are outside of the formal study area of this report and presented here to provide a broader perspective on channel change downstream of Mount Rainier.

Long-term trends at the Carbon (USGS 12093900, 12094000) and Cowlitz River (USGS 14226500) streamgages have generally been downward, with net lowering of about 3 ft relative to early-20th century high points of the two long-term records streamgages (Figure 26A, B, E). Lowering on the Cowlitz River accelerated starting around 1990. The Puyallup (USGS 12092000) and Nisqually River (USGS 12082500) streamgages have been characterized by numerous abrupt shifts up or down, with no secular long-term trend (Figure 26C, D; U.S. Geological Survey, 2025). At both of the latter streamgages, stage-discharge relations in the 2020s were similar to what they were at the start of their respective records in the mid-20th century, though the Puyallup River streamgage shifted downwards soon after the start of record and was lower than current [2024] conditions through most of the period of record.

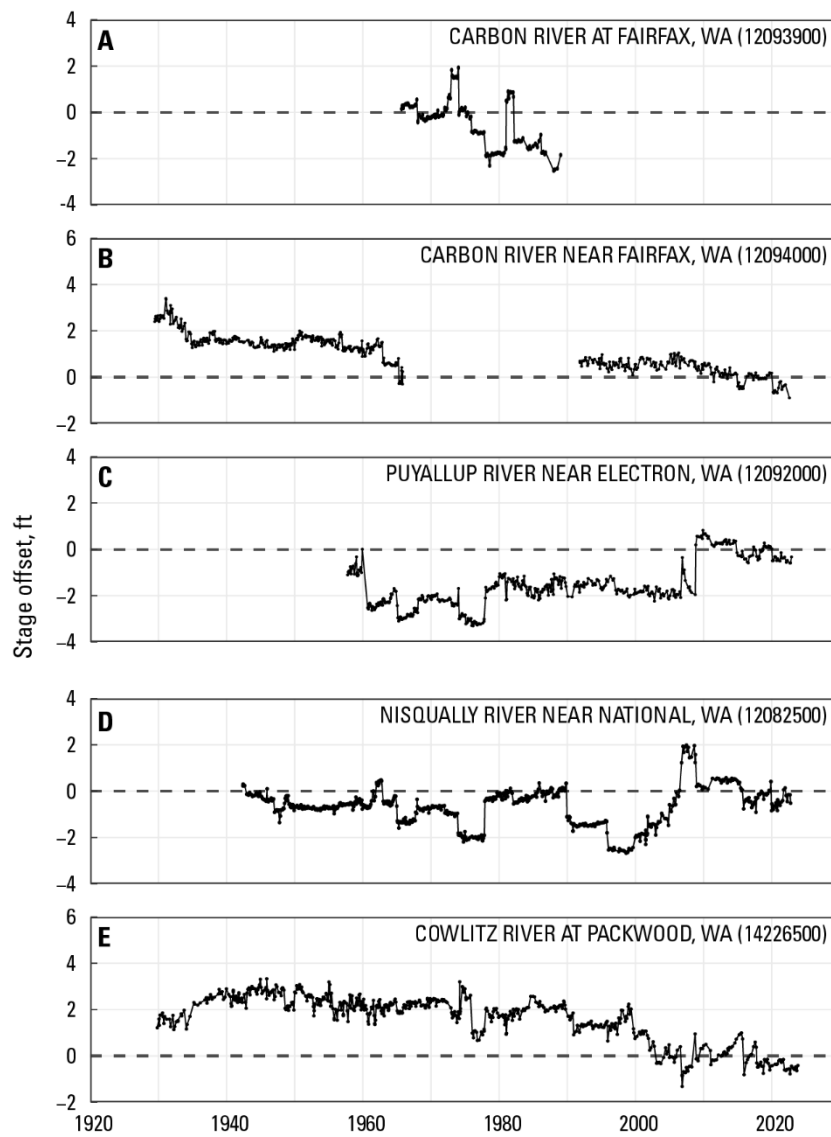


Figure 26. Changes in stage-discharge relations at upland streamgages draining Mount Rainier (U.S. Geological Survey, 2025).

Integrated Topographic Change and Watershed Sediment Budgets

The topographic change results from the lower (Table 6; Table 7) and upper (Figure 24; Table 9) Puyallup River watersheds were combined to provide an integrated view of sediment

storage trends across the watershed. Those integrated results were then combined with measurement-based estimates of sediment transport in the lower watershed and literature-based estimates of two major sediment source areas not assessed in this report—sub-glacial erosion and sediment delivery from non-glacial tributaries—to construct watershed-scale sediment budgets.

Sediment budgets were constructed to provide a better sense of the magnitude of river valley erosion and erosion in the proglacial headwaters relative to total watershed sediment transport rates. A synthesis of the topographic change results is presented to provide a high-level view of three major geomorphic process zones that characterize the sediment budgets.

Methods for Constructing Watershed Sediment Budgets

Sediment budgeting is a process of accounting for sediment sources and sinks in order to better understand dominant geomorphic processes over a given study area (Walling and Collins, 2008). A budget is considered complete if all major sediment sources and sinks are quantified. A budget is considered closed if the net sediment export implied by the sum of sources and sinks matches direct measurements of the sediment flux at the study area outlet with reasonable precision (Erwin and others, 2012).

The budgeting framework used here is based on bulk volumes of sediment, with no explicit consideration of grain size. While partitioning results by grain size or sediment transport mode would provide additional information (for example, Dietrich and Dunne, 1978), doing so would require accounting for both grain size distributions in many distinct source areas and the complex processes that modify grain size distributions moving downstream, such as lateral exchange and attrition. This is not possible with existing data in the Puyallup River watershed.

All components of the sediment budget are presented in terms of volumetric rates of erosion, deposition, or sediment transport (yd^3/yr). All volumes are expressed as effective volumes of unconsolidated sediment with a bulk density of 1.7 tons per cubic yards (t/yd^3), representative of mixed grain size deposits in natural rivers (Bunte and Abt, 2001). This effectively uses the volumes of erosion and deposition observed in the repeat topographic analyses as the common unit of budgeting analysis.

Distinct sediment budgets were created for the two major periods of topographic differencing (2002/04 to 2008/11 and 2008/11 to 2020/22). Using rates of change reduces, but does not eliminate, the issue of modestly different periods of analysis being combined to define the two distinct periods (Figure 5). The sediment budgets cover all areas upstream of the Puyallup River at Alderton, WA streamgage (USGS 12096500; Figure 1). This excludes the reaches downstream from the streamgage that are influenced by sediment delivery from the White River. Distinct sediment budgets were also constructed for the Puyallup and Carbon River watersheds upstream of the two locations with sediment transport data (USGS 12093510 and USGS 12094300, respectively; Figure 1).

The sediment budgets included five major components:

- 1) Sediment delivery from sub-glacial erosion, estimated based on previously published estimates of sub-glacial erosion rates and glacier area.
- 2) Sediment delivery from headwater areas, based on topographic differencing presented in this report (Table 9).

- 3) Net sediment storage changes along the major river valleys, based on topographic differencing presented in this report for both the lower and upper watersheds (Table 6, Table 7; Table 9).
- 4) Sediment delivery from non-glacial tributaries, estimated from previously published sediment transport studies in the region.
- 5) Estimates of sediment fluxes at three locations in the lower watershed, derived from limited direct measurements of sediment transport. A summary of those analysis methods is presented in this section, with more complete information presented in Appendix C.

In combination, the first four components cover all major sediment sources or sinks across the entire study area, providing a complete budget. Sediment transport estimates then allow an assessment of how well closed these budgets are.

Sediment Delivery from Sub-Glacial Erosion

Mills (1976; 1979) estimated modern sub-glacial erosion rates on Mount Rainier to be on the order of 0.12–0.31 inches per year (in/yr). While these estimates are based on limited data, they are consistent with predicted erosion rates based on glacier sliding velocity or precipitation (Cook and others, 2020). This range of values was recast as 0.22 ± 0.10 in/yr, providing a central estimate with associated uncertainty bounds. Vertical erosion rates were then multiplied by glacier-covered area (Beason and others, 2023) to estimate volumetric sediment production in cubic yards of bedrock. This was converted into a volume of unconsolidated sediment, using typical bulk densities of bedrock (~ 2.3 t/yd³) and unconsolidated deposits (~ 1.7 t/yd³; Bunte and Abt, 2001).

Sediment Delivery from Deglaciated Headwaters

The topographic differencing analyses presented here provide estimates of net sediment delivery from the recently deglaciated headwaters (Table 9). Delivery from the deglaciated headwaters was defined as the net export beyond the limits of logically connected deposition; if a debris flow eroded 1.0 million yd^3 from the headwaters and formed a distinct 0.4 million yd^3 deposit a short distance downstream, the net sediment delivery was considered to be 0.6 million yd^3 . Estimates of erosion and deposition based on 1991/2–2008 differencing were converted to rates under the assumption that all observed change happened between 2002 and 2008, as aerial imagery collected over that era suggests was largely the case. To the degree that some of the observed 1991/2–2008 erosion occurred prior to 2002, this simplification would overestimate headwater erosion rates.

In the Carbon River, only the deposits of early 2000s debris flows were observed in the available repeat topography (Figure 20A). Source area erosion and ultimate net delivery was estimated by assuming that the observed deposit represented between 30 and 70 percent of the up-valley erosion, based on a range of values observed in neighboring basins over comparable periods (Table 9; Anderson and Shean, 2021). This same approach was used to estimate the likely deposit volume associated with early 2000s debris flows in the South Mowich River headwaters (Figure 21A). In both watersheds, a range of plausible estimates were obtained by treating the fractional deposition value as 50 ± 20 percent, with the uncertainty propagated through the analysis.

Storage Changes Along Major River Valleys

Lidar-based estimates of sediment storage changes along the major river valleys from the upper and lower watersheds (Table 6, Table 7; Table 9) were summarized across long reaches for this sediment budget. Within a given period, reaches were sub-divided into spatially coherent extents of net erosion or net deposition, with additional breaks placed at the divide between upper and lower watersheds and at the location of streamgages with sediment load information.

Sediment Delivery from Non-glacial tributaries

Published suspended sediment yields from 10 non-glacial rivers in the region surrounding the study area range from 17 to 690 t/mi²/yr, averaging about 200 t/mi²/yr (Nelson, 1974; Czuba and others, 2012b). Drainage areas of these non-glacial watersheds ranged from 10 to 160 mi², averaging 65 mi². Based on these published values, the spatially averaged sediment yield from non-glacial tributaries across the study area was presumed to be between 100 and 300 t/mi²/yr (that is, 200 ± 100 t/mi²/yr). Czuba and others (2012a) arrived at similar estimates of sediment yields for forested terrain in the Puyallup River watershed by summing expected inputs from roads, landslides, and soil creep. However, Czuba and others (2012a) ultimately calibrated their process-based load estimates using published loads, including several from Nelson (1974), such that this similarity may largely a product of a shared underlying data source. The estimated sediment yield of 200 ± 100 t/mi²/yr was multiplied by the unglaciated contributing area to obtain a range of plausible sediment loads from non-glacial tributaries. Load estimates in tons were then converted into volumes using a bulk density of 1.7 t/yd³.

Measurement-based estimates of sediment transport

The USGS has made suspended sediment and bedload measurements at multiple locations in the Puyallup River watershed over the past 70 years, including at the Puyallup River at Alderton, WA (USGS 12096500), the Puyallup River at East Main Bridge at Puyallup, WA (12096505), the Puyallup River at or near Orting, WA (USGS 12093500 and 12093510), and the Carbon River near Orting, WA (USGS 12094300; U.S. Geological Survey, 2025; Figure 1). The available suspended-sediment data were used to define suspended-sediment concentration (SSC)-discharge rating curves (Figure 27), which were applied to available discharge records to estimate suspended sediment loads over the intervals bounded by repeat topography (Table 10). Bedload fluxes were estimated based on bedload to total load ratios observed in a limited number of paired SSC and bedload samples collected at the three sites (Table C1).

Given the relatively short distance between the Puyallup River at Orting, WA and the Puyallup River near Orting, WA streamgages and the lack of intervening tributaries, data from the two sites were combined and treated as an estimate of loads at the Puyallup River near Orting, WA streamgage. Data from the Puyallup River at Alderton, WA and the Puyallup River at East Main Bridge near Puyallup, WA streamgages were also combined and treated as an estimate of loads at the Puyallup River at Alderton, WA streamgage. A full discussion of the available sediment transport data, the rating curve fitting process, and limitations of the results is presented in Appendix C.

Suspended sediment rating curves for the three sites were based on 7–16 SSC measurements, almost all of which were collected in the mid-1980s. Bedload measurements made in the 1980s were judged to be unreliable; thus, bedload to total load ratios were estimated solely on one to two paired bedload-SSC measurements made at each site in WY 2013/14.

Between 50 and 70 percent of total estimated sediment loads occurred at discharges higher than the highest sampled discharge. The available sediment transport data are then limited in number, out of date, and involve substantial extrapolation above measured values. Although the resulting sediment load estimates are internally consistent and within the range of previously published observations in comparable watersheds around the region (Nelson, 1978; Czuba and others, 2012b; Jaeger and others, 2017; Anderson and others, 2019), they should be viewed as subject to substantial uncertainty.

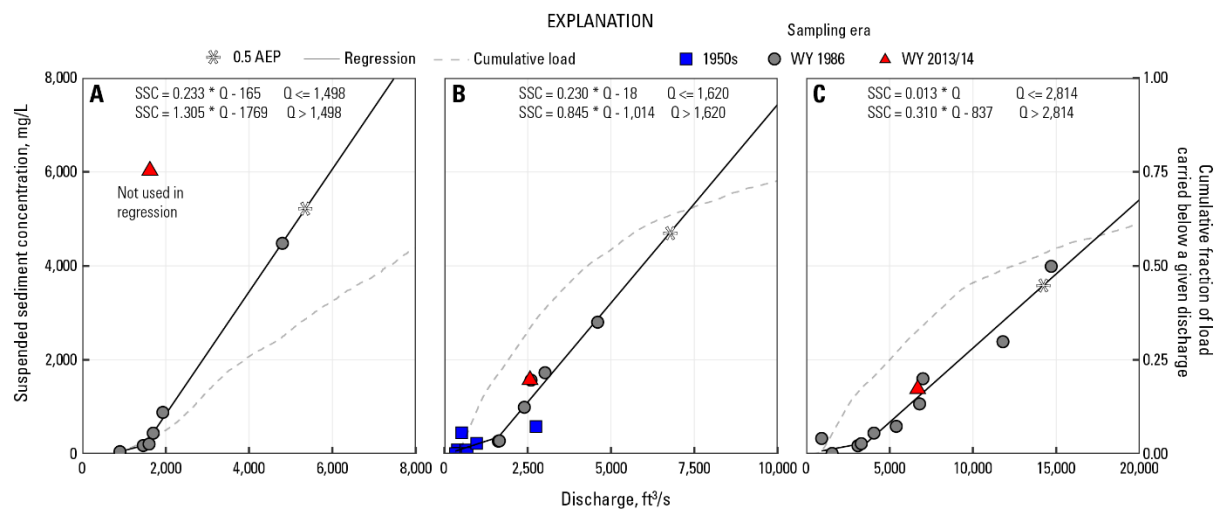


Figure 27. Suspended-sediment concentration (SSC)-discharge relations in the lower Puyallup River watershed, based on discrete SSC measurements, for A) the Carbon River near Orting, WA (USGS 12094300), B) combined records from the Puyallup River near Orting, WA (USGS 12093500) and the Puyallup River at Orting, WA (USGS 12093510), and C) combined records from the Puyallup River at Alderton, WA (USGS 12096500) and the Puyallup River at East Main Bridge at Puyallup, WA (USGS 12096505). Refer to Appendix C for details of input data and regressions. AEP – Annual exceedance probability, per Mastin and others (2016); WY – water year.

Table 10. Summarized sediment loads at selected sites in the lower Puyallup River watershed, 2004 to 2020. [ft³/s – cubic feet per second; mi² – square miles; WY – water year; yr – year]

February 4, 2004 to February 9, 2011									
Site	Site number	Drainage area, mi ²	Mean discharge, ft ³ /s	Three largest peaks, ft ³ /s (WY)	Load, tons/yr		Yield, tons/mi ² /yr		Sand fraction, suspended load
					suspended	bedload	Suspended	bedload	
Puyallup River at Orting	12093500; 12093510	175	740	21,500 (2007) 16,900 (2009) 15,200 (2009)	440,000	50,000	2,550	280	70
Carbon River at Orting	12094300	97	513	17,400 (2007) 14,040 (2009) 13,900 (2009)	390,000	43,000	3,990	440	75
Puyallup River at Alderton	12096500; 12096505	441	1,660	53,600 (2009) 51,600 (2007) 45,600 (2009)	960,000	20,000	2,160	45	66

February 9, 2011 to April 13, 2020									
Site	Site number	Drainage area, mi ²	Mean discharge, ft ³ /s	Three largest peaks, ft ³ /s	Load, tons/yr		Yield, tons/mi ² /yr		Sand fraction, suspended load
					suspended	bedload	Suspended	bedload	
Puyallup River at Orting	12093500; 12093510	175	820	17,200 (2016) 16,600 (2020) 16,500 (2015)	490,000	55,000	2,800	310	70
Carbon River at Orting	12094300	97	540	12,240 (2016) 11,540 (2016) 11,360 (2015)	220,000	25,000	2,310	260	75
Puyallup River at Alderton	12096500; 12096505	441	1,740	35,800 (2016) 34,600 (2020) 30,700 (2015)	750,000	15,000	1,690	35	66

The Carbon River near Orting, WA (USGS 12094300) and Puyallup River at Orting, WA (USGS 12093510), streamgages are located close to the transition between the eroding upper reaches and the depositional lower reaches along the Carbon and Puyallup Rivers, respectively (Figure 1, Figure 7, Figure 13). Conversely, most lowland deposition has occurred upstream of the Puyallup River at Alderton, WA (USGS 12096500; U.S. Geological Survey, 2025) streamgage. The three streamgages with sediment load information then bracket most of the depositional extents of the lower study area, such that the difference between the combined

bedload transport rates at the two upstream gages and the bedload transport rate estimate at the downstream gage provides an independent estimate of bed material deposition rates.

Synthesis of Observed Topographic Change

Compiled topographic changes over the past several decades in the Puyallup River watershed show spatially coherent trends that can be summarized into three major domains (Figure 28). The first and upstream-most domain has been defined by debris flow-related processes. This encompasses debris flow erosion and associated deposition observed in the early period, and the localized remobilization of debris flow material a short distance downstream observed in the late period. This first domain was generally limited to the first several miles downstream of 2022 glacier termini, and in all cases was fully contained within Mount Rainier National Park. The second and most expansive domain encompasses river reaches experiencing net erosion, which extended from roughly the Mount Rainier National Park boundary to the onset of lowland deposition near Orting. The third domain encompasses the depositional lowlands themselves, extending from just upstream of Orting downstream to VM 4 on the Puyallup River, the downstream limits of valid results obtained from repeat lidar. Given that 1984–2009 (Czuba and others, 2010) and 2009–23 repeat cross sections (Figure A1) both showed deposition continuing out the limits of the available data, this depositional third domain can reasonably be extended to the river’s mouth at Puget Sound.

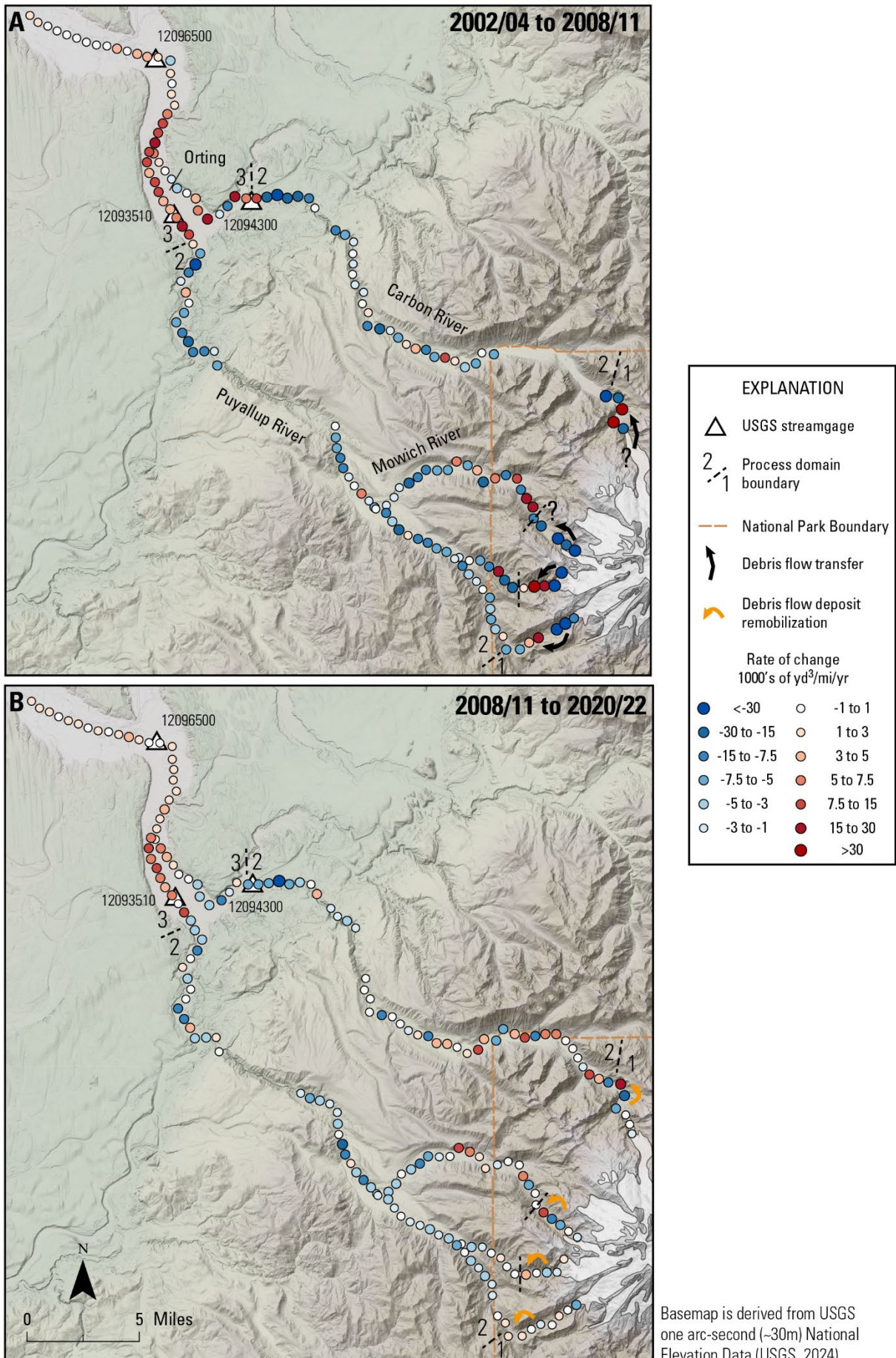


Figure 28. Compiled volumetric rates of change in the Puyallup River watershed from A) 2002/04 to 2008/11 and B) 2008/11 to 2020/22. In A, black arrows indicate specific plot points corresponding to early 2000s debris flow erosion and corresponding downstream deposition. Yellow arrows in B indicate plot points corresponding to erosion of early 2000s debris flow deposits and subsequent redeposition a short distance downstream. Question marks indicate instances in which either debris source area or likely debris flow deposition zones were not covered by repeat topographic data. Approximate boundaries between the three process domains described in the text are shown.

The three major process domains described here are purely a description of observed results for the ~2002–22 study period and do not imply that similar divisions have existed or will exist outside of that time window. This three-part division is also a broad simplification that does not encompass all local variability, such as time-varying trends observed near the Mount Rainier National Park boundary (Table 9) or near VM 6 along the Carbon River (Figure 13).

Watershed Sediment Budgets

The results of the watershed sediment budgets are presented for each of the two periods. Each period section first summarizes the major sources, sinks, and transport rates constrained by direct measurements (Figure 29), which are then integrated with literature-based estimates to develop the full budgets by sub-watershed (Table 11). The results are then aggregated over the full study period and study area to summarize relative sediment delivery to the depositional extents of the lower Puyallup River watershed by source area.

Early period - 2002/04 to 2008/11

Over the early period (2002/04 to 2008/11), net sediment delivery associated with major debris flows from the deglaciated headwaters was estimated to average $225,000 \pm 90,000 \text{ yd}^3/\text{yr}$ (Figure 29; Table 11). From the downstream edge of those debris flow deposits to the onset of deposition in the lower watershed, net erosion occurred along all of the study rivers, delivering material at a rate of $290,000 \pm 80,000 \text{ yd}^3/\text{yr}$. Fifty-five percent of that river valley erosion occurred in the upper Puyallup River watershed and 45 percent from the lower watershed. Deposition in the Puget Sound lowlands down to the USGS streamgage at Alderton was estimated to average $140,000 \pm 40,000 \text{ yd}^3/\text{yr}$. This includes overbank deposition along the Puyallup River.

The combined suspended sediment load passing the Carbon River near Orting, and Puyallup River at Orting streamgages was estimated to average $495,000 \text{ yd}^3/\text{yr}$ (Figure 29). The average estimated suspended load at the Puyallup River at Alderton over this same period was $570,000 \text{ yd}^3/\text{yr}$. The modest increase moving downstream is consistent with expectations that most suspended sediment would pass the lower reaches, with some additional material supplied by lowland tributaries. In contrast, the combined bedload flux from the two upper sites ($55,000 \text{ yd}^3/\text{yr}$) was substantially larger than the bedload flux at Alderton ($11,500 \text{ yd}^3/\text{yr}$), implying net deposition of coarse sediment (sand and gravel) at a rate of about $43,500 \text{ yd}^3/\text{yr}$. This is on the same order of magnitude as rate of floodway deposition estimated from repeat topography within the bounded reaches ($86,000 \pm 28,000 \text{ yd}^3/\text{yr}$; Figure 29).

Estimated sediment delivery from sub-glacial erosion and non-glacial tributaries were combined with estimated deliveries from proglacial debris flows and river valley erosion over the watersheds upstream of the Carbon River near Orting, WA and the Puyallup River at Orting,

WA streamgages. In both watersheds, sub-glacial erosion, net delivery from proglacial debris flows, and net erosion of river valleys over the early period each supplied about one-third of the total estimated sediment inputs (Table 11). Non-glacial tributaries supplied a relatively minor (4 percent) additional amount. In the Carbon River, the sum of sediment inputs matched the rating-curve derived sediment load at the outlet within 15 percent. In the Puyallup River, the estimated sum of inputs was about 75 percent higher than the rating-curve derived sediment load at the outlet.

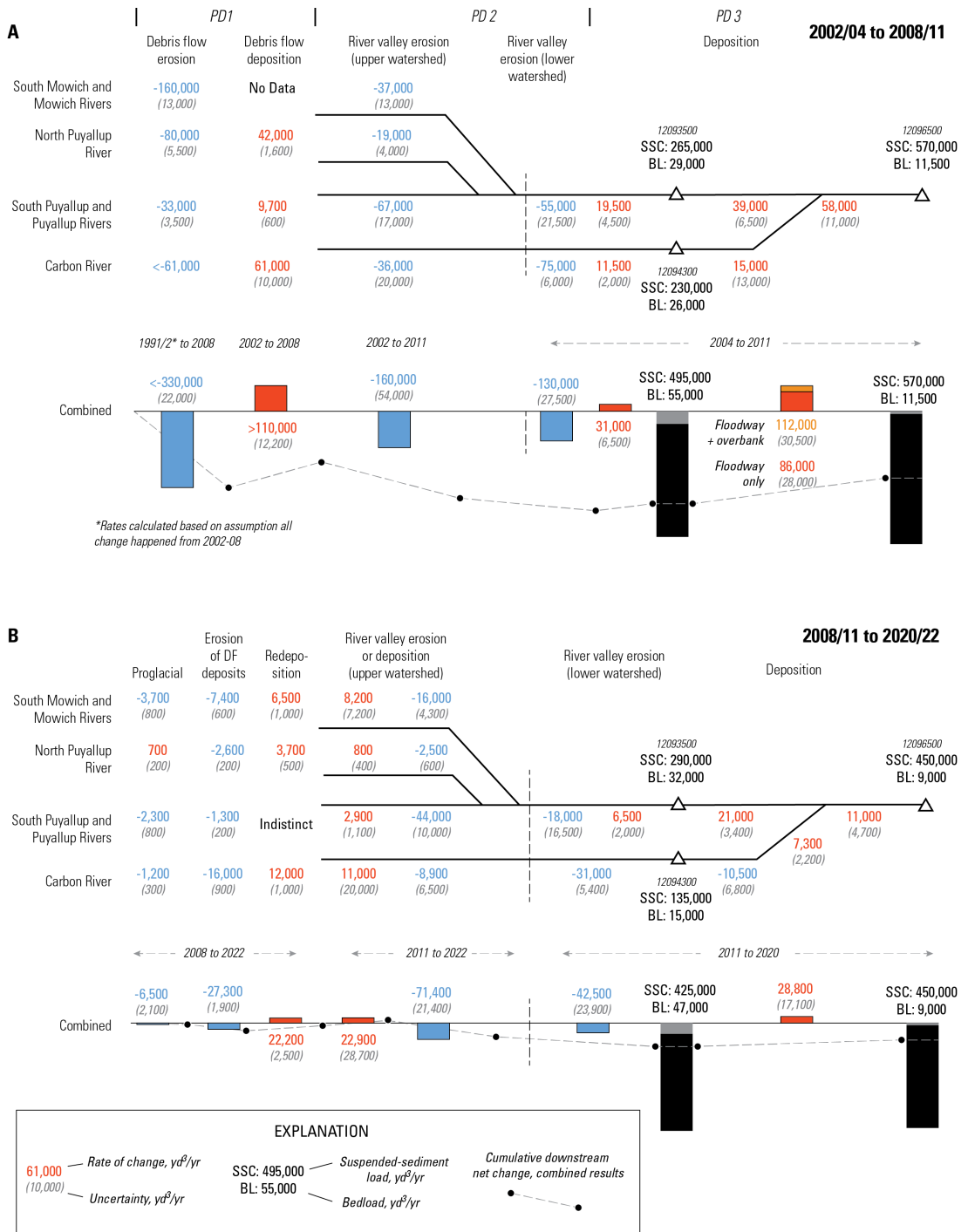


Figure 29. Observed sediment storage changes and estimated sediment transport rates in the Puyallup River watershed over two approximately decade-long intervals. A) Early period, combining observed change and transport over various intervals between 1991 and 2011 (Figure 5). Headwater results based on 1991-2008 differencing were converted to rates under the assumption that all change occurred between

2002 and 2008. B) Late period, combining observed change and transport over various intervals between 2008 and 2022. Primary columns describe the major processes observed in each period, which were largely the same across the different rivers. The relationship between those processes and the three broad process domains described figure 28 are indicated above panel A. DF – Debris flow; PD – Process domain.

Table 11. Sediment budgets for the Puyallup River watershed, partitioned by period and sub-watershed.
[yd³/yr – cubic yards per year]

Early period (2002/04-2008/11)				
	Carbon River		Puyallup River	
	Erosion or transport volume, yd ³ /yr	Percent of total	Erosion or transport volume, yd ³ /yr	Percent of total
Subglacial erosion ¹	97,000 ± 44,000	33 (20-46)	183,000 ± 83,000	36 (23-47)
Deglaciated headwater areas ²	84,000 ± 58,000	29 (11-43)	141,000 ± 32,000	28 (21-36)
Net river valley erosion	100,000 ± 28,000	34 (25-47)	158,000 ± 60,000	31 (21-42)
Non-glacial tributaries ³	12,000 ± 6,000	4 (2-6)	21,000 ± 11,000	4 (2-6)
Total	290,000 ± 80,000	-	500,000 ± 110,000	-
Rating-curve derived total sediment load	255,000 (USGS 12094300)	-	290,000 (USGS 12093510)	-

Late period (2008/11-2020/22)				
	Carbon River		Puyallup River	
	Erosion or transport volume, yd ³ /yr	Percent of total	Erosion or transport volume, yd ³ /yr	Percent of total
Subglacial erosion ¹	97,000 ± 44,000	64 (47-74)	183,000 ± 83,000	65 (49-77)
Deglaciated headwater areas ²	0-20,000	0 (0-12)	0-20,000	0 (0-7)
Net river valley erosion	40,000 ± 12,000	26 (18-39)	74,000 ± 33,000	26 (15-40)
Non-glacial tributaries ³	12,000 ± 6,000	8 (4-13)	21,000 ± 11,000	7 (4-12)
Total	153,000 ± 47,000	-	282,000 ± 90,000	-
Rating-curve derived total sediment load	144,000 (USGS 12094300)	-	320,000 (USGS 12093510)	-

¹ Erosion rate from Mills (1978); Glacier area from Beason and others (2023)

² Net export beyond upland debris flow deposition areas

³ Based on range of yields in Nelson (1974); Czuba and others (2012b)

Late period - 2008/11 to 2020/22

Over the late period (2008/11 to 2020/22), net erosion rates within proglacial areas and along early-2000s debris flow deposits ($34,000 \pm 4,000 \text{ yd}^3/\text{yr}$) were approximately balanced by re-deposition rates of the debris flow material and more diffuse deposition over the next 2-10 miles downstream ($45,000 \pm 31,000 \text{ yd}^3/\text{yr}$; Figure 29). This balance held for each of the four study rivers considered individually. While there was modest net erosion through the sub-aerial parts of the headwaters, an equivalent volume of sediment was deposited over the next 2-10 miles downstream. The aggregate average net change ($-11,000 \pm 35,000 \text{ yd}^3/\text{yr}$) implies that combined net sediment delivery from sub-aerial extents of the headwaters beyond 2–10 miles downstream was most likely less than $24,000 \text{ yd}^3/\text{yr}$, and more plausibly close to zero. Note that these values just describe change observed from repeat topography and do not account for sediment delivery from sub-glacial erosion. Moving downstream, net erosion occurred along all major river valleys from roughly the Mount Rainier National Park boundary to the onset of deposition in the Puget Sound lowlands, with a combined erosion rate of $114,000 \pm 43,000 \text{ yd}^3/\text{yr}$.

As in the early period, the combined suspended load at the two upstream streamgages (average of $425,000 \text{ yd}^3/\text{yr}$) was slightly less than the average suspended load passing the Puyallup River at Alderton, WA streamgage ($450,000 \text{ yd}^3/\text{yr}$), while the combined bedload flux at the two upstream streamgages ($47,000 \text{ yd}^3/\text{yr}$) was substantially higher than at Alderton ($9,000 \text{ yd}^3/\text{yr}$). The bedload imbalance between the streamgages, $38,000 \text{ yr}^3/\text{yr}$, was similar to the observed deposition rate within the bounded reaches ($28,800 \pm 17,100 \text{ yd}^3/\text{yr}$), all of which occurred within the floodway (Figure 7).

Over the late period, sediment budgeting implies total watershed sediment delivery to the Puget Sound lowlands was dominated by sub-glacial erosion (65 percent), with most of the remainder supplied by erosion along the major river valleys (26 percent; Table 11). Non-glacial tributaries supplied an additional 7–8 percent, while the median estimate of the input from the subaerial extents of Mount Rainier was zero. For both the Carbon and Puyallup River watersheds, the sum of estimated inputs matched rating-curve derived sediment load estimates within 15 percent.

Relative Sediment Delivery by Source Area, 2004–20

Averaged over the full study period and aggregated over the two sub-watersheds, the combined sediment inputs from sub-glacial erosion ($280,000 \pm 130,000 \text{ yd}^3/\text{yr}$), net delivery from recently deglaciated areas ($67,000 \pm 27,000 \text{ yd}^3/\text{yr}$), river valley erosion ($180,000 \pm 40,000 \text{ yd}^3/\text{yr}$), and non-glacial tributary inputs ($32,000 \pm 16,000 \text{ yd}^3/\text{yr}$) implied an estimated sediment load of $560,000 \pm 140,000 \text{ yd}^3/\text{yr}$ at the Carbon River near Orting, WA and Puyallup River at Orting, WA streamgages. As percentages, subglacial erosion provided about 50 (95 percent Confidence Interval: 35–61) percent of that total, river valley erosion provided 32 (24–43) percent, recently deglaciated headwaters provided 12 (7–18) percent, and non-glacial tributaries provided 6 (3–9) percent. The total combined sediment load estimated at the two outlet points from sediment rating curves was $500,000 \text{ yd}^3/\text{yr}$, within about 10 percent of the estimate based on summed inputs.

Sediment Budgeting Summary and Limitations

For all the uncertainties in the components of these sediment budgets, the results are both coherent and consistent. The relative magnitudes of the various input areas were generally

similar across the Carbon and Puyallup Rivers within a given period, and the summed input estimates were, with the modest exception of the Puyallup River over the early period, close to rating-curve derived estimates of sediment loads. This does not prove that the results are accurate but improves confidence that the results provide a reasonable guide to broad patterns of sediment delivery.

These sediment budgets imply that upwards of 95 percent of the total sediment load entering the depositional extents of the lower Puyallup River watershed has been balanced by sediment from Mount Rainier or the river valleys connecting Mount Rainier to the Puget Sound lowlands. This is consistent with the order of magnitude difference in sediment yields observed between glacial and non-glacial watersheds in the adjacent Nisqually River watershed (Czuba and others, 2012b). This budgeting further indicates that erosion along the river valleys between Mount Rainier and the Puget Sound lowlands has a key sediment source to the depositional lowlands in recent decades, providing about a third of the total downstream sediment load. From ~2004 to 2020, river valley erosion was second only to sub-glacial erosion as a sediment source, and supplied about three times more sediment than recently deglaciated areas on Mount Rainier.

These results come with several caveats. First, they are specific to the study period and may not be representative of longer-term average conditions. Given that the 20-year study period includes the exceptional debris flows of the early 2000s, the headwater erosion rates estimated over the study period are likely somewhat higher than average rates since at least the 1960s (Anderson and Shean, 2021). Observations along the river valleys are more difficult to contextualize, since it is currently unknown whether the erosion observed here occurred prior to the study period or whether it will continue into the future. It is then unclear if the basic direction

of sediment storage changes along these river valleys is representative of longer-term conditions, let alone the rate.

Second, the results are simply descriptions of bulk volumes of sediment, with no partitioning by grain size or typical transport mode. Most (~90 percent) of the sediment passing the watershed outlets is fine material carried suspension (Table 10). To first order, this sediment budget is probably most directly a suspended sediment budget. The source areas and transport dynamics of sand and gravel may be materially different than fine sediment and can't necessarily be inferred from simple scaling of the watershed sediment budget results presented here.

Long-term Channel Change in the Lower Puyallup River Watershed

The Puyallup River watershed has been subject to substantial natural change and human-caused modification over the past 100–150 years, extending well beyond the ~20-year timescales considered in the previous sections of this report (Czuba and others, 2010). Information about channel change over these centennial timescales is sparse but can provide important historical context for understanding contemporary river form and dynamics, as observed in the White River (Anderson and Jaeger, 2021). For this study, stage-discharge trends were assessed at the three long-term gages along the lower Puyallup River (USGS 12093500, 12096500, and 12101500; Figure 1; U.S. Geological Survey, 2025) using methods identical to those described in “Methods for assessing changes in stage-discharge relations.” Discharge measurement records at the three sites extend back to the early 20th century. Downstream of VM 12, detailed channel surveys from 1907 (Chittenden, 1907) were also used to assess channel planform and elevation change relative to modern (2009 or 2011) conditions. No long-term records of channel change on the Carbon River were available for analysis.

Methods for Assessing Channel Change Using 1907 Surveys

In 1907, Hiram Chittenden led a detailed survey of the lower extents of the White, Green, and Puyallup Rivers in response to the major drainage re-organization that occurred during the 1906 flood (Chittenden, 1907). Those 1907 surveys were preserved in detailed survey sheets, which include planform channel mapping, regular cross section surveys, water surface elevations at the time of survey, and high-water marks from the 1906 flood (Anderson and Jaeger, 2020; Anderson, 2025). These surveys were used to assess planform and vertical changes of the Puyallup River downstream of VM 12 from 1907 to 2009.

Survey sheets were obtained as scanned images and georeferenced based on road and bridge alignments, township and range lines, and prominent topographic features. Elevations from the 1907 surveys were adjusted to reference the North American Vertical Datum of 1988 (NAVD 88) by comparing elevations from 1907 survey points made outside of the river valley floors against 2011 lidar elevations. The mean offset ($Z_{1907} - Z_{2011}$), based on 103 comparison points, was 5.8 ± 2.3 ft (mean \pm one standard deviation). While the offset was noisy, the mean value was consistent along the length of the valley floor. This is also consistent with the expected datum offset between extreme low water in Puget Sound (“Puget Sound Datum”) referenced in the 1907 survey, and NAVD 88, estimated to be between 5.9 and 6.6 ft based on pre-1906 tide heights at Seattle, Washington (NOAA site 9447130; National Oceanic and Atmospheric Administration, 2025). All 1907 survey elevations were then lowered by 5.8 ft to obtain values referencing NAVD 88. These data were used to assess changes in planform position and thalweg

elevation, using channel positions from 2011 lidar and thalweg elevations from the 2009 cross section survey (Czuba and others, 2010) to represent modern conditions.

Long-term Stage-Discharge Trends in the Lower Puyallup River

Stage-discharge trends at the three long-term streamgages in the lower Puyallup River all show substantial lowering over the early- and mid-20th century (Figure 30). Lowering at the Puyallup River at Orting, WA streamgage near VM 22 started around 1960, with stage-discharge relations dropping five feet through 1975 (Figure 30A). This lowering reversed an upward trend that had persisted since the establishment of the streamgage in the 1930s. The onset of lowering at the Puyallup River at Orting, WA streamgage coincided in time with the construction of narrow, straight, levees in the reaches upstream and downstream of the streamgage. Given that channel incision is a common response to straightening (Simon, 1989; Simon and Thomas, 2002), the observed drop in stage-discharge relations through the 1960s may plausibly be a response to those channel modifications.

Lowering at the Puyallup River at Puyallup, WA and Puyallup River at Alderton, WA streamgage started in the 1910s, and has previously been attributed to dredging and river straightening projects conducted in the wake of the 1906 White River avulsion (Sikonia, 1990; Czuba and others, 2010). Both sites show a net drop of about 6 feet in the stage-discharge relations since the start of records in 1914 (Figure 30B, C). At the Puyallup River at Puyallup streamgage, punctuated lowering occurred in the late 1910s and early 1930s, reaching its lowest elevation by the late 1930s. At the Puyallup River at Alderton streamgage, lowering occurred progressively through at least the late 1950s, but then ended sometime before 1990. Gaps in the record preclude a more exact description of the timing and nature of trends at the Alderton streamgage.

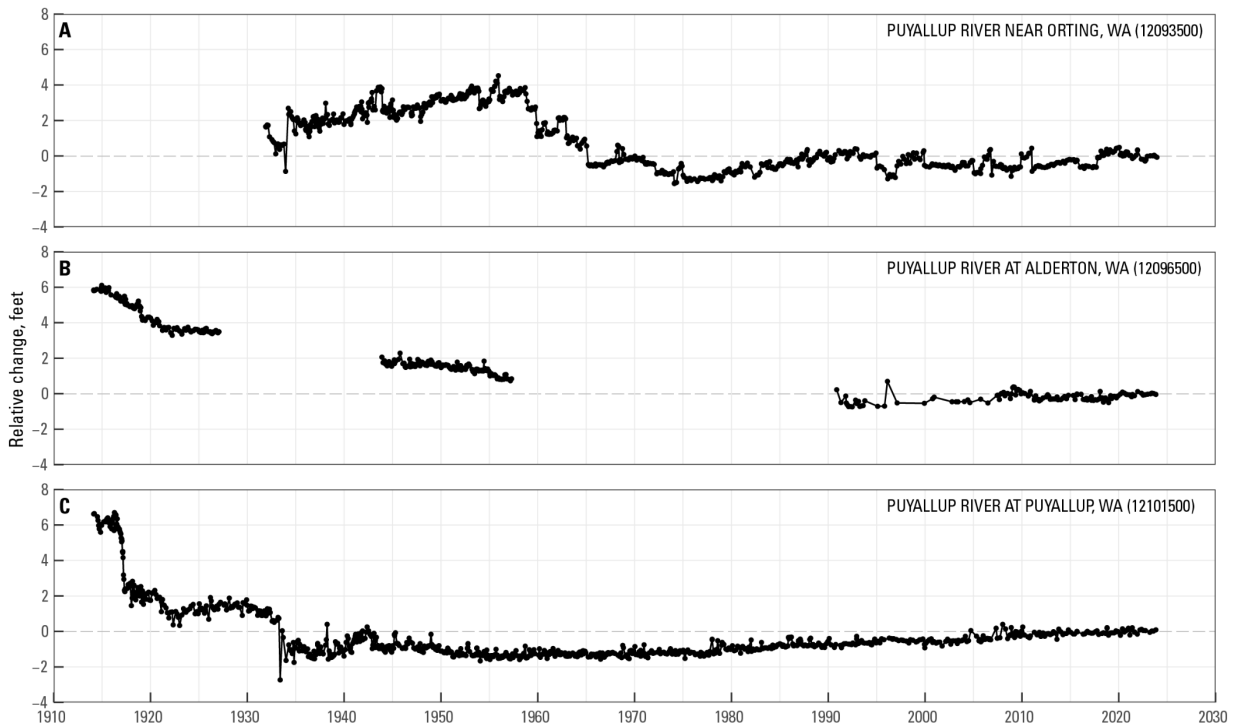


Figure 30. Long-term stage-discharge trends at A) the Puyallup River near Orting, WA (USGS 12093500), B) the Puyallup River at Alderton, WA (USGS 12096500), and C) the Puyallup River at Puyallup, WA (USGS 12101500; U.S. Geological Survey, 2025). Increasing values over time generally indicate aggradation while decreasing values over time indicate erosion, though results are also influenced by changing roughness or width.

After reaching low points in the mid- to late-20th century, stage-discharge relations at all three long-term streamgages have generally been trending back up, though the scale of changes have been small relative to lowering over the early to mid-20th century. The Puyallup River at Puyallup, WA streamgage shows a relatively consistent upwards trend, with stage-discharge relations going up at about 0.25 ft/decade since approximately 1970 (Figure 30C). Changes at the Puyallup River at Alderton, WA and Puyallup River near Orting, WA streamgages show a combination of short-term trends and abrupt shifts that have resulted in net higher stage-discharge relations. The net effect at the Puyallup River at Alderton, WA streamgage has been an

increase of about 0.5 ft since 1990, the start of the most recent period of record. At the Puyallup River near Orting, WA streamgage, there has been a net increase of about 1.5 ft above the low point in the mid-1970s. Most of that increase occurred from the late 1970s to about 1990. Since 1990, change has been marked by variability on the order of 0.5–1.0 ft with little net change. Notably, stage-discharge trends at the Puyallup River near Orting streamgage do not show any obvious response to the re-widening of the surrounding reaches through the 1990s and early 2000s (Figure 2).

Channel Change in the Lower Puyallup River, 1907 to 2009

Comparisons of 1907 and 2011 channel planforms demonstrate that the contemporary Puyallup River downstream of VM 10 is substantially straighter than it was in 1907, a result of manual straightening through the early 20th century (Figure 31; Table 12). This straightening reduced the length of the channel by about 25 percent. In contrast, between VM 10 and 12, the contemporary

channel planform is similar to conditions observed in 1907, both in terms of overall length and specific meander patterns.

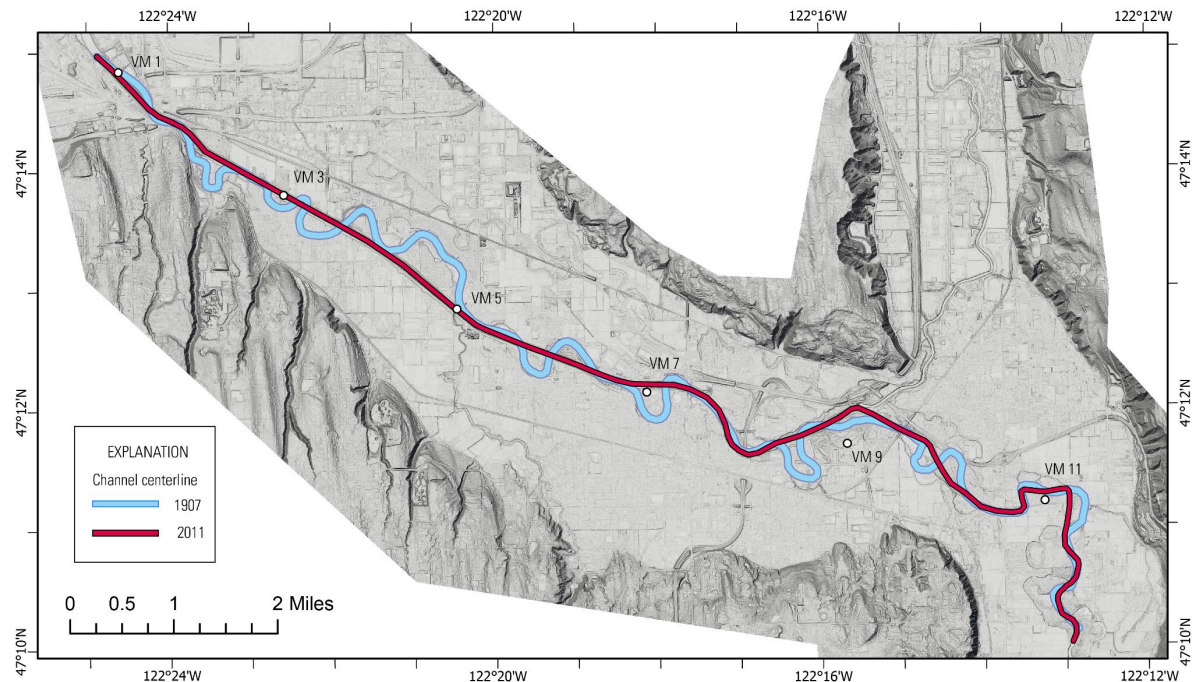


Figure 31. Comparisons of 1907 and 2011 channel centerlines of the lower Puyallup River, Washington.

Base map is derived from 2011 aerial lidar provided by the Washington Geological Survey (2011).

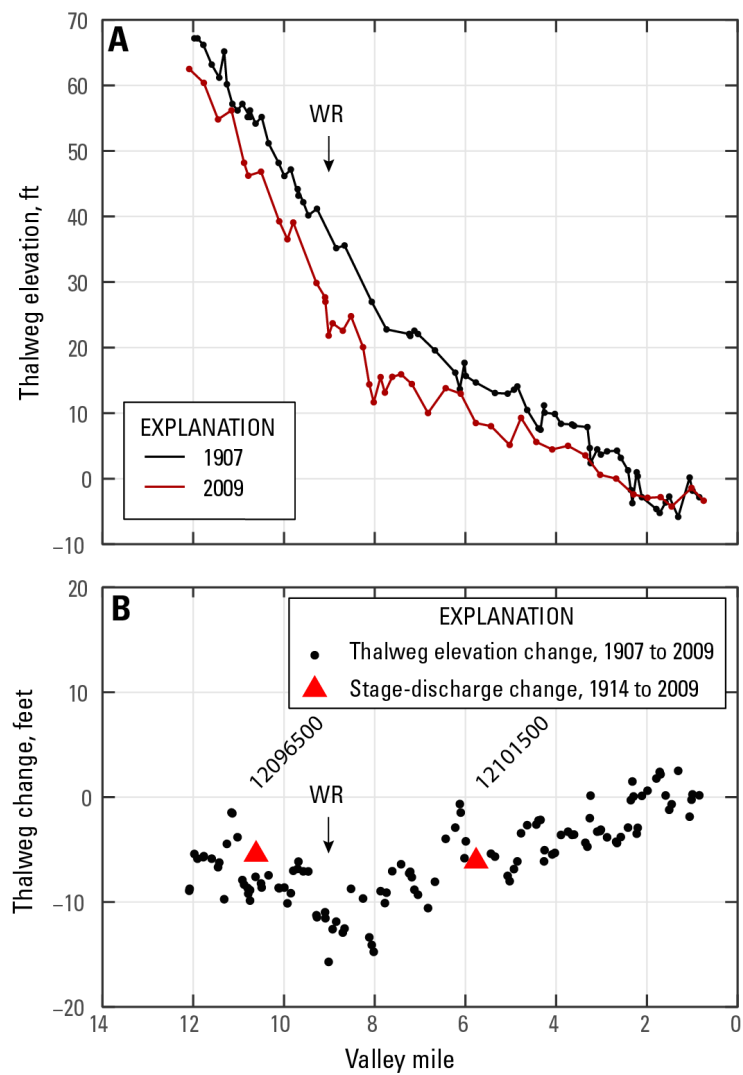


Figure 32. Change in channel thalweg elevations along the lower Puyallup River, Washington, between 1907 and 2009. A) Surveyed thalweg elevations B) Change in thalweg elevations. Vertical channel change inferred from changing stage-discharge relations for the Puyallup River at Puyallup, WA (USGS 12101500) and Puyallup River at Alderton, WA (USGS 12096500) streamgages (Figure 30). WR – White River

Comparison of 1907 and 2009 channel thalweg elevations indicates widespread lowering over the intervening century (Figure 32). Changes in stage-discharge relations from 1914 to 2009

at the two long-term streamgages in the reach corroborate the direction and general scale of lowering observed in the 1907–2009 thalweg elevation comparison, cross-validating the two methods (Figure 32B). Thalweg lowering between 1907 and 2009 was most substantial at the White River confluence (VM 9), where elevations dropped 10–15 ft. The magnitude of lowering then generally declined both upstream and downstream from that confluence. Downstream from the White River confluence, thalweg lowering tapered to essentially 0 feet by VM 2. Upstream from the confluence, lowering tapered to 5–8 feet near VM 12, the upstream limit of the 1907 survey.

Table 12. Comparison of 1907 and 2009 channel characteristics of the lower Puyallup River, Washington.
[VM - valley miles].

	<i>Mouth to White River confluence (VM 0-9)</i>		<i>White River confluence to end of survey (VM 9-12)</i>	
	1907	2009	1907	2009
Channel length, miles	12.15	8.74	4.40	3.61
Channel slope, feet/feet	0.00064	0.00064	0.00125	0.00167
Mean thalweg elevation change, 1907-2009, feet		-5.9		-6.6

Despite substantial changes in planform and profile elevations, the average slope (rise over run) of the Puyallup River downstream of the White River confluence was the same in 2009 as it was in 1907 (Table 12). This is a result of offsetting influences of planform and vertical changes. The modern straightened river has a shorter “run,” which, on its own, would increase slope. However, the spatial pattern of lowering, which was large at the upstream end of the reach but got progressively smaller moving downstream, has reduced the “rise” over this reach. The percent change in rise and run were the same, resulting in no change in the reach-average slope.

This distinct spatial pattern of tapered lowering, on a scale that exactly recovered the pre-modification channel slope, supports an interpretation that lowering of the Puyallup River downstream of the White River confluence was primarily a channel response to the straighter and steeper channel imposed by early-20th century channel modifications. Similar incision in response to river engineering has been documented in rivers around the world (Simon and Hupp, 1987; Harmar and others, 2005; Ylla Arbós and others, 2021) and attributed to the fact that modified channels tend to be shorter (and so steeper), narrower, and/or smoother, all of which would tend to increase shear stress and promote channel incision. This is also consistent with the timing of lowering in the reach, which began coincident with those major straightening projects (Figure 30). Implicit in this interpretation is that the quasi-equilibrium channel slope of the Puyallup River did not change as a result of the new water and sediment inputs from the White River. This interpretation also implies that while dredging and major floods may have influenced local channel change dynamics or the exact timing of channel change, the basic fact that incision occurred, along with the magnitude and spatial pattern of that incision, were primarily dictated by the slope adjustments.

Upstream of the White River confluence, the upstream-tapering pattern of lowering has increased the local channel slope, compounding slope increases associated with modest channel shortening. The 2009 channel slope is about 35 percent steeper than it was in 1907 (Table 12). No data exist to assess how channel elevations or slopes have changed upstream of VM 12 over similar timescales.

Estimated Bedload Transport Capacity Response to Projected Changes in High Flows

There is a broad consensus that changes in climate are likely to increase the frequency and intensity of fall and winter high flows across western Washington rivers (Tohver and others, 2014; Salathé and others, 2014; Mass and others, 2022). Because bedload transport capacity generally increases non-linearly with streamflow (Recking, 2013), changes in the frequency of high flows can increase average bedload transport capacity even if the total annual flow volume does not change. In the sediment-rich Puyallup River, such an increase in bedload transport capacity would likely increase the sediment load delivered to the lower Puyallup River watershed and, in turn, coarse sediment deposition rates (Czuba and others, 2012a). While actual changes in sediment transport and deposition will depend on concurrent changes in sediment supply and reach-scale hydraulics, projections of future streamflow were used to assess the potential scale of changes in bedload transport capacity over the 21st century.

Methods for Assessing Projected Bedload Transport Capacity

There is substantial uncertainty in projections of future regional hydrology, particularly for hydrologic extremes. Chegwidden and others (2019) assessed how sensitive projected changes in flows were to different modeling methodologies for many streamgages across the Pacific Northwest, including the Puyallup River near Orting, WA (USGS 12093500). That assessment included two different emissions scenarios (defined in terms of representative concentration pathways, or RCPs, 4.5 and 8.5, describing moderate and high-end warming scenarios, respectively), ten different climate models, two down-scaling methods, and four hydrologic models. This resulted in 160 different realizations of daily discharge records from

1950 to 2100. RCP 8.5 is generally considered to be an extreme, worst-case emissions scenario that is unlikely to occur (Ritchie and Dowlatabadi, 2017). Results using the RCP 8.5 scenario are then presented as a conservative upper bound on possible future conditions and also provide a measure of the sensitivity of the results to assumptions regarding emissions pathways.

The projected discharge records were assessed via the same methodology described in the “Methods of Characterizing Sediment Transport Capacity” section, in which the power-law bedload-discharge rating curve presented in Figure 37 of Czuba and others (2012a) was applied to each of the 160 daily discharge simulations. As in that previous section, predicted loads were interpreted as approximate estimates of bedload transport capacity and not true estimates of sediment load. For each of the 160 realizations, transport capacity estimates were normalized by the mean annual value from 1977 to 2011, such that the mean value from 1977 to 2011 was exactly one in all 160 realizations. Values in out years then represent relative change from that baseline. The 1977–2011 normalization period represents the intersection of the 1950–2011 calibration period used by Chegwidden and others (2019) and years when historical deposition rates along the Puyallup River are reasonably well known (Figure 17). Model projections then start in 2012 and were summarized over sequential 20-year windows, starting with the truncated window of 2012–2030.

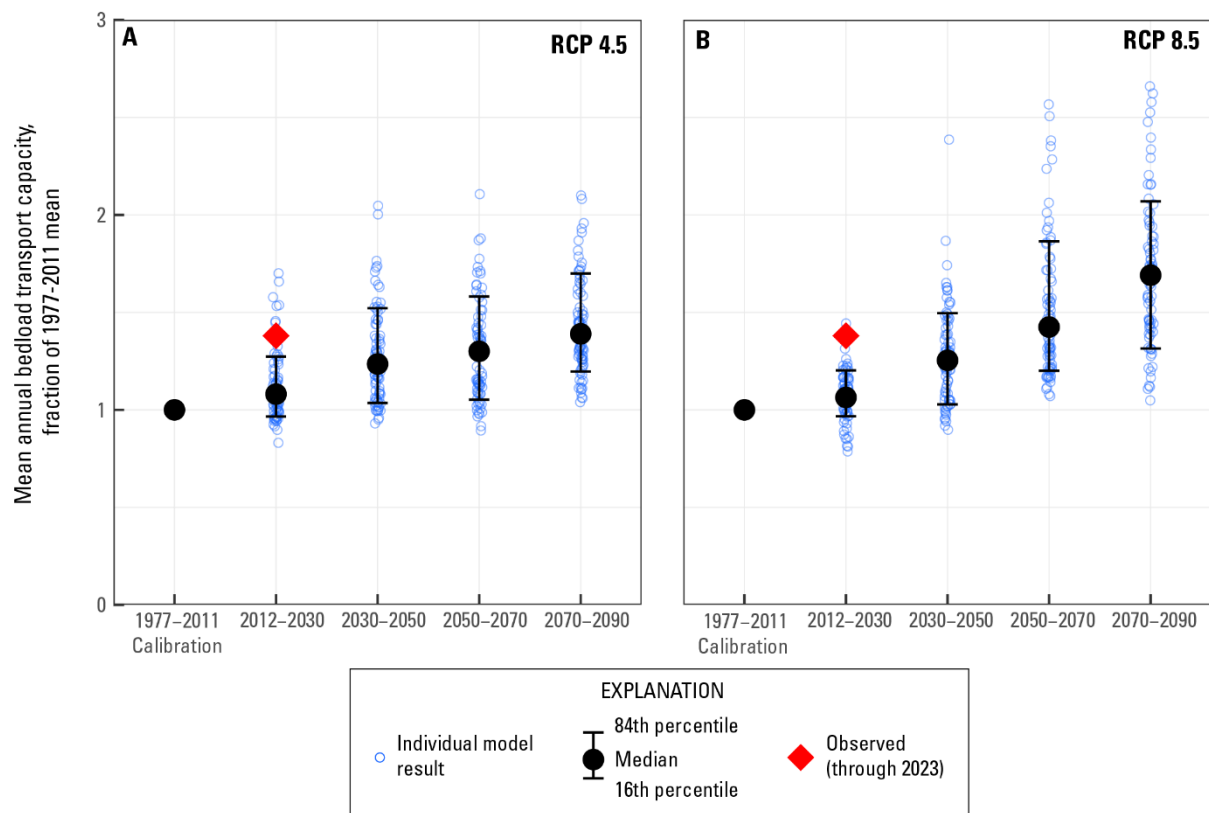


Figure 33. Estimated trends in bedload transport capacity at the Puyallup River near Orting, WA (USGS 12093500) streamgage. Results are based on application of the empirical bedload-discharge rating curve presented in Czuba and others (2012a) to the ensemble of 160 different model realizations of daily discharge presented in Chegwidden and others (2019) using either A) representative concentration pathway (RCP) 4.5 or B) RCP 8.5.

Projected Changes in Bedload Transport Capacity through 2090

Relative to 1977–2011 conditions, discharge projections based on RCP 4.5 show a median increase in bedload transport capacity of 20–25 percent in the mid-21st century, increasing to about 40 percent by the end of the century (Figure 33A). There is substantial spread across the full population of estimates, ranging from essentially zero to 100 percent increases from 2030 through the end of the modeling period. Modeling approaches using RCP 8.5 show modestly larger increases, particularly in the second half of the 21st century, with median estimated increases of about 50 percent in the 2050–70 interval, and nearly 75 percent in the 2070–90 window. The spread of estimates from the different individual realizations ranged from essentially no change to a 200 percent increase in all intervals starting after 2030 (Figure 33B).

These results are similar to results presented in Czuba and others (2012a), who estimated that bedload transport capacity in the White River would increase 30–50 percent by the mid-21st century. Since the results presented here and those in Czuba and others (2012a) both used essentially the same bedload-discharge rating curve to estimate sediment transport capacity, this agreement primarily indicates a consistency in projections of how flows will change over the century.

Applying this same analysis method to the observed discharge values at the Puyallup River near Orting, WA streamgage during 2012–2023 shows a 37 percent increase in estimated bedload transport capacity relative to the 1977–2011 baseline (Figure 33; U.S. Geological Survey, 2025). This is within the range of modeled outcomes for the 2012–2030 interval, though towards the upper end of that range. The Puyallup River was unique among neighboring rivers in

terms of how active 2011-20 flood hydrology was (Figure 18), such that the relatively large increase observed at that site does not seem to be regionally representative.

Summary and Discussion of Major Findings

This report has presented a large swath of analyses of channel change and sediment transport within the Puyallup River watershed, encompassing results from repeat topographic surveys, long-term streamgage records, and estimates of sediment transport (Table 2). Given their breadth, the major findings are summarized here, followed by a discussion of how those findings inform flood hazard management in the lower Puyallup River watershed and broader understanding of sediment delivery and transport across the watershed. Discussion topics cover the spatial patterns of deposition in the lowlands and their potential controls; the expected persistence of flood conveyance benefits from levee setback projects in the lower Puyallup River; and a consideration watershed-scale sources of coarse sediment delivered to the depositional lowlands.

Summary of Major Findings

The major findings of this report are summarized here, organized into three sections corresponding to the three major process domains described in Figure 29—the depositional lowlands, the eroding river valleys, and the headwaters on the flanks of Mount Rainier. Because the eroding river valleys span the upper and lower watershed, the presentation order of findings in this summary differs slightly from ordering in the main text. There are then sections summarizing the integrated sediment budget findings and analyses of longer-term historical channel change and forecasted future changes in bedload transport capacity.

Depositional Lowlands

During 2004–2020, 1.3 ± 0.3 million yd^3 of sediment were deposited along the lower 20 VMs of the Puyallup River (Figure 7; Table 6). Deposition occurred in both the 2004–11 and 2011–20 intervals. About 25–30 percent of this material was deposited in overbank areas outside of the floodway, and the remaining 70–75 percent was deposited within the floodway. The deposition observed from 2004–20 continued a trend that extends back to at least 1976/77 (Figure 17; Prych, 1988; Czuba and others, 2010). Variations in deposition rates since 1976/77 generally correlated with variations in estimated bedload sediment transport capacity between 1977 and 2011. However, during 2011–20, deposition rates dropped with no concurrent change in estimated sediment transport capacity, indicating the variables were no longer correlated (Figure 17, Figure 18). It is unclear whether this represents actual changes in other factors that influence deposition rates, such as sediment supply or local hydraulic conditions, or bias in the discharge records used to estimate transport capacity. Net deposition was also observed over the lower six miles of the Carbon River during 2004–2020 (Figure 13; Table 7). However, the volume (0.15 ± 0.09 million yd^3) was substantially lower than along the Puyallup River.

Observed and Projected Change in Levee Setback Reaches

During 2004–11, volumetric deposition rates along the Soldiers Home levee setback were roughly four times higher than adjacent reaches, with high deposition rates logically related to the setback project itself (Figure 9, Figure 10). In contrast, deposition rates during 2011–20 along the three major levee setback projects downstream of VM 20 on the Puyallup River were not appreciably different from surrounding unmodified reaches. The three major levee setback projects along the lower Puyallup River increased the cross-sectional area of the local floodway, a rough proxy for flood conveyance, by 50 to 200 percent. Assuming recent deposition rates hold

steady, cross-sectional areas within these setback projects would be expected to return to 2004 values by 2050–90 (Figure 12).

Eroding River Valleys

Between the depositional lowlands and approximately the boundary of Mount Rainier National Park, net erosion occurred along most of the length of the Puyallup, Carbon, and Mowich Rivers (Figure 28, Figure 29). Net erosion along these river valleys totaled 3.4 ± 0.6 million yd^3 , equivalent to $190,000 \pm 35,000 \text{ yd}^3/\text{yr}$ (Table 6, Table 7, Table 9). Net erosion was the result of bank and bluff erosion outpacing deposition occurring over lower surfaces in the active channel, as opposed to downcutting across the entire active channel (Figure 9, Figure 15, Figure 25). Substantial net erosion along the Puyallup River upstream of VM 20 from 2004 to 2020 nominally contrasts with substantial 1984–2009 deposition reported between VM 19 and 22 by Czuba and others (2010). However, estimates of 1984–2009 deposition in those upper reaches were likely biased high due to incomplete accounting of bank erosion (Figure 16).

River reaches within Mount Rainier National Park generally saw net erosion during 2002–08 and modest net deposition during 2008–22, with 2002–22 net changes typically within measurement uncertainty (Table 9). Long-term stage-discharge trends on four upland rivers draining Mount Rainier show either net lowering or dynamic variability with no long-term trend over the past 60–100 years (Figure 26).

Recently Deglaciated Headwaters

All four recently deglaciated headwater areas assessed in this study produced major debris flows between 2002 and 2008, due at least in part to an extreme November 2006 storm (Figure 20, Figure 21, Figure 22, Figure 23). Detectable erosion totaled about 2.1 million yd^3

(Table 9), most of which was sourced from erosion along the primary valley floors. These debris flows formed distinct deposits extending one to two miles downstream from source areas, with measured deposition totaling 0.9 ± 0.1 million yd³. In the two watersheds where both debris flow erosion and down-valley deposition were largely captured within the available data extents, deposits accounted for 30 and 50 percent of upstream erosion (Table 9, Figure 24).

During 2008–2022, no major debris flows were observed in any of the four headwater areas, and overall geomorphic change in those headwater areas was relatively modest. All four rivers eroded through the debris flow deposits emplaced over the prior interval but deposited similar volumes of material within about half a mile downstream (Figure 24).

Watershed Sediment Budgets

Topographic change results presented in this study were combined with measurement-based estimates of sediment transport rates in the lower watershed (Figure 27; Appendix C) and literature-based estimates of subglacial erosion and non-glacial tributary sediment yields to construct watershed sediment budgets (Figure 29). During 2004–2020, over 90 percent of the total sediment load entering the depositional extents of the lower Carbon and Puyallup Rivers was balanced by inputs from a combination of sub-glacial erosion (33–60 percent), river valley erosion (25–45 percent), and headwater debris flows (7–17 percent; Table 11). Non-glacial tributaries provided the remaining 3–9 percent. The relative magnitudes of these inputs were consistent across the Carbon and Puyallup River watersheds and, with the exception of the Puyallup River budget from 2004–11, the sum of estimated sediment inputs matched rating-curve derived estimates of sediment loads at watershed outlets within about 15 percent (Table 11). These sediment budgets are necessarily specific to the study period and are most directly a

description of the suspended sediment budget, which makes up most of the total sediment load passing the watershed outlets.

Long-term Historical Channel Change and Projected Changes in Bedload Transport Capacity in the Lower Puyallup River

Comparisons of 1907 and 2011 channel surveys and long-term stage-discharge trends at USGS streamgages both show substantial (4–12 ft) of lowering in the lower 12 valley miles of the Puyallup River (Figure 32). This lowering was inferred to be a response to the substantial straightening, and thus steepening, of the river as a result of early-20th century management actions. Streamgage records near VM 22 similarly show 4–6 ft of lowering coincident with 1960s channel straightening and levee construction in the surrounding reaches (Figure 30).

Projected changes in flood hydrology (Chegwidden and others, 2019) at the Puyallup River near Orting (USGS 12093500) streamgage are projected to increase mean annual bedload transport capacity by 20–60 percent by the mid to late 21st century (Figure 33). Actual changes in deposition rates will also depend on concurrent changes in sediment supply and local hydraulics.

Observed Patterns of Lowland Deposition and Potential Controls

Channel change in the lower Puyallup River watershed over the past several decades has exhibited three consistent patterns: first, deposition has occurred in the lower extents of the Puyallup River over every analysis interval since the start of records in 1977 (Figure 17). Second, while there has also been some net deposition along the lower 6 miles of the Carbon River during 2004–20, deposition rates along the Carbon River have been markedly lower than those observed in the Puyallup River (Table 6, Table 7). Third, in both the Puyallup and Carbon Rivers, the transition from pervasive net erosion to net deposition occurred approximately where

rivers exited post-glacial valley and entered the broader glacial valleys (Figure 28; Collins and Montgomery, 2011). The potential causes of these patterns are discussed in the following subsections, with the primary goal of better understanding whether these patterns are likely to persist in the future. These three sections broadly address (1) why sediment is consistently being deposited in the lower reaches of these rivers; (2) why more sediment is being deposited along the Puyallup River than the Carbon River; and 3) factors that determine where the onset of that deposition occurs.

The Role of Channel Slope in Lowland Sediment Deposition

River channel slope is a primary control on the shear stress acting on a riverbed, which, in turn, defines a river's ability to transport sand and gravel as bedload (Yager and others, 2018). River channel slopes generally decline moving downstream through the Puyallup River watershed, and particularly so where the rivers leave the mountain front and enter the Puget Sound lowlands (Czuba and others, 2012a). Czuba and others (2010, 2012a) pointed to declining slope as a primary cause of deposition in the lower reaches of the Puyallup River watershed, and the low-gradient Puget Sound lowlands have generally functioned as depositional settings over the past 16,000 years since the retreat of continental glaciers (Dragovich and others, 1994, Collins and Montgomery, 2011).

The observations presented in this report support the conclusion that deposition along the lower Puyallup River downstream of VM 20 is fundamentally a product of declining slope through the lower watershed. Supporting observations include the persistence of deposition at relatively consistent rates over the historical record (Figure 17), which is more consistent with a simple structural explanation than a transient channel response to a pulse of sediment supply. Deposition is also a logical outcome of the abundant gravel transport that occurs just upstream of

Orting; given that almost no gravel is expected to exit out into Puget Sound (Czuba and others, 2012a), and that the distance from Orting to Puget Sound is too short for attrition to meaningfully reduce gravel to finer material that could be carried suspension (Pfeiffer and others, 2022), the imbalance between upstream gravel input and downstream gravel output must be accommodated by deposition.

Coherence between measured slope and observed channel change adds additional support to this interpretation (Figure 34). In both rivers, the transition from erosion to deposition occurred when slope drops below ~ 0.007 – 0.010 ft/ft, while the highest rates of deposition along the lower Puyallup River (\sim VM 14–20) correspond to a reach in which slope decreased particularly rapidly moving downstream. The transition to lower deposition rates from VM 9-14 likewise corresponds to a reach in which slope remains more steady moving downstream, though lower deposition rates may also be influenced by an exhaustion of coarse sediment to be deposited and/or extra bedload transport capacity provided by the Carbon River.

Looking forward, reach-scale slopes along the Puyallup River are unlikely to change in a way that reduces or eliminates lowland deposition. Given abundant coarse sediment supply throughout the watershed, and expectations that average sediment transport capacity upstream of the depositional lowlands will remain steady or increase in the coming decades (Figure 33), coarse sediment deposition is likely to be a persistent management issue in the lower Puyallup River.

Assessing how deposition rates may change over time remains difficult. The synthesis of historical deposition rates presented here (Figure 17), estimated impacts of climate on bedload transport capacity (Figure 33), and sediment transport modeling results over multiple periods (Czuba and others, 2010; Appendix A) all show variability within a factor of two, as opposed to

orders of magnitude, providing some sense of potential scale. On their own, projected changes in flood hydrology would be expected to increased sediment transport capacity on the order of 20–60 percent by the mid-21st century (Figure 33), but projecting actual changes in sediment transport rates remains difficult in the absence of a clear understanding of how sediment supply to the lower watershed may change.

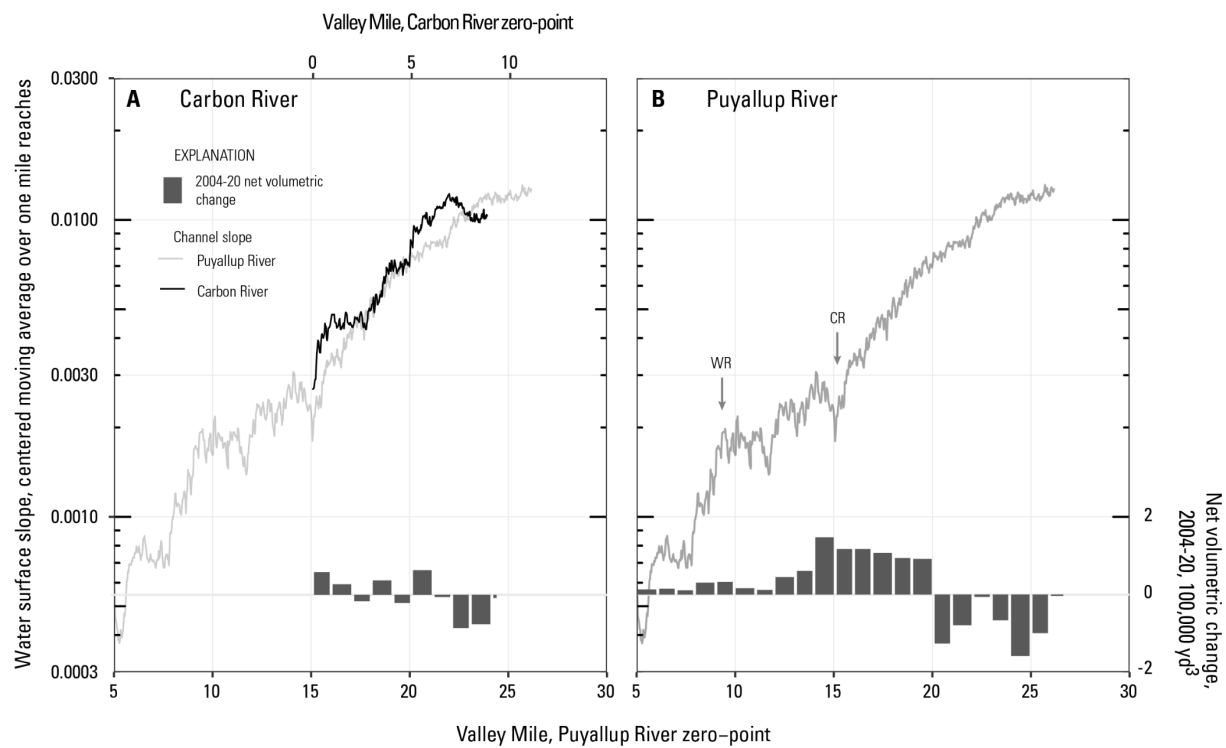


Figure 34. Longitudinal profiles of channel slope in the lower A) Carbon River and B) Puyallup River. Slope of the Puyallup River is also shown in panel A to facilitate direct comparison. Inset bar charts show net volumetric change from 2004–20 based on repeat topographic analyses, summarized over one mile reaches. WR – White River; CR – Carbon River.

Low Relative Deposition Rates of the Carbon River

During 2004–2020, deposition rates per unit valley length in the lower six miles of the Carbon River (~1,500 yd³/mi/yr; Table 7) were about one-sixth of the concurrent deposition rates along the equivalent reach of the Puyallup River (VM 15–20; ~9,200 yd³/mi/yr; Table 6) despite draining watersheds with similar areas and physiographic characteristics. Similarly, Czuba and others (2010) found that 1984–2009 sediment storage changes along the lower Carbon River were neutral to negative, contrasting with widespread deposition observed along the lower Puyallup River over the same period.

Czuba and others (2012a) suggested that the relative lack of deposition in the lower Carbon River was most likely a result of lower rates of incoming bedload. The bedload transport rates estimated in this report partially corroborate this finding, in that the estimated 2004–20 bedload flux at the Carbon River near Orting streamgage was about 60 percent of what passed the Puyallup River at Orting streamgage (Table 10). However, this does not fully explain the six-fold difference in deposition rates. Another possible factor is channel slope, which is, in least in some reaches, modestly steeper than the Puyallup River at equivalent distances upstream from their confluence (Figure 34).

A third plausible factor explaining lower deposition rates on the Carbon River is the additional discharge, and thus increased sediment transport capacity, provided by Voight and South Prairie Creeks, both of which enter the Carbon River near VM 5 (Figure 1). The contributing area of the Carbon River more than doubles as a result of those two tributaries, from 97 mi² near just upstream of the tributary confluences to 228 mi² downstream of those confluences. In contrast, the contributing area of the Puyallup River increases by only 10 percent between the onset of deposition near VM 20 and the Carbon River confluence (VM 15). The

combination of modestly lower incoming coarse sediment loads, modestly steeper channel slopes, and additional discharge from two large lowland tributaries likely all contribute to relatively lower deposition rates in the Carbon River, though the relative importance of these three factors remains unclear.

Looking forward, the location of the lowland tributaries and reach-scale channel slope are functionally fixed over management-relevant timescales. Whether the Carbon River will continue to receive somewhat less incoming bedload than the Puyallup River is less clear. The differences in bedload scale with differences in drainage area and mean runoff volume, suggesting they may be a simple function of transport capacity in transport-limited systems. If so, then it seems likely that the Carbon River will continue to experience lower deposition rates than the Puyallup River barring a major increase in sediment supply specific to the Carbon River.

Geologic Controls on Spatial Patterns of Lowland Deposition

During 2004–20, the Puyallup and Carbon Rivers experienced consistent net erosion through their respective post-glacial valleys, which were created via incision into glacial deposits left by the Cordilleran Ice Sheet (Collins and Montgomery, 2011). Conversely, there was consistent net deposition along the wider glacial valleys, formed over the Holocene through post-glacial sediment deposition (Figure 28). This suggests that modern storage trends could simply represent ongoing landscape adjustments to the retreat of the Cordilleran Ice Sheet about 16,000 years ago. On one hand, this is consistent with Collins and Montgomery's (2011) discussion of an *ongoing* river profile response to continental glacier retreat, and the legacy of continental glaciation clearly continues to influence modern sediment dynamics in the region (for example, Collins and Montgomery, 2011; Scott and Collins, 2021). However, several lines of evidence suggest that an explanation of modern sediment storage trends in the lower Puyallup River

watershed as just an ongoing response to the retreat of continental ice sheets may be overly simplistic.

First, regional studies have generally found that river incision through continental glacial deposits was largely accomplished within several thousand years of initial retreat (Beechie and others, 2001; LaHusen and others, 2016). Direct monitoring of river profile response to modern disturbances corroborates that regional river profile adjustments tend to occur rapidly (Major and others, 2012; Zheng and others, 2014; Ritchie and others, 2018). This implies that, at least in the incising post-glacial valleys, profile adjustments would be expected to be substantially complete. Lateral erosion of glacial deposits can continue to supply sediment long after initial vertical profile adjustments have largely ended (LaHusen and others, 2016; Scott and Collins, 2021), and substantial erosion of tall glacial bluffs in the lower Carbon River provides a clear local example of that on-going impact (Figure 15). However, much of the erosion occurring throughout the lower Puyallup River watershed involved relatively low surfaces likely composed of modern alluvium, not glacial bluffs (Figure 9, Figure 25).

Second, there are multiple more recent disturbances that seem likely to have influenced reach-scale channel geometry and disequilibrium conditions. These include the ~5,600 year old Osceola Mudflow and the 500 year-old Electron Mudflow; a geologic cross section shown on Plate 1 of Crandell (1963) indicates that the modern Puyallup River near VM 24 remains perched well above pre-Electron Mudflow alluvial deposits. Incision triggered by early-20th century channel straightening (Figure 32) may have influenced reach-scale channel geometry and disequilibrium conditions, and the recent removal of confining levees could also be a factor in the Puyallup River between VM 20 and 26 (Figure 2). However, disentangling the relative, and likely interacting, impacts of these historical events is not possible with current data. The fact

that 2004–20 spatial patterns of erosion and deposition correspond to the long-term patterns of landscape response to continental glacier retreat is therefore presented as an observation awaiting a full explanation.

Expected Persistence of Flood Conveyance Benefits from Levee Setback Projects

Levee setbacks have become a key strategy for managing flood hazards in the Puyallup River watershed, increasing the cross-sectional area available to convey high flows. Ongoing deposition in the lower extents of the watershed would be expected to progressively reduce that flood conveyance, gradually undoing the benefits provided by the setbacks. Understanding the timescales over which those reductions occur is important for assessing the viability of individual projects and for developing an integrated long-term flood hazard management plan.

The results presented in this report imply that sediment deposition is expected to progressively reduce the mean floodway cross-sectional areas within the three major levee setback projects downstream of VM 20 back to pre-project conditions (~2004) by 2050–90 (Figure 12). This equates to approximately 30–80 years of flood conveyance benefits since the completion of the projects. These projections rest on two key assumptions: The first is that recent deposition rates do not change markedly in the coming decades. The second is that relative changes in floodway cross-sectional area provide a reasonable proxy for actual changes in flood conveyance. Given relatively modest variability (~factor of two) in deposition rates over the historical period (Figure 17) and the fact that relative changes in flood conveyance have typically scaled closely with changes in channel geometry (Sikonia, 1990), both assumptions are considered reasonable enough that the general timescale of the conveyance benefits—decades, as opposed to years or centuries—is considered reasonable. These estimates could be improved with the use of two-dimensional hydraulic models and channel geometries and vegetation extents

observed in the various lidar datasets to directly assess changes in flood conveyance. Ongoing monitoring of channel change will also help better constrain variability and controls on deposition rates over time.

In theory, levee setbacks, by allowing high flows to spread and slow, may increase local deposition rates (Czuba and others, 2010). High volumetric deposition rates within the Soldiers Home levee setback during 2004–11 provide an example of this dynamic (Figure 10). However, the absence of high deposition rates along the setback projects during 2011–20 suggests that elevated 2004–11 deposition rates may have been contingent on high flows during WY 2007 and 2009 storm events (Figure 3), which allowed sediment-rich water to access lower-velocity areas within the floodway. Regardless, potential increases in volumetric deposition rates (relative to a no-action alternative) does not inherently imply that such setback projects do not provide conveyance benefit; the increase just reduces the expected period of benefits relative to a projection that assumes that the project has no impact on long-term deposition rates. To that point, the cross-sectional area of Soldiers Home levee setback reach as of 2020 remained substantially higher than both pre-project values and in adjacent reaches that have remained in place, elevated 2004-11 deposition rates notwithstanding (Figure 11).

High 2004–11 deposition rates in the Soldiers Home levee setback project were largely the result of widespread deposition across the forested river-left surface reconnected via the setback (Figure 9). Given the height of this surface, much of the deposited material was likely suspended silt and sand. Since the completion of the setback, that forested surface has been progressively eroded away by lateral channel migration at its upstream and downstream ends and through incision of a side channel cut through its middle. All of these erosional processes were generally not possible prior to the levee setback. As that forested surface erodes away, fine

material will be flushed out into Puget Sound, opening up space for flood conveyance and/or future sand and gravel deposition (Nelson and others, 2024). The replacement of hydraulically rough forested surfaces with relatively smooth bare gravel surfaces would also help to maintain flood conveyance. These observations highlight that the long-term conveyance benefits provided by levee setbacks partly depend on the degree to which the river is able to migrate laterally into reconnected overbank areas and re-establish cycles of floodplain turnover (Nelson and others, 2024). How much that occurs is in turn influenced by project design factors, including the overall width and length of setbacks, whether bank protection is fully removed versus truncated or notched, and the presence of local constrictions that may inhibit the development or migration of channel meanders (Nelson and others, 2024).

The degree to which lateral migration influences sediment storage response following a loss of confinement is well illustrated by the Puyallup River between VM 20 and 26. Over those 6 miles, levees have either been eroded away or setback in a way that has allowed the river access to most of the corridor width observed in the 1940s, prior to levee construction (Figure 2). Those reaches have experienced persistent net erosion since 2004 as a result of extensive bank erosion (Table 6). While it remains unclear whether that erosion has been ongoing since the initial loss of confinement in the 1990s, the re-evaluation of 1984–2009 change presented here (Figure 16) indicates that mean channel elevation change over that early period was, at the very least, much lower than reported in Czuba and others (2010). These observations illustrate that increased deposition is not an inherent response to reduced confinement; the sediment storage response to the removal of confining levees may vary widely depending on project design and local geomorphic context.

Finally, while this discussion has focused on levee modifications in the Puyallup River, the re-activation of erosion of the tall glacial bluffs along the Carbon River due to loss of the Ski Park Bluff levee system likely represents one of the more substantial changes to the lower watershed sediment budget in recent years (Table 7; Figure 29). Over the 2004–11 interval, erosion of those bluffs likely provided 10–15 percent of the total sediment load entering the depositional extents of the lower Puyallup River watershed (Figure 29). However, in the absence of information about the relative amounts of coarse and fine material stored in those bluffs, assessing how significant those inputs may be in terms of sand and gravel deposition remains difficult.

Sediment Sources to the Lower Puyallup River Watershed

In the Puyallup River watershed, it has generally been assumed that the recently deglaciated terrain within headwater areas on Mount Rainier are major sources of sand and gravel, such that variations in sediment delivery from those headwater areas were key to understanding downstream sediment transport and channel change (Czuba and others, 2010; 2012b). Rivers linking Mount Rainier to the Puget Sound lowlands have generally been presented as either quasi-equilibrium systems periodically perturbed by pulses of headwater sediment delivery (Czuba and others, 2012a; Ahammad and others, 2021), or, at least in their upper extents, as aggrading in response to an inferred increase in headwater sediment delivery (Beason, 2007; Beason and others, 2014).

In contrast, the results presented here indicate that, at least over the past two decades, rivers upstream of the depositional Puget Sound lowlands have generally been eroding, acting as a substantial source of sediment to the lower Puyallup River watershed (Table 12; Figure 28; Figure 29). Conversely, while erosion rates over recently deglaciated areas on the flanks of

Mount Rainier are unambiguously high when compared to adjacent forested terrain, the net sediment delivery from that erosion has not dominated watershed sediment budgets over the past two decades; net delivery beyond upland zones of debris flow deposition amounted to about 7–18 percent of the total sediment load entering the Puget Sound lowlands, or about a third the volume supplied by river valley erosion (Table 11). Further, that headwater input was almost entirely a product of the large debris flows of the early 2000s. During 2008–2022, erosion of deglaciated headwater areas was small in comparison to sediment transport rates in the lower watershed, and most mobilized material was deposited within several miles of source areas (Figure 29).

Whether recent river valley erosion is representative of long-term conditions remains unclear. Czuba and others (2012a) documented that active channel widths in upland rivers draining Mount Rainier had generally increased from 1994 to 2009. This increase in width was attributed to the active flood hydrology over that time period, contrasting with more muted flood hydrology and limited channel width change observed from 1965–94 (Czuba and others, 2012a; Figure 4). Czuba and others (2012a) noted that this widening could recruit sediment and, combined with approximate of mean bank heights, estimated potential rates of lateral sediment recruitment (1,500–11,000 $\text{yd}^3/\text{mi}/\text{yr}$) that bracket rates observed via repeat lidar since 2002 (1,630–5,600 $\text{yd}^3/\text{mi}/\text{yr}$). Widespread river valley erosion observed here may then be, at least in part, a response to the relatively active flood hydrology since the 1990s (Figure 4), but additional studies would be needed to confirm this hypothesis.

More broadly, results in the Puyallup River add to the growing body of work highlighting that an appreciable fraction of sediment loads in many western Washington rivers may come from erosion of sediment already stored along river valleys (Anderson and others, 2019; Collins

and others, 2019; Anderson and Jaeger, 2021; Scott and Collins, 2021). Conversely, while recently deglaciated areas of regional stratovolcanoes supply a substantial volume of sediment, particularly relative to their relatively small spatial footprint, that input does not dominate watershed-scale sediment budgets (Schwat and others, 2023) and the downstream impacts may be muted by persistent storage of material in upland areas (Anderson and Shean, 2021).

Comparisons with the White River

Observations in the Puyallup and Carbon Rivers are broadly consistent with findings on the White River, both in terms of the high relative importance of river valley erosion as a coarse sediment source to the lowlands and the somewhat ambiguous importance of the deglaciating headwaters (Anderson and Jaeger, 2021). However, there are key differences between observations in the White River and the results presented here, particularly in terms of how lower-watershed channel change over the past decades may relate to early 20th-century disturbances.

In the White River, lower-watershed erosion through its post-glacial valley (the ‘canyon reach;’ Anderson and Jaeger, 2021) was interpreted as a response to the drop in downstream base-level associated with the 1906 avulsion and subsequent dredging (Anderson and Jaeger, 2021). Deposition in the downstream glacial valley (the ‘fan reach’) was, at least in part, attributed to the unique geometry of the valley floor arising from complex patterns of late-Holocene river drainage re-organizations (Anderson and Jaeger, 2021). Spatial patterns of erosion and deposition were logically related to the location of the 1906 avulsion and associated drop in base-level, with an upstream tapering pattern of erosion located upstream of the avulsion node and a relatively abrupt transition to deposition downstream of the avulsion node.

The Puyallup and Carbon Rivers nominally contain all these same features: both rivers have experienced net erosion through their respective post-glacial valley over the past decades, with a relatively abrupt transition to deposition where they enter their respective glacial valleys (Figure 28). Channel elevations in the lower Puyallup River watershed have also lowered substantially in response to 20th century river management activities (Figure 30; Figure 32). However, unlike in the White River, spatial patterns of erosion and deposition over the past several decades in the Puyallup and Carbon Rivers do not show a clear or straightforward relation to early-20th century channel lowering. Most notably, the reaches just upstream of the substantial drop in local base-level near VM 9, at the White River confluence, have been aggrading in recent decades. The downstream drop in base-level at VM 9 was also partly accommodated by steepening of the Puyallup River up to at least VM 12, reducing the relative base-level drop experienced by reaches farther upstream.

Given the limited extents of long-term channel change data, including gaps in river reaches impacted by levee construction through the 1950s and 1960s, and the potential for complex sequences of incision and aggradation in response to a drop in base-level (Schumm, 1993), modern sediment storage trends could still plausibly be substantially influenced by early- and mid-20th century channel lowering. However, at present, the nature of any such influence is unclear and remains unconfirmed.

The White River also differs from the Carbon and Puyallup Rivers in that river valley erosion in the upper White River watershed was a relatively modest and somewhat ambiguous source of sediment to the lower river (Anderson and Jaeger, 2021), contrasting with the substantial inputs observed from the upper Puyallup and Carbon River watersheds (Figure 29). Given that the White River travels over 90 miles between headwaters on Mount Rainier and

Puget Sound, compared to 40–50 miles for the Puyallup and Carbon Rivers (Czuba and others, 2012a), lower average slope along the White River provides one plausible explanation for this difference, though more data on recent erosion rates along the upper White River would be needed to better determine the direction and rate of modern sediment storage trends.

Considerations of Grain Size by Source Area

Most of this report is based on estimates of erosion and deposition that are undifferentiated by grain size. In the Puget Sound lowlands, about 90 percent of the sediment load carried by the Puyallup and Carbon Rivers is fine material (sand, silt and clay) moving in suspension, and so it stands to reason that the sediment budget results presented here are, to first order, primarily an accounting of the sources, sinks, and transport of that finer material. However, sediment deposited in the lower Puyallup River floodway is primarily sand and gravel carried as bedload, such that the coarse fraction of the sediment budget is most relevant for management questions. The varied nature of the sediment sources across the watershed, and the complexities of lateral sediment exchange and attrition, precludes any simple transformation of the total sediment budgets into bed-material load or bedload specific budgets. However, river valley erosion may be a more significant source of downstream sand and gravel than implied by the bulk sediment budgets alone.

Sub-glacial erosion is the dominant watershed source of the total sediment load (Table 11). However, prior studies have suggested that most of the material exiting these glaciers is fine sediment carried in suspension (Fahnestock, 1963; Mills, 1979). While these findings were based on qualitative observations and limited to the summer melt season, the modest rates of channel re-working right at glacier outlets during ‘typical’ hydrologic conditions (for example, Figure 23B; Anderson and Shean, 2021) and the relative absence of cases in which upland deposition

substantially exceeded observed erosion from areas upstream, which would imply an unmeasured source of bed material, provides some support for this claim.

Debris flow source areas on Mount Rainier typically contain a substantial fraction of coarse material (Mills, 1978), but that coarse material is preferentially deposited high in the watersheds (Walder and Driedger, 1994; Scott and others, 1995). The material transported beyond those initial depositional zones is generally composed of finer material, including large volumes of silt, sand, and clay likely to travel in suspension or hyper-concentrated flows. Material sourced from Mount Rainier must also necessarily transit the full length of the river valleys to reach the lowlands, during which time abrasion is likely to break down some fraction of the coarse inputs into finer material. This may be particularly important in areas where volcanic source rocks are hydrothermally altered and relatively weak (Pfeiffer and others, 2022). The estimates of net sediment delivery from headwater debris flows estimated here are then likely to preferentially consist of finer material carried in suspension, while a large fraction of the initially mobilized coarse material has been emplaced in the distinct debris flow deposits. While some of that deposited material was subsequently remobilized, remobilization distances seem to have been less than half a mile over 14 years, implying that ultimately delivery to the lower watershed would require substantial time.

Preferential transport of fine material and abrasion also impact the ultimate grain size of material supplied by river valley erosion, which necessarily involves varied deposits with a wide range of grain sizes. The fact that observed river valley erosion exceeded, by a good margin, both the estimated bedload flux at the onset of lowland deposition and bed material deposition with the Puget Sound lowlands clearly illustrates that a large fraction of the net erosion from the river valleys must be fine material moving in suspension (Figure 29). However, many valley

floor deposits consist of a sizeable fraction of coarse material, and that material is typically entrained into the river, more or less by definition, when and where the river is competent to move bed material downstream. Transport paths to the depositional lowlands may also be relatively short for erosion occurring lower down in the watershed, and because much of the material has already been subject to transport and the loss of relatively weaker clasts, what remains is likely preferentially resistant to abrasion (Pfieffer and others, 2022). River valley erosion then represents a well-connected sediment source with a sizeable fraction of coarse, durable bed material. The arguments presented here largely follow a similar discussion put forth by Scott and Collins (2021) on the potential importance of glacial bluff erosion as a source of bed material in rivers across western Washington State.

Ultimately, the observations presented here do not provide any simple answers to the question of how upland sediment supply and sediment delivery to the Puget Sound lowlands may change in the coming decades. However, these observations indicate that the answer to that question will almost certainly be influenced by sediment storage dynamics down the length of the major river valleys and may not be strongly or directly tied to changing sediment delivery from the exposed flanks of Mount Rainier. Observations in the Puyallup River watershed also do not support the general aggradation of upland rivers downstream of Mount Rainier. While there have been areas subject to local deposition, most notably in areas of distinct debris flow deposition, such areas are fairly limited in extent, while both recent (Figure 24) and long-term (Figure 26) records of channel change generally show neutral to negative sediment storage trends. These results do not negate the hazards posed by lateral channel migration or large floods to infrastructure at Mount Rainier National Park.

Conclusions

Sediment deposition and associated loss of flood conveyance in the lower Puyallup River watershed has been a persistent issue. In recent decades, flood hazard management actions have primarily involved the removal or set back of existing levees, though there have been few assessments of the long-term viability of those projects in the face of on-going deposition, nor is there a clear understanding of whether changes in flood hydrology and/or upstream sediment supply may substantially alter sediment transport and channel change dynamics in the coming decades. The work presented here supports the conclusion that deposition along the Puyallup River downstream of VM 20, and more muted deposition along the lower Carbon River, are both fundamentally a result of downstream declines in channel slope as the rivers enter the Puget Sound lowlands. Given the abundant supply of sand and gravel available to be transported downstream, deposition is likely to continue for the foreseeable future. Recent levee setbacks in the depositional extents of the Puyallup River are estimated to provide several decades of increased flood conveyance relative to 2004 channel conditions. The widespread net erosion that has followed the loss of levee confinement upstream of VM 20 illustrates that the deposition in the lower extents is a product of geomorphic context, and not an inherent response to reduced confinement. Over the past two decades, the river valleys linking Mount Rainier to the Puget Sound lowlands saw widespread erosion, supplying three times more material than recently deglaciated areas on Mount Rainier. While projecting how overall sediment delivery and deposition rates in the lower watershed may evolve in the coming decades remains difficult, the answer is likely to depend strongly on sediment storage dynamics through the major river valleys and not just varying sediment delivery from the flanks of Mount Rainier. Continued watershed-scale monitoring via repeat high-resolution topographic surveys, more accurate and up-to-date

lower-watershed sediment transport estimates, and information allowing for better partitioning of grain size in sediment budgeting would help further improve understanding of sediment and its relation to flood hazard management in the Puyallup River watershed.

References Cited

Ahammad, M., Czuba, J.A., Pfeiffer, A.M., Murphy, B.P. and Belmont, P., 2021. Simulated dynamics of mixed versus uniform grain size sediment pulses in a gravel-bedded river. *Journal of Geophysical Research: Earth Surface*, 126(10), p.e2021JF006194.

Anderson, S.W., Konrad, C.P., Grossman, E.E., and Curran, C.A., 2019, Sediment storage and transport in the Nooksack River basin, northwestern Washington, 2006–15: U.S. Geological Survey Scientific Investigations Report 2019-5008, 43 p., <https://doi.org/10.3133/sir20195008>.

Anderson, S. and Pitlick, J., 2014. Using repeat lidar to estimate sediment transport in a steep stream. *Journal of Geophysical Research: Earth Surface*, 119(3), pp.621-643.

Anderson, S.W., 2019. Uncertainty in quantitative analyses of topographic change: error propagation and the role of thresholding. *Earth Surface Processes and Landforms*, 44(5), pp.1015-1033.

Anderson, S.W. and Konrad, C.P., 2019. Downstream-propagating channel responses to decadal-scale climate variability in a glaciated river basin. *Journal of Geophysical Research: Earth Surface*, 124(4), pp.902-919.

Anderson, S.W., and Jaeger, K.L., 2020, Supporting data for sediment studies in the White River watershed, U.S. Geological Survey data release, <https://doi.org/10.5066/P9HT46KB>.

Anderson, S.W., and Jaeger, K.L., 2021, Coarse sediment dynamics in a large glaciated river system: Holocene history and storage dynamics dictate contemporary climate sensitivity: *Bulletin*, 133(5-6), pp.899-922.

Anderson, S.W., and Shean, D., 2021, Spatial and temporal controls on proglacial erosion rates: A comparison of four basins on Mount Rainier, 1960 to 2017: *Earth Surface Processes and Landforms*, 47(2), pp.596-617.

Anderson, S.W., 2025, Supporting datasets for analyses of sediment transport and channel change in the Puyallup River watershed: U.S. Geological Survey Data Release, <https://doi.org/10.5066/P149MBYG>.

Ballantyne, C.K., 2002. Paraglacial geomorphology. *Quaternary Science Reviews*, 21(18-19), pp.1935-2017.

Beason, S. R. 2007, The environmental implications of aggradation in major braided rivers at Mount Rainier National Park, Washington. Thesis. University of Northern Iowa, Cedar Falls, Iowa, USA

Beason, S.R., L.C. Walkup, and P.M. Kennard, 2014, Aggradation of glacially-sourced braided rivers at Mount Rainier National Park, Washington: Summary report for 1997-2012: Natural Resource Technical Report NPS/MORA/NRTR-2014/910, National Park Service,

Beason, S.R., T.R. Kenyon, R.P. Jost, and L.J. Walker, 2023, Changes in glacier extents and estimated changes in glacial volume at Mount Rainier National Park, Washington, USA from 1896 to 2021: Natural Resource Report NPS/MORA/NRR—2023/2524, National Park Service, 63 p

Beechie, T.J., Collins, B.D. and Pess, G.R., 2001. Holocene and recent geomorphic processes, land use, and salmonid habitat in two north Puget Sound river basins. *Geomorphic processes and riverine habitat*, 4, pp.37-54.

Booth, D.B., 1994. Glaciofluvial infilling and scour of the Puget Lowland, Washington, during ice-sheet glaciation. *Geology*, 22(8), pp.695-698.

Brunner, G.W., 2020: HEC-RAS, River Analysis System Hydraulic Reference Manual: U.S. Army Corps of Engineers Computer Program Documentation CPD-69, 520 p.

Bunte, Kristin; Abt, Steven R. 2001. Sampling surface and subsurface particle-size distributions in wadable gravel- and cobble-bed streams for analyses in sediment transport, hydraulics, and streambed monitoring. Gen. Tech. Rep. RMRS-GTR-74. Fort Collins, CO: U.S. Department of Agriculture, Forest Service, Rocky Mountain Research Station. 428 p.

Chegwidden, O.S., Nijssen, B., Rupp, D.E., Arnold, J.R., Clark, M.P., Hamman, J.J., Kao, S.C., Mao, Y., Mizukami, N., Mote, P.W. and Pan, M., 2019. How do modeling decisions affect the spread among hydrologic climate change projections? Exploring a large ensemble of simulations across a diversity of hydroclimates. *Earth's Future*, 7(6), pp.623-637.

Chittenden, H.M., 1907, Report of an investigation by a board of engineers of the means of controlling floods in the Duwamish-Puyallup Valleys and their tributaries in the state of Washington: Seattle, Washington, Lowman and Hanford S. and P. Co., 32 p.

Chow, V.T. (1959), *Open Channel Hydraulics*, 660 pp., McGraw-Hill Book Company, Inc., New York.

Church, M., 2006. Bed material transport and the morphology of alluvial river channels. *Annu. Rev. Earth Planet. Sci.*, 34(1), pp.325-354.

Cleveland, W.S. and Devlin, S.J., 1988. Locally weighted regression: an approach to regression analysis by local fitting. *Journal of the American statistical association*, 83(403), pp.596-610.

Collins, B.D. and Montgomery, D.R., 2011. The legacy of Pleistocene glaciation and the organization of lowland alluvial process domains in the Puget Sound region. *Geomorphology*, 126(1-2), pp.174-185.

Collins, B.D., Dickerson-Lange, S.E., Schanz, S. and Harrington, S., 2019. Differentiating the effects of logging, river engineering, and hydropower dams on flooding in the Skokomish River, Washington, USA. *Geomorphology*, 332, pp.138-156.

Cook, S.J., Swift, D.A., Kirkbride, M.P., Knight, P.G. and Waller, R.I., 2020. The empirical basis for modelling glacial erosion rates. *Nature communications*, 11(1), p.759.

Copeland, E.A., 2009. Recent periglacial debris flows from Mount Rainier, Washington. Masters Thesis, Oregon State University

Crandell, D.R., 1963, Surficial geology and geomorphology of the Lake Tapps quadrangle, Washington: U.S. Geological Survey Professional Paper 388

Crandell, D.R. and Fahnestock, R.K., 1965: Rockfalls and avalanches from Little Tahoma Peak on Mount Rainier, Washington: U.S. Geological Survey Bulletin 1221A

Crandell, D.R., 1969. Surficial geology of Mount Rainier National Park, Washington: U.S. Geological Survey Bulletin 1288

Crandell, D.R., 1971. Postglacial lahars from Mount Rainier volcano, Washington. U.S. Geological Survey Professional Paper 677, 75 pg.

Crandell, D.R. and Miller, R.D., 1974. Quaternary stratigraphy and extent of glaciation in the Mount Rainier region. Washington. U.S. Geological Survey Professional Paper 847, 59 pg.

Czuba, J.A., Czuba, C.R., Magirl, C.S., and Voss, F.D., 2010, Channel-conveyance capacity, channel change, and sediment transport in the lower Puyallup, White, and Carbon Rivers, western Washington: U.S. Geological Survey Scientific Investigations Report 2010-5240, 104 p.

Czuba, J.A., Magirl, C.S., Czuba, C.R., Curran, C.A., Johnson, K.H., Olsen, T.D., Kimball, H.K., and Gish, C.C., 2012a, Geomorphic analysis of the river response to sedimentation downstream of Mount Rainier, Washington: U.S. Geological Survey Open-File Report 2012-1242, 134 p.

Czuba, J.A., Olsen, T.D., Czuba, C.R., Magirl, C.S., and Gish, C.C., 2012b, Changes in sediment volume in Alder Lake, Nisqually River Basin, Washington, 1945–2011: U.S. Geological Survey Open-File Report 2012-1068, 30 p.

Dietrich, W. E., and Dunne, T., 1978, Sediment Budget for a Small Catchment in Mountainous Terrain: *Zeitschrift für Geomorphologie*, 29, 191-206.

Dragovich, J.D., Pringle, P.T. and Walsh, T.J., 1994. Extent and geometry of the mid-Holocene Osceola Mudflow in the Puget Lowland: Implications for Holocene sedimentation and paleogeography. *Washington Geology*, 22(3), pp.3-26.

Driedger, C.L. and Fountain, A.G., 1989. Glacier outburst floods at Mount Rainier, Washington state, USA. *Annals of Glaciology*, 13, pp.51-55.

Dunne, T., 1986, Sediment transport and sedimentation between RMs 5 and 30 along the White River, Washington: Bellevue, Wash., 39 p.

Erwin, S.O., Schmidt, J.C., Wheaton, J.M. and Wilcock, P.R., 2012. Closing a sediment budget for a reconfigured reach of the Provo River, Utah, United States. *Water Resources Research*, 48(10).

Fahnestock, R.K., 1963. Morphology and hydrology of a glacial stream — White River, Mount Rainier, Washington. *U.S. Geological Survey Professional Paper 422-A*

Fiske, R.S., Hopson, C.A. and Waters, A.C., 1964. Geologic map and section of Mount Rainier National Park, Washington: *U.S. Geological Survey Miscellaneous Geologic Investigations Map I-432*

Fonstad, M.A., Dietrich, J.T., Courville, B.C., Jensen, J.L. and Carboneau, P.E., 2013. Topographic structure from motion: a new development in photogrammetric measurement. *Earth surface processes and Landforms*, 38(4), pp.421-430.

Gessese, A.F., Sellier, M., Van Houten, E. and Smart, G., 2011. Reconstruction of river bed topography from free surface data using a direct numerical approach in one-dimensional shallow water flow. *Inverse Problems*, 27(2), p.025001.

Harmar, O.P., Clifford, N.J., Thorne, C.R. and Biedenharn, D.S., 2005. Morphological changes of the Lower Mississippi River: geomorphological response to engineering intervention. *River Research and Applications*, 21(10), pp.1107-1131.

Herrera Environmental Consultants, 2010, Summary of sediment trends, lower White River—RM 4.44 to RM 10.60: Report prepared for King County, February 10, 2010, Seattle, Wash., 66 p.

James, L.A., 1991. Incision and morphologic evolution of an alluvial channel recovering from hydraulic mining sediment. *Geological Society of America Bulletin*, 103(6), pp.723-736.

Jaeger, K.L., Curran, C.A., Anderson, S.W., Morris, S.T., Moran, P.W., and Reams, K.A., 2017, Suspended sediment, turbidity, and stream water temperature in the Sauk River Basin, Washington, water years 2012–16: U.S. Geological Survey Scientific Investigations Report 2017-5113, 47 p.

Juracek, K.E. and Fitzpatrick, F.A., 2009. Geomorphic applications of stream-gage information. River Research and Applications, 25(3), pp.329-347.

Katz, S., S. Dickerson-Lange, J. Jay, D. STratten, S. Higgins, and T. Abbe. 2022. Puyallup river watershed flood storage assessment. Prepared by Natural Systems Design, Seattle, Washington. Prepared for Floodplains for the Future, Puyallup, Washington. 50 pp.

Konrad, C.P. and Dettinger, M.D., 2017. Flood runoff in relation to water vapor transport by atmospheric rivers over the western United States, 1949–2015. Geophysical Research Letters, 44(22), pp.11-456.

Knuth, F., Shean, D., Bhushan, S., Schwat, E., Alexandrov, O., McNeil, C., Dehecq, A., Florentine, C. and O’Neil, S., 2023. Historical Structure from Motion (HSfM): Automated processing of historical aerial photographs for long-term topographic change analysis. Remote Sensing of Environment, 285, p.113379.

LaHusen, S.R., Duvall, A.R., Booth, A.M. and Montgomery, D.R., 2016. Surface roughness dating of long-runout landslides near Oso, Washington (USA), reveals persistent postglacial hillslope instability. Geology, 44(2), pp.111-114.

Lane, E.W. 1954. The Importance of Fluvial Morphology in Hydraulic Engineering. Hydraulic Laboratory Report No. 372. United States Department of the Interior, Bureau of Reclamation. Denver, CO.

Legg, N.T., Meigs, A.J., Grant, G.E. and Kennard, P., 2014. Debris flow initiation in proglacial gullies on Mount Rainier, Washington. *Geomorphology*, 226, pp.249-260.

Major, J.J., O'Connor, J.E., Podolak, C.J., Keith, M.K., Grant, G.E., Spicer, K.R., Pittman, S., Bragg, H.M., Wallick, J.R., Tanner, D.Q., Rhode, A., and Wilcock, P.R., 2012, Geomorphic response of the Sandy River, Oregon, to removal of Marmot Dam: U.S. Geological Survey Professional Paper 1792, 64 p.

Mantua, N.J. and Hare, S.R., 2002. The Pacific decadal oscillation. *Journal of oceanography*, 58, pp.35-44.

Mass, C.F., Salathé Jr, E.P., Steed, R. and Baars, J., 2022. The mesoscale response to global warming over the Pacific Northwest evaluated using a regional climate model ensemble. *Journal of Climate*, 35(6), pp.2035-2053.

Mastin, M.C., Konrad, C.P., Veilleux, A.G., and Tecca, A.E., 2016, Magnitude, frequency, and trends of floods at gaged and ungaged sites in Washington, based on data through water year 2014 (ver 1.2, November 2017): U.S. Geological Survey Scientific Investigations Report 2016-5118, 70 p.

McCabe, G.J., Clark, M.P. and Hay, L.E., 2007. Rain-on-snow events in the western United States. *Bulletin of the American Meteorological Society*, 88(3), pp.319-328.

Mills, H.H., 1976. Estimated erosion rates on Mount Rainier, Washington. *Geology*, 4(7), pp.401-406.

Mills, H.H., 1978. Some characteristics of glacial sediments of Mount Rainier, Washington. *Journal of sedimentary research*, 48(4), pp.1345-1356.

Mills, H.H., 1979. Some implications of sediment studies for glacial erosion on Mount Rainier, Washington. *Northwest Sci*, 53(3), pp.190-199.

Nelson, A.D., Collins, V.D., Payne, J.S. and Abbe, T.B., 2024. Proactive river corridor definition: Recommendations for a process-based width optimization approach illustrated in the context of the coastal Pacific Northwest. *Wiley Interdisciplinary Reviews: Water*, 11(3), p.e1711.

Nelson, L.M., 1974. Sediment transport by streams in the Deschutes and Nisqually River basins, Washington, November 1971-June 1973. U.S. Geological Survey Open-File Report 74-1078, 33 p.

Nelson, L.M., 1978. Sediment transport by the White River into Mud Mountain Reservoir, Washington, June 1974-June 1976. U.S. Geological Survey Water-Resources Investigations Report 78-133, 26 p.

Nolan, M., Post, A.S., Hauer, W., Zinck, A. and O'Neil, S., 2017. Photogrammetric scans of aerial photographs of North American glaciers. Arctic Data Center. [doi:10.18739/A2VH5CJ8K](https://doi.org/10.18739/A2VH5CJ8K).

National Oceanic and Atmospheric Administration, 2025; water levels for Seattle, Washington (station ID 9447130). Accessed at <https://tidesandcurrents.noaa.gov/waterlevels.html?id=9447130> on September 1, 2025

Nuth, C. and Kääb, A., 2011. Co-registration and bias corrections of satellite elevation data sets for quantifying glacier thickness change. *The Cryosphere*, 5(1), pp.271-290.

Nylen, T.H., 2004, Spatial and temporal variations of glaciers (1913-1994) on Mt. Rainier and the relation with climate: M.S. Thesis, Portland State University, 128 p.

Pfeiffer, Allison M., Susannah Morey, Hannah M. Karlsson, Edward M. Fordham, and David R. Montgomery, 2022, Survival of the Strong and Dense: Field Evidence for Rapid, Transport-Dependent Bed Material Abrasion of Heterogeneous Source Lithology. *Journal of Geophysical Research: Earth Surface* 127, no. 6 (2022): e2021JF006455.

Prych, E.A., 1988, Flood-conveyance capacities and changes in channels of the lower Puyallup, White, and Carbon Rivers in western Washington. U.S. Geological Survey Water-Resources Investigations Report 87-4129, 43 p.

Recking, A., 2013. An analysis of nonlinearity effects on bed load transport prediction. *Journal of Geophysical Research: Earth Surface*, 118(3), pp.1264-1281.

Reid, M.E., Sisson, T.W. and Brien, D.L., 2001. Volcano collapse promoted by hydrothermal alteration and edifice shape, Mount Rainier, Washington. *Geology*, 29(9), pp.779-782.

Ritchie, A.C., Warrick, J.A., East, A.E., Magirl, C.S., Stevens, A.W., Bountry, J.A., Randle, T.J., Curran, C.A., Hilldale, R.C., Duda, J.J. and Gelfenbaum, G.R., 2018. Morphodynamic evolution following sediment release from the world's largest dam removal. *Scientific reports*, 8(1), p.13279.

Ritchie, J. and Dowlatbadi, H., 2017. Why do climate change scenarios return to coal? *Energy*, 140, pp.1276-1291.

Salathé, E.P., Hamlet, A.F., Mass, C.F., Lee, S.Y., Stumbaugh, M. and Steed, R., 2014. Estimates of twenty-first-century flood risk in the Pacific Northwest based on regional climate model simulations. *Journal of Hydrometeorology*, 15(5), pp.1881-1899.

Schwat, E., Istanbulluoglu, E., Horner-Devine, A., Anderson, S., Knuth, F. and Shean, D., 2023. Multi-decadal erosion rates from glacierized watersheds on Mount Baker, Washington, USA, reveal topographic, climatic, and lithologic controls on sediment yields. *Geomorphology*, 438, p.108805.

Scott, D.N. and Collins, B.D., 2021. Frequent mass movements from glacial and lahar terraces, controlled by both hillslope characteristics and fluvial erosion, are an important sediment source to Puget Sound rivers. *Water Resources Research*, 57(4), p.e2020WR028389.

Scott, K.M., Vallance, J.W. and Pringle, P.T., 1995. Sedimentology, behavior, and hazards of debris flows at Mount Rainier, Washington. U.S. Geological Survey Professional Paper 1547, 56 p.

Schumm, S.A., 1993. River response to baselevel change: Implications for sequence stratigraphy. *Journal of Geology*, v. 101, p. 279-294.

Sigafoos, R.S. and Hendricks, E.L., 1972. Recent activity of glaciers of Mount Rainier, Washington. US Geological Survey Professional Paper 387, 23 pg.

Sikonia, W.G., 1990, Sediment transport in the lower Puyallup, White, and Carbon Rivers of western Washington: U.S. Geological Survey Water-Resources Investigations Report 89-4112, 204 p.

Simon, A., and Hupp, C.R., 1987, Channel evolution in modified alluvial streams.

Transportation Research Record, p. 9

Simon, A., 1989. A model of channel response in disturbed alluvial channels. *Earth surface processes and landforms*, 14(1), pp.11-26.

Simon, A. and Thomas, R.E., 2002. Processes and forms of an unstable alluvial system with resistant, cohesive streambeds. *Earth Surface Processes and Landforms*. The Journal of the British Geomorphological Research Group, 27(7), pp.699-718.

Smith, D.L., Miner, S.P., Theiling, C.H., Behm, R.L. and Nestler, J.M., 2017. Levee setbacks: an innovative, cost-effective, and sustainable solution for improved flood risk management. US Army Engineer Research and Development Center, Environmental Laboratory.

Tohver, I.M., Hamlet, A.F. and Lee, S.Y., 2014. Impacts of 21st-century climate change on hydrologic extremes in the Pacific Northwest region of North America. *JAWRA Journal of the American Water Resources Association*, 50(6), pp.1461-1476.

Turley, M., Hassan, M.A. and Slaymaker, O., 2021. Quantifying sediment connectivity: Moving toward a holistic assessment through a mixed methods approach. *Earth Surface Processes and Landforms*, 46(12), pp.2501-2519.

U.S. Geological Survey, 2024, USGS 1 Arc Second Digital Elevation Models – USGS National Map 3DEP Downloadable Data Collection, accessed August 15, 2024 at
<https://www.usgs.gov/the-national-map-data-delivery>

U.S. Geological Survey, 2025, USGS water data for the Nation: U.S. Geological Survey National Water Information System database, accessed June 10, 2025, at
<https://doi.org/10.5066/F7P55KJN>.

Vallance, J.W. and Scott, K.M., 1997. The Osceola Mudflow from Mount Rainier: Sedimentology and hazard implications of a huge clay-rich debris flow. Geological Society of America Bulletin, 109(2), pp.143-163.

Walder, J.S. and Driedger, C.L., 1994. Rapid geomorphic change caused by glacial outburst floods and debris flows along Tahoma Creek, Mount Rainier, Washington, USA. Arctic and Alpine Research, 26(4), pp.319-327.

Walling, D.E. and Collins, A.L., 2008. The catchment sediment budget as a management tool. Environmental science & policy, 11(2), pp.136-143.

Washington Geological Survey, 2003, Rainier West 2002 project [lidar data]: originally contracted by National Aeronautics and Space Administration. [accessed Dec. 1, 2022, at <http://lidarportal.dnr.wa.gov>]

Washington Geological Survey, 2005, Puget Lowlands 2005, Pierce County 2004 sub-project [lidar data]: originally contracted by the Puget Sound Lidar Consortium. [accessed Dec. 1, 2022, at <http://lidarportal.dnr.wa.gov>]

Washington Geological Survey, 2009, Rainier 2007 project [lidar data]: originally contracted by the National Park Service. [accessed Dec. 1, 2022, at <http://lidarportal.dnr.wa.gov>]

Washington Geological Survey, 2011, Pierce 2011 project [lidar data]: originally contracted by Pierce County. [accessed Dec. 1, 2022, at <http://lidarportal.dnr.wa.gov>]

Washington Geological Survey, 2020, Pierce 2020 project [lidar data]: originally contracted by Pierce County. [accessed Dec. 1, 2022, at <http://lidarportal.dnr.wa.gov>]

Washington Geological Survey, 2022, Surface geology 1:250,000-GIS data, May 2022: Washington Geological Survey Digital Data Series 26, version 4.0, previously released June 2010.

Washington Geological Survey, 2023a, Puyallup Watershed Wall 2022 project [lidar data]: originally contracted by Washington Dept. of Natural Resources. [accessed Dec. 1, 2022, at <http://lidarportal.dnr.wa.gov>]

Washington Geological Survey, 2023b, Rainier Wali 2022 project [lidar data]: originally contracted by Washington Dept. of Natural Resources. [accessed Dec. 1, 2022, at <http://lidarportal.dnr.wa.gov>]

Wheaton, J.M., Brasington, J., Darby, S.E. and Sear, D.A., 2010. Accounting for uncertainty in DEMs from repeat topographic surveys: improved sediment budgets. *Earth surface processes and landforms: the journal of the British Geomorphological Research Group*, 35(2), pp.136-156.

Wheaton, J.M., Brasington, J., Darby, S.E., Kasprak, A., Sear, D. and Vericat, D., 2013. Morphodynamic signatures of braiding mechanisms as expressed through change in sediment storage in a gravel-bed river. *Journal of Geophysical Research: Earth Surface*, 118(2), pp.759-779.

Yager, E.M., Venditti, J.G., Smith, H.J. and Schmeeckle, M.W., 2018. The trouble with shear stress. *Geomorphology*, 323, pp.41-50.

Ylla Arbós, C., Blom, A., Viparelli, E., Reneerkens, M., Frings, R.M. and Schielen, R.M.J., 2021. River response to anthropogenic modification: Channel steepening and gravel front fading in an incising river. *Geophysical Research Letters*, 48(4), p.e2020GL091338.

Zheng, S., Wu, B., Thorne, C.R. and Simon, A., 2014. Morphological evolution of the North Fork Toutle River following the eruption of Mount St. Helens, Washington. *Geomorphology*, 208, pp.102-116.

Appendix A—Supplemental Channel Change Analyses

As part of this work, several analyses of channel change were conducted that provided cross-validations or interesting comparisons with the lidar-based change estimates but did not materially add to understanding of watershed-scale sediment dynamics beyond what was already gleaned from those lidar-based analyses. The first was an assessment of 2009–23 change based on repeat cross-section surveys, which provided a rough cross-validation of 2011–20 repeat lidar change estimates. The repeat cross sections also provide estimates of channel change in the tidally influenced lower four miles of the Puyallup River, where the discharge-normalization approach to lidar differencing used here are not applicable. The second was a comparison of observed 2004–20 channel change against modeled estimates of channel change presented in Czuba and others (2010) based on one-dimensional HEC-RAS sediment transport modeling, providing a test of whether relatively simple sediment transport modeling was able to predict the observed channel change trends in the lower Puyallup River watershed.

Channel Change Estimates from Repeat Cross Sections, 2009 to 2023

In the summer of 2023, David Evans and Associates, Inc., (DEA) re-surveyed cross sections surveyed in 2009 by Czuba and others (2010), including 80 sections on the Puyallup River between its mouth and VM 25 and 17 sections on the Carbon River between its confluence with the Puyallup River and VM 8 (Figure 1; Anderson, 2025). Surveys were conducted using a combination of differential Global Navigation Satellite System (GNSS) and boat-based single-beam depth sounders; refer to Anderson (2025) for details. These data were used to assess channel change during 2009–2023.

The first goal of this analysis was to provide a check on channel change estimates based on 2011–20 aerial lidar, particularly in the confined lower reaches of the watershed where lidar-based change estimates primarily involve comparisons of discharge-normalized water surface elevations. The second goal was to assess how well repeat cross sections at the spacing used by Czuba and others (2010) are able to estimate reach-scale channel change. That second goal was accomplished by comparing change from 2011–2020 repeat aerial lidar against change estimated from synthetic 2011 and 2020 cross sections cut from those same lidar datasets at the locations of 2009 and 2023 cross section surveys. Because these synthetic cross sections are just a down-sampled version of the full lidar datasets, differences between change estimates from the two sources are an indication of how much error may be introduced via interpolation of cross section survey data.

Comparisons of elevation and horizontal positions of stable levee crests in 2009 and 2023 datasets showed no significant or systematic offsets between the two datasets; thus, no adjustments were made to the 2023 data prior to assessing change. For all 97 cross sections, change in cross-sectional area and mean elevation was assessed over the overlapping extents of the two surveys. Volumetric change from repeat cross sections was estimated using average end-area methods (Czuba and others, 2010).

Synthetic 2011 and 2020 cross sections were created by sampling aerial lidar from 2011 and 2020 at the locations of the 2009 and 2023 survey points, respectively. Mean elevation and volumetric change were assessed based on these synthetic cross sections using the same methods described for the 2009–23 change analysis.

Comparisons of local mean elevation change estimated from 2009–23 repeat surveys against local mean elevation change estimates based on 2011–20 synthetic cross sections provide

a spatially consistent comparison of the two survey methods, addressing the question of whether the discharge-normalization process accurately captures the broad trends observed in the repeat cross sections. This is an imperfect check, given that 2009–23 interval encompasses five years more change than the repeat lidar. Because the different time intervals of analysis would most likely reduce agreement between the methods, rather than improve it, the comparison is considered a conservative estimate of methodologic agreement.

In contrast, the comparison of reach-scale volumetric change based on end-area averaging methods applied to synthetic 2011 and 2020 cross sections against results from the continuous 3.3 ft resolution 2011–20 repeat lidar differencing indicates how much error might be introduced by interpolating change between discrete cross section estimates. For the purposes of that comparison, 2011–20 repeat lidar results were limited to change in the floodway zone in the Puyallup River and the active channel zone in the Carbon River, excluding overbank deposition in the Puyallup River and bank erosion in the Carbon River. This better aligned the lidar results with the spatial extent of the 2009 and 2023 cross sections, which typically did not extend out into overbank deposition areas or up the full height of bluffs along the Carbon River.

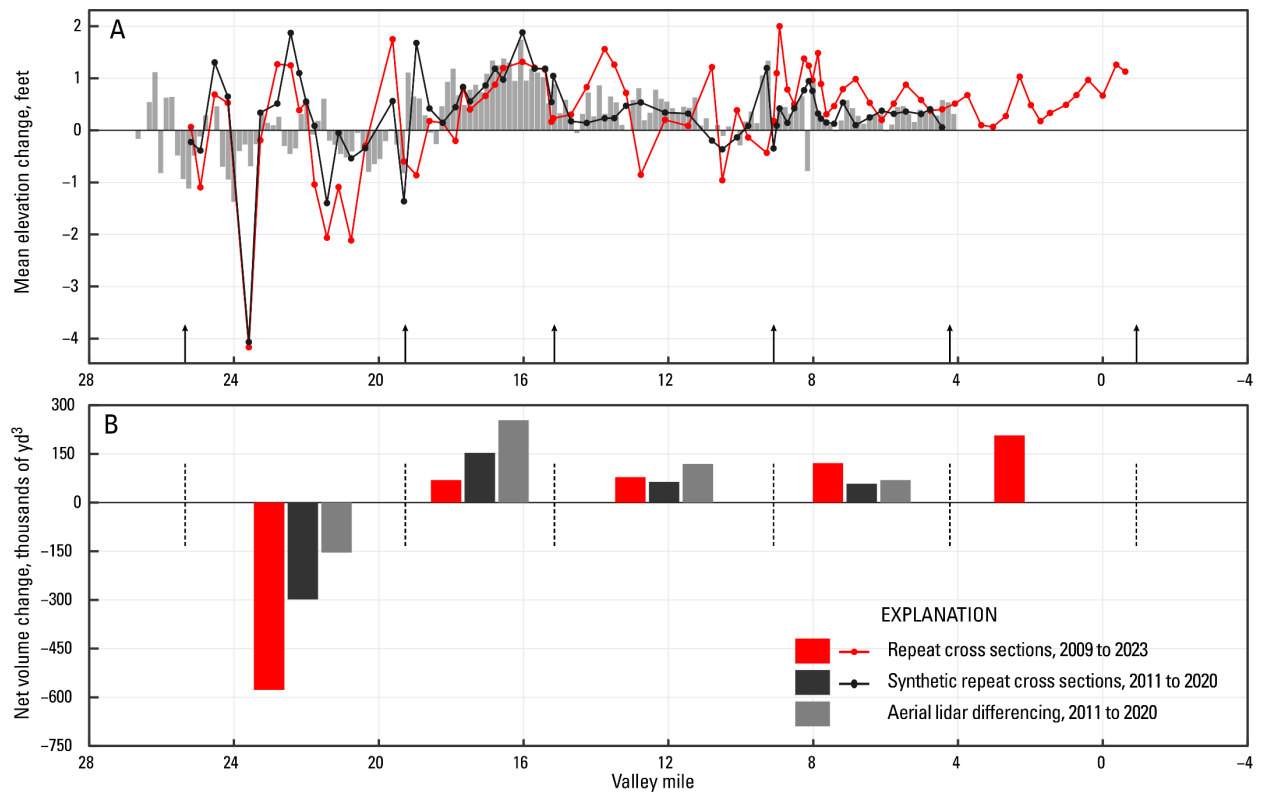


Figure A1. Comparisons of change in the Puyallup River based on 2009–23 repeat cross sections and 2011–2020 repeat aerial lidar in terms of A) mean elevation change and B) volumetric change, summarized over several sub-reaches. Differences between results from the synthetic 2011–2020 repeat cross sections and the full lidar differencing indicate the scale of error that may be introduced by using cross sections at current spacings to interpolate reach-scale estimates of volumetric change.

Cross Section-Based Estimates of Channel Change, 2009–23

In the Puyallup River, channel change estimated from 2009 and 2023 repeat cross sections indicates net erosion upstream of VM 20, albeit with substantial local variability, and net deposition downstream (Figure A1A). There is a reasonable correspondence between local change observed in 2009–23 repeat cross sections and 2011–20 synthetic repeat cross sections, particularly upstream of VM 15. The repeat cross sections also indicate there was 0.5–1.0 ft of

mean elevation increase in the reach downstream of VM 4, beyond the limits of usable repeat lidar results, with the largest changes occurring downstream of VM 2. Total volumetric deposition downstream of VM 4 from 2009 to 2023 was approximately 180,000 yd³.

Volumetric change estimated from synthetic 2011–20 cross sections was up to a factor of two different than the volumetric change estimated from the full 2011–20 repeat lidar (Figure A1B). Moreover, the fact that the synthetic cross sections correctly show net erosion upstream of VM 20 is also entirely the result of significant local lowering measured in one section near VM 24, where the section cut crossways through a localized scallop of bank erosion. Omitting that cross section from the change analysis would result in an estimated net change of weak aggradation from VM 20 to 24 (not shown).

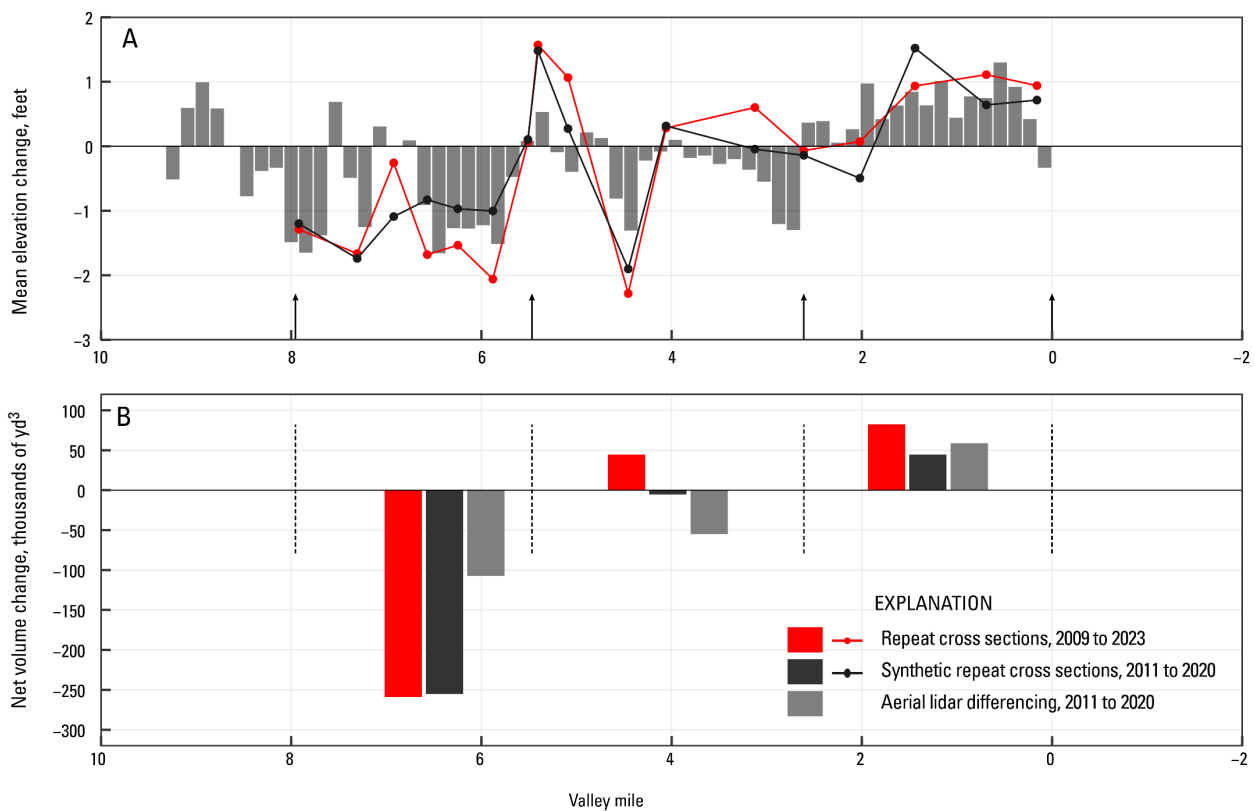


Figure A2. Comparisons of change in the Puyallup River based on 2009–23 repeat cross sections and 2011–2020 repeat aerial lidar in terms of A) mean elevation change and B) volumetric change, summarized over several sub-reaches. Differences between results from the synthetic 2011–2020 repeat cross sections and the full 2011–20 lidar differencing solely reflect the impact of the reduced spatial resolution of the synthetic cross sections.

In the Carbon River, local mean elevation changes from 2009–23 repeat cross sections generally match change estimated from synthetic 2011–2020 cross sections within 0.7 ft, with clear correspondence in terms of general spatial trends (Figure A2). As with the Puyallup River, reach-scale volumetric change estimated from synthetic 2011–20 cross sections was up to a factor of two different than estimates from the full 2011–20 lidar differencing, though the repeat cross sections do capture the general trend of net erosion upstream of VM 6 and net deposition downstream.

Taken together, the reasonable agreement between at-a-section change estimates from 2009–23 repeat cross sections and the 2010–20 synthetic cross sections increases confidence that results based on discharge-normalized repeat aerial lidar provide usable estimates of channel change in the Puyallup River watershed. This is particularly true given that some of the disagreement that exists likely indicates real change that occurred during 2009–2011 and 2020–2023. The 2009–23 cross section comparison also indicates that approximately 180,000 yd³ of sediment accumulated along the tidally influenced lower four VMs of the Puyallup River (Figure A1), where the repeat lidar analysis was unable to provide information.

In contrast, the comparison of change estimates from synthetic 2011–20 cross sections against the full 2011–20 repeat lidar results indicate that the cross section spacing used by Czuba and others (2010) is likely not dense enough to provide accurate reach-scale estimates of volumetric change within a factor of two. This is particularly true in the relatively wide and braided reaches of the Puyallup River upstream of VM 20, where estimates of reach-scale volumetric change based on synthetic 2011–20 cross section only got the basic direction of change correct because of substantial negative change observed in a single unrepresentative cross section. In those upper reaches, it seems plausible that the current cross section spacing could get the sign of the change wrong and not just the rate.

Comparisons of Observed and HEC-RAS Model-Estimated Channel Change

Czuba and others (2010) used a one-dimensional HEC-RAS sediment transport model to estimate bedload transport and channel change along the lower Puyallup and Carbon Rivers. Here, modeled estimates of net erosion and deposition by reach were compared against observed change from 2004 to 2020 to assess how well that model was able to capture broad spatial trends.

The sediment transport model used by Czuba and others (2010) was developed using cross sections and bed material grain size distributions collected in 2009. Bedload transport was estimated using the Wilcock and Crowe (2003) equation and validated using the limited available bedload measurements from the late 1980s (Sikonia, 1990). The derived bedload-discharge rating curve for the Carbon River was used to estimate sediment inputs from the two major lowland tributaries entering that river (South Prairie Creek and Voight Creek; Figure 1). Input cross sections were limited to the within-bank extents, and hydraulic output was not calibrated for large floods. Coupled with the relative scarcity of sediment transport validation data, Czuba and others (2010) presented model results as approximate and best used to assess broad spatial trends or relative differences between model runs with different management options implemented.

Czuba and others (2010) presented model output using hydrology from WYs 1999 to 2003, a period of relatively moderate flood hydrology, and from WYs 2005 to 2009, a period with significant high flows. Spatial patterns and average rates of bedload transport for the two intervals were almost identical (refer to Czuba and others, 2010, figures 49 and 51). The comparison with observed change presented below is based on the WYs 1999–2003 output, though using the WYs 2005–09 output would not materially change the results. Given the similarity in model output using the two different hydrologic inputs, and the fact that the model was developed using channel and grain size information collected near the middle of the 2004–20 study period used in this report, model output was interpreted here as a general estimate of average trends as opposed to an estimate of 1999–2003 change specifically. Model results based on 1999–2003 hydrology were then compared against observed change from both 2004–11 and 2011–20. In the Puyallup and Carbon Rivers, model outputs were compared against observed

change only within the floodway, excluding overbank deposition along the Puyallup River and bluff erosion along the Carbon River. All comparisons were based on mean annual rates of channel change (yd^3/yr).

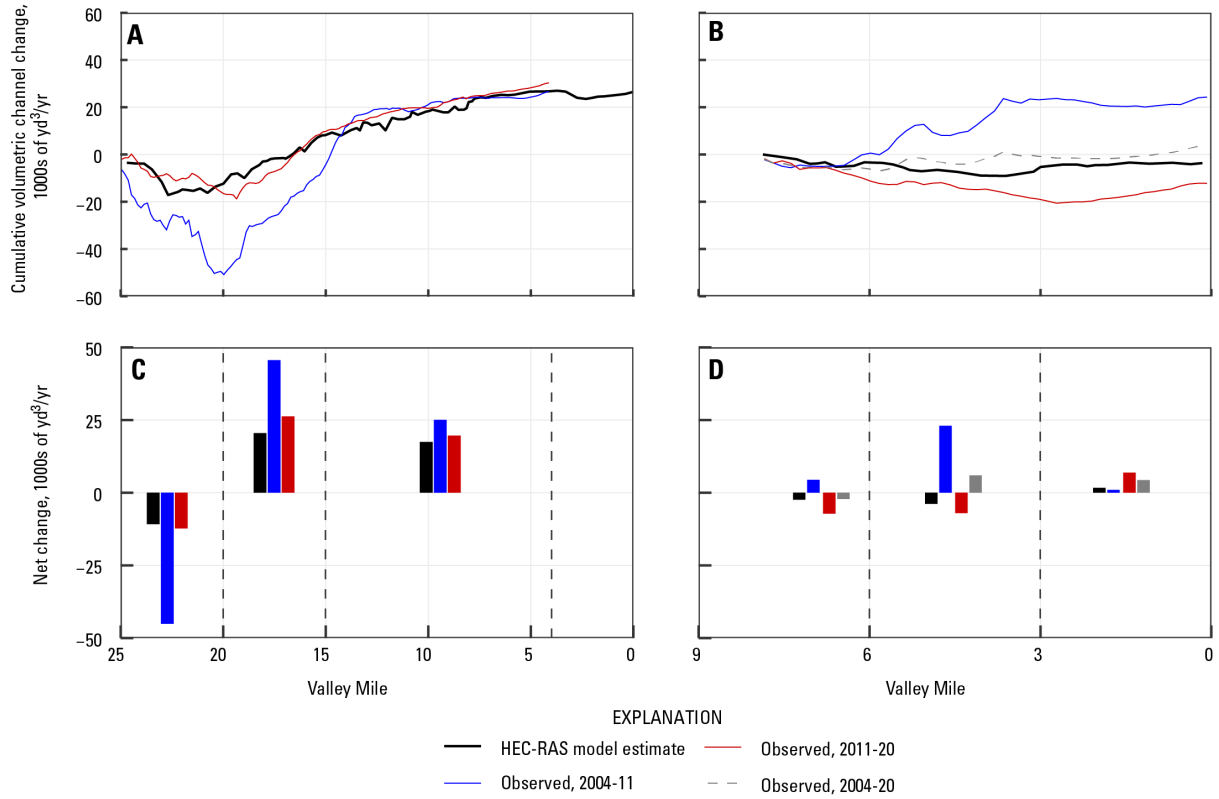


Figure A3. Comparison of modeled (Czuba and others, 2010) versus observed volumetric channel change in the Puyallup River, Washington, based on differencing of repeat aerial lidar (Table 6). Results presented as cumulative sum of net change for A) the Puyallup River and B) the Carbon River, showing local spatial patterns; reach-aggregate net change over 3–10-mile sub-reaches are also shown for the C) Puyallup River and D) Carbon River.

HEC-RAS model estimates of channel change in the Puyallup River match the spatial patterns of change observed from both 2004–11 and 2011–20, with negative to neutral trends upstream of roughly VM 20 and deposition downstream of VM 20 (Figure A3). Model agreement was particularly good with the 2011–2020 observational period. Model-estimated

deposition downstream of VM 20 averaged 41,000 yd³/yr, similar to observed rates of 49,000 yd³/yr from 2011–2020, and the model accurately captured the observed reduction in deposition rates downstream of the Carbon River confluence. During 2004–2011, observed erosion upstream of VM 20 and deposition from VM 20 to 14 were both larger than modeled; observed deposition downstream of VM 14 was modestly lower than modeled, though the difference is minor.

In the Carbon River, modeled estimates of channel change were qualitatively similar to observations during 2011–2020, with modest erosion in the upper reaches, modest deposition in the lower reaches, and overall low rates of change relative to the Puyallup River (Figure A3). However, model output tended to underestimate the magnitude of change and did not capture the substantial deposition observed over the 2004–11 interval between VMs 3.5 and 7. It seems likely that this deposition and subsequent re-erosion of deposited material during 2011–2020 were likely both short-term responses to large sediment loading associated with major floods in the 2004–2011 interval. Aggregating the observed change over the full 2004–2020 period, which should average out those short-term adjustments to some extent, brings observed and modeled change into closer agreement, with weak net erosion in the upper reaches, weak net deposition farther downstream, and substantially lower overall rates of change than observed in the Puyallup River.

Taken together, the one-dimensional sediment transport modeling of Czuba and others (2010) seems to have accurately captured the major features of recent change in the lower Puyallup and Carbon Rivers. This is particularly true for the Puyallup River during 2011–2020, the period that most logically aligns with model inputs collected in 2009. Mismatches between observed and modeled change in the Carbon River are plausibly attributable to transient channel

response to significant sediment loading in the early 2000s, and aggregating change over the full 2004–20 interval improved agreement between model-estimated channel change and observations.

Appendix B—Validation of Discharge-Normalization Approach on the Nooksack River

Direct validation of the ‘discharge-normalized’ approach to lidar differencing described in the ‘Accounting for Cross-Survey Differences in Discharge’ section requires bathymetric data collected concurrently with all near-infrared (NIR) lidar surveys, providing an independent estimate of change based directly on surveyed elevations in submerged areas. No such data exist within the Puyallup River watershed. However, such datasets exist over an extent of the Nooksack River near Everson, Washington (Figure B1). The Nooksack River is a dynamic gravel-bedded system in northwest Washington with headwaters on Mount Baker, another glacier-covered stratovolcano of the Cascade Range. NIR lidar and dense cross sections were both collected in the summer of 2006, while blue-green topobathymetric lidar and NIR lidar were collected concurrently in 2022 (Washington Geological Survey, 2008, 2022). These data provide the means to estimate change using both complete bathymetric data and NIR lidar via the discharge-normalization process described in this report. Within the reach of river covered by the relevant survey data, the Nooksack River varies between an anastomosing planform and a relatively confined single-threaded channel (Figure B1), with a width and planform character similar to much of the lower Puyallup and Carbon Rivers.

Mean elevation change in the Nooksack River was first estimated using 2006 cross sections and 2022 topobathymetric lidar. Analyses were based on synthetic 2022 cross sections

cut at identical locations as the 2006 survey data. These results represent estimates of change in which the submerged channel was directly surveyed in both datasets. The discharge-normalization procedure described above was then applied to the 2022 NIR lidar, raising the water surface to elevations expected at the discharge observed in the 2006 NIR lidar. Both the 2006 and 2022 NIR lidar were then sampled at the location of 2006 cross section survey points to create synthetic cross sections and used to assess local mean elevation change. These results represent change estimates in which the impact of change over the submerged channel has been inferred from discharge-normalized water surface elevations.

Aggregated across 129 cross sections collected over six river miles of the Nooksack River, the difference in differences between the two change estimation methods was 0.04 ± 0.70 ft (mean value, uncertainty bounds encompass 90 percent of observations; Figure B1), indicating minimal bias and reasonable precision for the discharge-normalized approach. Local section-to-section variability was very similar across both methods. While results on the Nooksack River do not guarantee that results in the Puyallup River watershed are similarly accurate, they do demonstrate the general validity of the approach in a similar geomorphic setting.

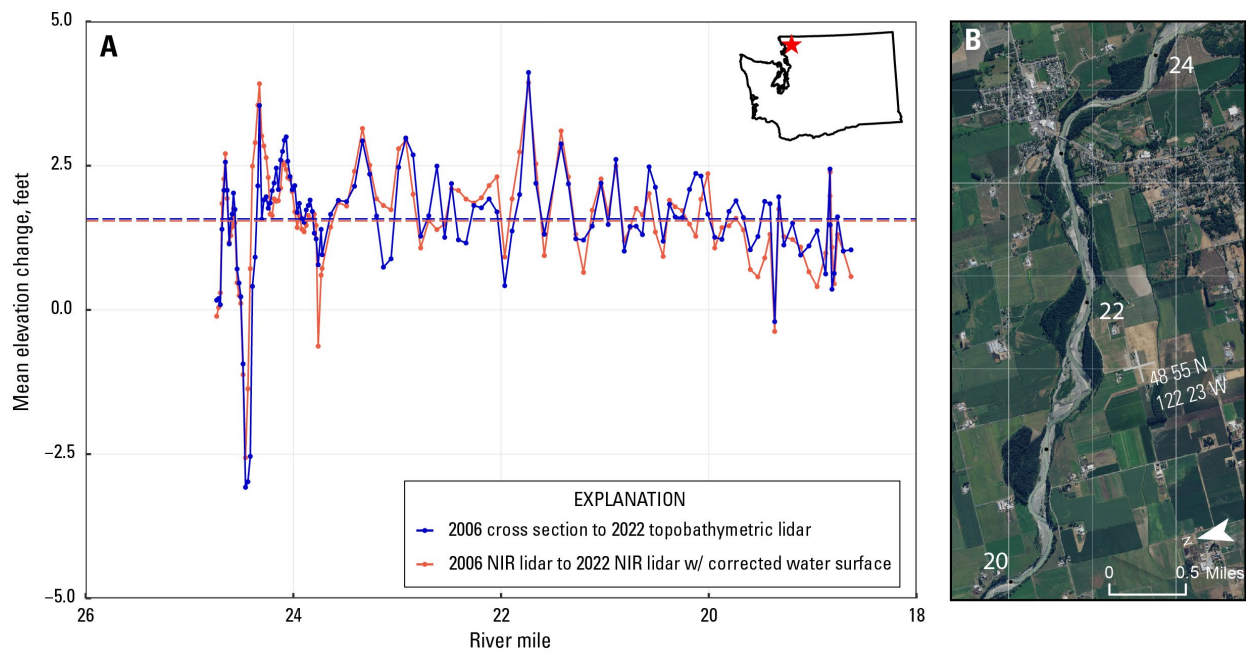


Figure B1. Comparison of discharge-normalized lidar differencing to traditional repeat cross sections on the Nooksack River near Everson, Washington. A) Methodologic comparison; horizontal dashed lines show reach-average elevation change. B) Aerial imagery showing the Nooksack River within extents of the analysis. Base from U.S. Department of Agriculture National Agricultural Imagery Program, 2019.

Appendix C—Methods for Estimating Sediment Loads

The USGS has made suspended sediment and bedload measurements at multiple locations in the Puyallup River watershed over the past 70 years, including at the Puyallup River at Alderton, WA (USGS 12096500), the Puyallup River at East Main Bridge at Puyallup, WA (12096505), the Puyallup River at or near Orting, WA (USGS 12093500 and 12093510), and the Carbon River near Orting, WA (USGS 12094300; U.S. Geological Survey, 2025; Figure 1). All data were collected using standard USGS methods (Edwards and Glysson, 1999) and publicly archived (U.S. Geological Survey, 2025).

Data from USGS 12093500 and USGS 12093510 were combined and treated as an estimate of sediment transport at USGS 12093510, where most high-discharge measurements were made. Similarly, data from USGS 12096500 and USGS 12096505 were combined, and outputs were treated as estimates of transport at USGS 12096500 (Figure 1). The general methods of analysis and limitations of the datasets common to all sites are presented first, followed by site-specific presentation of rating curve development and load estimation methods.

At all sites, a limited number (7–16) of suspended-sediment measurements were used to define suspended-sediment concentration (SSC)-discharge rating curves, and suspended sediment loads were estimated over the two intervals bounded by repeat topography. Suspended sediment samples were collected using a mix of D-61, D-74, and D-77 samplers. Bedload fluxes were estimated based on bedload to total load ratios estimated from limited paired SSC and bedload sampling conducted throughout the watershed. The goals of these analyses were to assess the state of knowledge of sediment transport in the lower Puyallup River watershed and to

place volumes of erosion and deposition observed via repeat topography into the context of watershed-scale sediment transport rates and overall sediment budget.

At all sites, there were not enough SSC measurements collected in summer months to meaningfully characterize typical concentrations over the glacial melt period, when SSC and discharge are generally not well correlated (Czuba and others, 2012a). However, while concentrations in the summer are likely high (Czuba and others, 2012a), discharges tend to be low, and in mainstem rivers well downstream from glacier source areas, the summer suspended sediment load tend to make up a small fraction of the annual load (Nelson, 1978; Jaeger and others, 2017; Curran and others, 2018). SSC-discharge rating curves defined by measurements primarily made in the fall, winter, and spring were then applied to discharge records over the summer without correction, recognizing that this likely modestly underestimates sediment loads.

Sediment-discharge rating curves are commonly developed by fitting a linear relation to log-transformed variables (power-law relations). However, initial attempts to fit power law relations to data at the Puyallup River at Orting and the Carbon River near Orting sites resulted in predictions of extremely high SSC values during unexceptional high flows, comparable to the highest concentrations measured on the Toutle River in the immediate aftermath of the 1980 Mount Saint Helens eruption (U.S. Geological Survey, 2025). Estimated mean annual suspended sediment yields were about an order of magnitude larger than yields in similar watersheds in the region. These unrealistically high concentrations most likely were a result of not accounting for a reduction in the slope of the SSC-discharge relation that often occurs at higher discharges (Warrick and others, 2013; Anderson and others, 2022, 2023). Rating curves fit using segmented linear relations (Muggeo, 2008) on untransformed variables were found to fit the available data as well as power laws and resulted in concentration and load estimates considered more

plausible. Loads at the two upstream sites were then estimated using segmented linear relations on untransformed inputs. At the Puyallup River at Alderton streamgage, power-law regression and segmented linear regression fits produced almost identical rating curves and load estimates. Segmented linear relations were used at Alderton for consistency with the other two sites.

Carbon River near Orting, WA

Seven SSC measurements have been made at the Carbon River near Orting, WA streamgage (USGS 12094300; U.S. Geological Survey, 2025). Of those, six were made in water year (WY) 1986 and one was made in WY 2014. Samples were collected at discharges between 900 and 4,800 ft³/s. Based on drainage area-scaled peak flow statistics from the Carbon River near Fairfax, WA streamgage (USGS 12094000), the 0.5 annual exceedance probability (0.5 AEP, or two-year flood) at the sediment sampling site is roughly 5,400 ft³/s (Mastin and others, 2016). All WY 1986 samples were collected in late fall or winter, while the lone WY 2014 measurement was made in early fall.

SSC for the WY 2014 sample was an order of magnitude higher than SSC for WY 1986 measurements made at similar discharges. With a single measurement, it is not possible to assess if this indicates a systematic shift in SSC-discharge relations, a short-term pulse of elevated sediment, sampling error, or some combination of the above. For the purposes of this work, the SSC-discharge rating curve was fit to just the six measurements made in the 1980s. The discrepancy with the lone WY 2014 measurements underscores the uncertainty of these estimates.

The relation between SSC and discharge was fit with a segmented linear relation using the ‘segmented’ R-package (Muggeo, 2008; R Core team, 2024; Figure C1A). The resulting fit

had an R^2 of 0.99, though this good agreement is largely a reflection of the limited number of data points.

Fifteen-minute discharge records were estimated for the Carbon River near Orting site based on the long-term discharge records at the Carbon River near Fairfax (USGS 12094000), which accounts for about 80 percent of drainage area at the sediment sampling site. Minor gaps in the 15-minute record were filled, in preferential order, using a regression with 15-minute data at the Puyallup River at Orting, WA streamgage (accounting for 0.2 percent of the total estimated load) and daily discharge records from the Carbon River near Fairfax, WA streamgage (much less than 0.1 percent of total estimated sediment load). All discharge records were scaled by 1.2, the drainage area ratio between the sampling site and the Carbon River near Fairfax streamgage. Over the 2004–20 study period, 31 percent of the total estimated sediment load was transported at or below the maximum sampled discharge (Figure C1A).

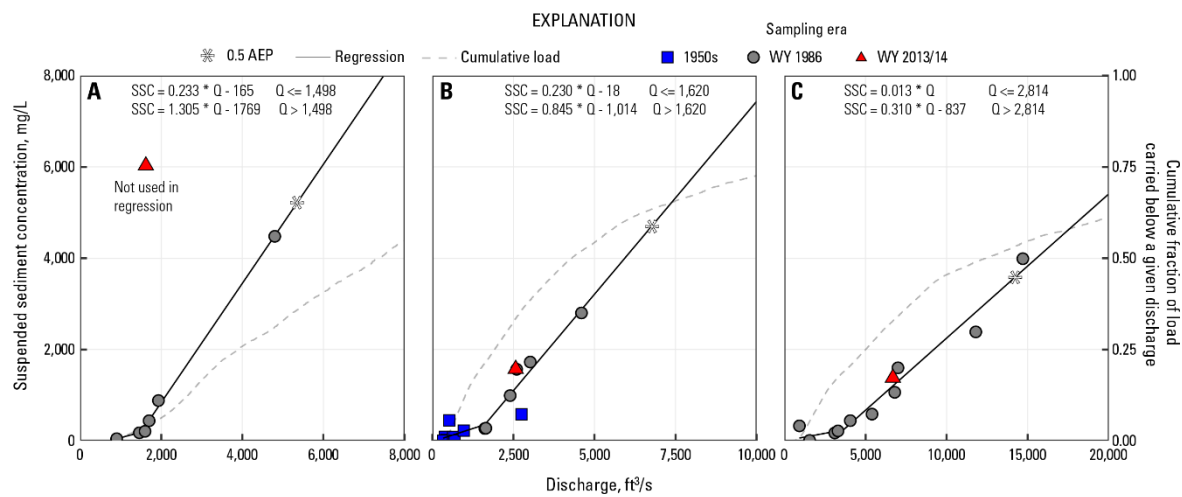


Figure C1. Suspended-sediment concentration (SSC)-discharge relations in the lower Puyallup River watershed, based on discrete SSC measurements, for A) the Carbon River near Orting, WA (USGS 12094300), B) the Puyallup River at Orting, WA (USGS 12093510), and C) the Puyallup River at Alderton,

WA (USGS 12096500). The 0.5 annual exceedance probability discharge (0.5 AEP) for each site is indicated and based on results from Mastin and others (2016).

Puyallup River at or Near Orting, WA

A total of 16 SSC measurements were available at the Puyallup River at Orting, WA streamgage (USGS 12093510; U.S. Geological Survey, 2025). This includes nine measurements made at the Puyallup River near Orting streamgage (USGS 12093500), about three miles upstream, all made in the 1950s at low (less than 1,000 ft³/s) discharges. The remaining seven measurements were made on the same days as the measurements available for the Carbon River at Orting, WA streamgage, with six collected in WY 1986 and one in WY 2014. The highest sampled discharge was 4,600 ft³/s, about 70 percent of the 0.5 AEP at the Puyallup River near Orting, WA streamgage (6,800 ft³/s; Mastin and others, 2016). The single WY 2014 SSC measurement plotted almost directly on top of a WY 1986 measurement made at a similar discharge.

All available measurements were used to define a segmented linear relation between SSC and discharge, again fit using the ‘segmented’ R package (Muggeo, 2008; Figure B1B). The adjusted R² was 0.92. Loads were estimated using 15-minute discharge records from the Puyallup River near Orting, WA streamgage, with gaps filled using regressions with 15-minute records from the Puyallup River at Electron, WA streamgage (USGS 12092000) after accounting for the 2.25 hour lag between sites (3.0 percent of load), and then daily discharge records from the Puyallup River near Orting site (much less than 0.1 percent of load). Over the 2004–20 study period, 52 percent of the total estimated load was transported at or below the maximum sampled discharge (Figure B1B).

Puyallup River at Alderton, WA

A total of 11 SSC measurements were available for the Puyallup River at Alderton, WA streamgage (USGS 12096500; U.S. Geological Survey, 2025). This includes measurements made at the Puyallup River at East Main Bridge at Puyallup, WA streamgage (USGS 12096505), located about 2 miles downstream (Figure 1). Of those 11 measurements, 10 were collected between WY 1983 and WY 1986, and 1 was collected in WY 2014. Measurements were collected up to 14,700 ft³/s, equivalent to the estimated 0.5 AEP flow of 14,300 ft³/s (Mastin and others, 2016). The single WY 2014 SSC measurement closely matched 1980s SSC measurements collected at similar discharges.

All available measurements were used to define a segmented linear regression with an R^2 of 0.97 (Figure B1C). Gaps in the primary discharge record were filled, in preferential order, using a regression with 15-minute records from the Puyallup near Orting, WA streamgage (13 percent of load), daily discharge estimates from the Puyallup River at Alderton, WA streamgage (much less than 0.1 percent of load), and a regression with daily discharge records at the Puyallup River near Orting, WA streamgage (0.4 percent of load). Over the 2004–20 study period, 48 percent of the total estimated load was transported at or below the maximum sampled discharge (Figure B1C).

Bedload Measurements and Bedload-to-Total Load Ratios

Two to three bedload sampling efforts have occurred at each site. In all cases, one bedload sample was collected in WY 2014 and the remainder in WY 1986. Samples from 1986 were collected using a Helley-Smith sampler, with a 3" x 3" opening and a mesh bag with 0.001" (0.25 cm) openings (Childers, 1999). Samples from WY 2014 were collected with Elwha (8" x

4" opening) or Toutle River II -2 (12" x 6" opening) samplers, with 0.5 mm mesh bags. All bedload samples were collected concurrent with SSC sampling.

A review of the data suggests that the WY 1986 bedload samples are unreliable, particularly for the steep channels at the Puyallup River at Orting, WA and Carbon River near Orting, WA streamgages. Common features of concern in the WY 1986 bedload samples include a substantial fraction of fine sand, which likely would be transported in suspension; limited collection of gravel in sizes that make up much of the bed (Sikonia, 1990; Czuba et al., 2010), and low bedload to total load ratios (Table C1).

An oversampling of suspended sand and under-sampling of coarse gravel is consistent with field tests of Helleys-Smith samplers (Emmett, 1980) and gravel collection would ultimately be limited by the 3" (76 mm) opening. Bedload to total load ratios for the 1986 samples were typically below three percent, while modern samples have bedload to total load ratios between 10 and 15 percent. These higher values are more consistent with results in similar rivers in the region (Czuba and others, 2012; Anderson and others, 2019) and expectations from a global compilation of paired sediment samples (Turowski and others, 2010). Bedload to total load ratios were then estimated based only the modern paired measurements. Paired measurements at the Carbon River near Orting, WA and the Puyallup River at Orting, WA streamgages both show bedload to total load ratios around 10 percent, and this value was used to estimate bedload at both sites. Bedload to total load ratio for the lone usable paired measurement at the Puyallup River near Alderton was two percent, and this value was used to estimate bedload at the site.

Summary of Estimated Sediment Loads

Suspended and bedload flux estimates were made over the two intervals bracketed by repeat lidar in the lower Puyallup River watershed. Because the lidar datasets were collected over a range of dates, the average collection dates were used to define the periods, which were February 4, 2004, February 9, 2011, and April 13, 2020. Total loads over the intervals were divided by the number of days in the interval and then multiplied by 365 to cast results as effective mean annual loads (tons/yr) and then divided by drainage area to obtain annual yields (tons/mi²/yr; Table 10).

Table C1. Summary of bedload measurements in the lower Puyallup River watershed (U.S. Geological Survey, 2025). [ft³/s – cubic feet per second; mm – millimeters]

Site	Site Number	Date	Discharge, ft ³ /s	Flux, tons/day	Percent <2 mm	Percent <0.5 mm	Bedload as percent of total load
Puyallup River at Orting	12093510	1/19/1986	2,600	80	95	73	1.4
		2/24/1986	4,800	252	69	56	0.8
		9/29/2013	2,493	1,100	34	6	9.1
Carbon River near Orting	12094300	1/19/1986	1,600	67	76	54	3.0
		2/24/1986	4,700	817	24	15	1.9
		9/29/2013	2,000	3,460	59	13	9.8
Puyallup River at Alderton	12096500	2/24/1986	11,000	330	29	27	0.5
		12/2/2013	8,238	640	33	13	2.2

Appendices References Cited

Anderson, S.W., Konrad, C.P., Grossman, E.E., and Curran, C.A., 2019, Sediment storage and transport in the Nooksack River basin, northwestern Washington, 2006–15: U.S. Geological Survey Scientific Investigations Report 2019-5008, 43 p., <https://doi.org/10.3133/sir20195008>.

Anderson, S.W., Jaeger, K.L., Rasmussen, N., Seguin, C.M., Wilkerson, O.A., and Curran, C.A., 2022, Suspended-sediment data for the Bogachiel and Calawah Rivers, WA for water years 2019-2021: U.S. Geological Survey data release, <https://doi.org/10.5066/P9YT9CN2>.

Anderson, SW, Curran, CA, Wilkerson, OA, and Seguin, CM, 2023, Suspended-sediment data for the Chehalis, Satsop and Wynoochee Rivers in Washington State, water years 2019-2022: U.S. Geological Survey Data release, <https://doi.org/10.5066/P9SBJP4S>.

Anderson, S.W., 2025, Supporting datasets for analyses of sediment transport and channel change in the Puyallup River watershed: U.S. Geological Survey Data Release, <https://doi.org/10.5066/P149MBYG>.

Childers, D., 1999, Field comparison of six pressure-difference bedload samplers in high-energy flow: U.S. Geological Survey Water Resources Investigations Report 92-4068

Curran, C.A., Anderson, S.W., and Foreman, J.R., 2018, Suspended sediment concentration and loads in the Nooksack River Basin, northwest Washington: U.S. Geological Survey data release, <https://doi.org/10.5066/F7TX3DK3>

Czuba, J.A., Czuba, C.R., Magirl, C.S., and Voss, F.D., 2010, Channel-conveyance capacity, channel change, and sediment transport in the lower Puyallup, White, and Carbon Rivers, western Washington: U.S. Geological Survey Scientific Investigations Report 2010-5240, 104 p.

Czuba, J.A., Magirl, C.S., Czuba, C.R., Curran, C.A., Johnson, K.H., Olsen, T.D., Kimball, H.K., and Gish, C.C., 2012, Geomorphic analysis of the river response to sedimentation downstream of Mount Rainier, Washington: U.S. Geological Survey Open-File Report 2012-1242, 134 p.

Edwards, T.E., and G.D. Glysson. 1999. Field methods for measurement of fluvial sediment. U.S. Geological Survey Techniques of Water-Resources Investigations, Book 3.

Emmett, W.W., 1980. A field calibration of the sediment-trapping characteristics of the Helleysmith bedload sampler: U.S. Geological Survey Professional Paper 1139, 44 p.

Jaeger, K.L., Curran, C.A., Anderson, S.W., Morris, S.T., Moran, P.W., and Reams, K.A., 2017, Suspended sediment, turbidity, and stream water temperature in the Sauk River Basin, Washington, water years 2012–16: U.S. Geological Survey Scientific Investigations Report 2017-5113, 47 p.

Mastin, M.C., Konrad, C.P., Veilleux, A.G., and Tecca, A.E., 2016, Magnitude, frequency, and trends of floods at gaged and ungaged sites in Washington, based on data through water year 2014 (ver 1.2, November 2017): U.S. Geological Survey Scientific Investigations Report 2016-5118, 70 p.,

Muggeo, V.M.R., 2008, Segmented: an R package to fit regression models with broken-line relationships. *R News*, 8/1, 20-25.

Nelson, L.M., 1978. Sediment transport by the White River into Mud Mountain Reservoir, Washington, June 1974-June 1976. U.S. Geological Survey Water-Resources Investigations Report 78-133, 26 p.

R Core Team. (2024). R: A language and environment for statistical computing (Version 4.2.1) [Computer software]. R Foundation for Statistical Computing. <https://www.R-project.org>

Sikonia, W.G., 1990, Sediment transport in the lower Puyallup, White, and Carbon Rivers of western Washington: U.S. Geological Survey Water-Resources Investigations Report 89-4112, 204 p.

Turowski, J.M., Rickenmann, D. and Dadson, S.J., 2010. The partitioning of the total sediment load of a river into suspended load and bedload: a review of empirical data. *Sedimentology*, 57(4), pp.1126-1146.

U.S. Geological Survey, 2025, USGS water data for the Nation: U.S. Geological Survey National Water Information System database, accessed June 10, 2025, at <https://doi.org/10.5066/F7P55KJN>.

Warrick, J.A., Madej, M.A., Goñi, M.A. and Wheatcroft, R.A., 2013. Trends in the suspended-sediment yields of coastal rivers of northern California, 1955–2010. *Journal of hydrology*, 489, pp.108-123.

Washington Geological Survey, 2008, North Puget USGS 2006 project [lidar data]: originally contracted by U.S. Geological Survey. [accessed Dec. 1, 2022, at <http://lidarportal.dnr.wa.gov>]

Washington Geological Survey, 2022, Nooksack River Topobathy 2022 [lidar data]: originally contracted by Whatcom County. [accessed Dec. 1, 2022, at <http://lidarportal.dnr.wa.gov>]

Wilcock, P.R. and Crowe, J.C., 2003. Surface-based transport model for mixed-size sediment. *Journal of hydraulic engineering*, 129(2), pp.120-128.